2007

Dissecting the Entry Pathways of Hepatitis C and Bovine Viral Diarrhea Viruses

Donna M. Tscherne

DISSECTING THE ENTRY PATHWAYS OF HEPATITIS C AND BOVINE VIRAL DIARRHEA VIRUSES

A Thesis Presented to the Faculty of

The Rockefeller University

in Partial Fulfillment of the Requirements for

the degree of Doctor of Philosophy

by

Donna M. Tscherne

June 2007

DISSECTING THE ENTRY PATHWAYS OF HEPATITIS C AND BOVINE VIRAL DIARRHEA VIRUSES

Donna M. Tscherne, Ph.D.
The Rockefeller University 2007

Hepatitis C virus (HCV) and bovine viral diarrhea virus (BVDV) are closely related members of the family *Flaviviridae* and are important human and animal pathogens, respectively. In this work, I investigated how these viruses interact with and enter both naïve and previously infected cells, specifically, the mechanisms of superinfection exclusion, the phenomenon by which previous viral infection prevents reinfection of the same cell, and the pathways of entry into target cells for these viruses. BVDV-acutely infected cells establish two blocks to superinfection, at the levels of virus entry and RNA replication. The former is mediated by the BVDV E2 protein, which was also identified as a transdominant inhibitor of BVDV entry in a screen of a random fragment BVDV cDNA library. The inhibitory region was further mapped to the E2 ectodomain and the block to entry was shown to occur downstream of CD46 receptor expression and BVDV binding, suggesting interference with a yet unidentified BVDV entry factor. In contrast to BVDV, HCV-infected and replicon-containing cells exhibit a post-entry block to superinfection, at one or more steps in viral replication.

The entry pathways of both BVDV and HCV into target cells were also examined and found to be pH-dependent. In addition, these viruses were shown to be very acid-resistant, suggesting that they require an activation step to trigger pH-dependent entry. The role of the cellular receptors/coreceptors, CD81, scavenger receptor class B type 1 (SR-BI), and claudin-1 (CLDN1), in mediating HCV entry and their modulation during persistent HCV replication were also investigated. This work highlights common features shared between BVDV and HCV and provides insight into the cellular environment required for productive virus entry and RNA replication.

To my parents

Acknowledgements

First and foremost, I thank my Thesis Advisor Charlie Rice. I am so appreciative of his patience and willingness to mentor me, especially in my early days in the lab; his knowledge and excitement about virology has inspired my work from the very beginning. Charlie has taught me how to be a scientist in every aspect, from experimental design and technique to the ability to evaluate data and to present it in a logical manner. I truly respect and admire him as a scientist.

I am also grateful for the support, encouragement, and generosity of many current and former members of the Rice lab. From my first day in the lab, Matthew Evans has assisted me with experiments, critiqued my writing, and provided me with sound advice. I value his friendship and appreciate all of his help. In addition, Thomas von Hahn, Shihyun You, Chris Jones, Drew Syder, John Law, John-William Carroll, Glenn Randall, and Arash Grakoui have made my experience in the lab productive and enjoyable. A special thank you to Peggy MacDonald who took the time to teach and assist me in experiments when I first joined the lab and has continued to provide me additional support (and a bench!) throughout the years. I also thank my dear friend Catherine Murray who has shared with me the ups and downs of

graduate school and consoled me time and again with her “layers of the onion” analogy.

I express sincere gratitude to my Thesis Committee, Mike Rout, Magda Konarska, and David Ho, who generously gave of their time to provide me with guidance and constructive criticism, which were indispensable for my growth as a scientist. I have also benefited from generous contributions of reagents from collaborators at other institutions, especially Till Rümenapf, Kenny Brock, James Cunningham, Kartik Chandran, and David Leib.

This work would not have been possible without the administrative and scientific support staff in the Rice lab, particularly Patricia Holst, Lily Zhang, Santa Pecoraro, Anesta Webson, Jodie Tassello, and Maryline Panis, who have made the lab a pleasant and productive place to do research. In addition, I very much appreciate the assistance provided by the administrative staff in The Rockefeller University Dean’s Office, especially by Sid Strickland, Marta Delgado, and Kristen Cullen.

Finally, I wish to thank my parents, who encouraged and supported me in my quest for this degree of persistence and to whom this thesis is dedicated. Their ability to provide sound advice and to empathize with my

experiences was vital for maintaining my confidence and composure over the years.

Table of Contents

Chapter 1. Introduction 1

1.1 Introduction to the family *Flaviviridae* 2

1.2 Features of bovine viral diarrhea virus (BVDV) 4

- *BVDV genome organization and encoded proteins* 4
- *BVDV entry and cellular entry factors* 7
- *BVDV pathogenesis and isogenic infectious clones* 10

1.3 Features of hepatitis C virus (HCV) 11

- *HCV genome organization and encoded proteins* 12
- *Evolution of model systems for HCV research* 14
- *HCV entry and cellular entry factors* 16

1.4 Objectives 21

Chapter 2. Materials and methods 22

- *Cells* 23
- *Chemicals* 23
- *BVDV RNA transcription, transfection, and virus stocks* 24
- *HCV replicons and cells harboring HCV replicons* 25
- *HCV RNA transcription, transfection, and virus stocks* 26
- *Generation of HCVpp stocks and HCVpp infection* 28

- *Vesicular stomatitis virus, Sindbis virus, and herpes simplex virus-1 stocks* 29
- *BVDV plaque and focus forming assays* 30
- *Construction of random BVDV cDNA library* 31
- *Packaging and screening of the random BVDV library* 33
- *Analysis of resistant MDBK clones* 34
- *Construction of pLenti6-EGFP, pLenti6-E1*E2p7*, pLenti6-Sig-E2, and pLenti6-Sig-E2** 35
- *BVDV Binding Assay* 36
- *Immunoblotting* 37
- *Immunostaining and flow cytometry* 39
- *Luciferase assays* 40
- *Real-time quantitative reverse transcription PCR (qRT-PCR)* 41
- *Bafilomycin A1, concanamycin A, and NH_4Cl inhibitor experiments* 43
- *Low pH treatment* 44
- *HCV, BVDV, and SIN entry at the plasma membrane* 45
- *Cathepsin B/L inhibitor experiments* 45
- *Transduction of J6/JFH-FLneo cells with TRIP-CD81 or TRIP-CD9* 46
- *Treatment of HCV replicon-containing cells with BILN 2061* 46

- *Construction of VEE-AP180c-GFP and inhibition of clathrin-mediated endocytosis* 47
- *HCVcc binding assay* 48
- *HCV glycoprotein-mediated cell fusion assay* 49

Chapter 3. A transdominant screen of bovine viral diarrhea virus reveals an inhibitor of virus entry 52

3.1 Introduction 53

3.2 BVDV E2 as a transdominant inhibitor of BVDV entry 54

- *A functional genomics approach to identify essential interactions in the BVDV life cycle* 54
- *Naïve cells expressing E1*E2p7* are resistant to homologous BVDV infection* 59
- *Expression of the BVDV E2 ectodomain is sufficient for BVDV inhibition* 66
- *BVDV is blocked prior to translation in MDBK-E1* E2p7* cells* 69
- *CD46 expression and BVDV binding on MDBK-E1* E2p7* cells is similar to control cells* 72

3.3 Discussion 75

Chapter 4. The mechanisms of BVDV and HCV superinfection exclusion 81

4.1 Introduction 82

4.2 Background information for BVDV superinfection exclusion 83

- *MDBK cells acutely infected with ncp BVDV are protected from CPE when superinfected with cp BVDV, but not with VSV* 84
- *Superinfection exclusion is established rapidly* 87
- *BVDV persistently infected cells lose the ability to exclude superinfecting virus* 88
- *Superinfecting BVDV is blocked at the level of viral entry* 91
- *Transfection of BVDV RNA reveals a second block at replication, but not translation* 96
- *Level of RNA replication correlates with the extent of superinfection exclusion* 102

4.3 Additional studies of BVDV superinfection exclusion 106

- *BVDV superinfection exclusion is transient and lost upon passaging* 106
- *Decreased RNA levels during persistent ncp BVDV infection render cells susceptible to superinfection* 110

4.4 HCV superinfection exclusion 112

- *Superinfection exclusion in HCVcc-infected and replicon-containing Huh-7.5 cells* 112

- *Treatment with BILN 2061 restores HCV permissiveness* 116
- *Superinfection exclusion occurs downstream of viral entry* 120
- *Examination of the post-entry superinfection block* 124
- *An additional defect in J6/JFH-FLneo selected cells* 127

4.5 Discussion 138

Chapter 5. Analysis of the BVDV and HCV entry pathways 146

5.1 Introduction 147

5.2 Mechanism of BVDV entry 148

- *BVDV entry is pH-dependent* 148
- *BVDV infectivity is unaffected by low pH treatment* 150

5.3 Mechanism of HCV entry 154

- *HCV entry is pH-dependent* 154
- *HCV infectivity is unaffected by low pH treatment* 160
- *HCV fails to enter bafilomycin A1 treated cells when exposed to low pH* 162
- *HCV entry is not dependent on cathepsin B or L* 163
- *Evidence that additional post-binding steps are required to activate HCV for entry* 164

- *An inhibitor of clathrin-mediated endocytosis reduces the efficiency of HCV entry* 168

5.4 Role of HCV entry factors 171

- *SR-BI enhances HCV binding to CHO cells* 171
- *CLDN1 enhances HCV glycoprotein-mediated cell fusion* 173

5.5 Discussion 177

Chapter 6. Unanswered questions and future directions 182

6.1 Mechanism of E1*E2p7* inhibition of BVDV entry 183

6.2 BVDV and HCV superinfection exclusion mechanisms 185

- *Superinfection exclusion at the level of RNA replication* 185
- *Cellular alterations induced by persistent ncp BVDV infection* 189
- *Role of superinfection exclusion in vivo* 193
- *HCV JFH-1 induced cytotoxicity in CD81-expressing cells* 195

6.3 Studies of the BVDV and HCV entry pathways 198

- *Mechanism of HCV and BVDV activation for pH-triggered entry* 198
- *Comparing HCVpp and HCVcc entry* 202

6.4 Perspectives 203

List of Figures

Chapter 1

Figure 1.1 The life cycle of the *Flaviviridae* 3

Figure 1.2 Genome organization of pestiviruses and hepaciviruses 5

Figure 1.3 Structure of CD46 9

Figure 1.4 Cellular factors for HCV entry 17

Chapter 3

Figure 3.1 Scheme for BVDV library screening 56

Figure 3.2 A genetic screen identifies the BVDV E1*E2p7* sequence as a transdominant inhibitor of BVDV replication 58

Figure 3.3 Cells expressing BVDV E1*E2p7* are resistant to homologous BVDV infection 60

Figure 3.4 The MDBK-E1*E2p7* cell population contains a small subset of permissive cells 62

Figure 3.5 Putative membrane topology of BVDV E2 64

Figure 3.6 E2 expression in MDBK-E1*E2p7* cells 65

Figure 3.7 E2 expression constructs 67

Figure 3.8 The E2 ectodomain is sufficient for BVDV inhibition 68

Figure 3.9 MDBK-E1*E2p7* cells have a defect at the level of BVDV entry 71

Figure 3.10 CD46 expression on MDBK-E1*E2p7* cells is similar to control pBabe cells 73

Figure 3.11 BVDV binding to MDBK-E1*E2p7* cells is similar to control pBabe cells 74

Chapter 4

Figure 4.1 MDBK cells acutely infected with ncp BVDV are protected from CPE when superinfected with homologous cp BVDV, but not with VSV 85

Figure 4.2 Superinfection exclusion is established within 30-60 minutes of primary BVDV infection 89

Figure 4.3 Superinfection exclusion is transient and lost upon passaging 90

Figure 4.4 Homologous BVDV superinfecting particles are blocked at the level of viral entry 94

Figure 4.5 Transfected ncp NADLJiv90^{-}*pac* RNA fails to replicate in ncp NADLJiv90^{-} infected cells 97

Figure 4.6 ncp NADLJiv90^{-}ΔS-*luc* viral RNA transfected into ncp NADLJiv90^{-}-infected MDBK cells is competent for translation, but not for replication 100

Figure 4.7 The level of primary viral RNA replication correlates with the degree of superinfection exclusion at viral RNA replication 105

Figure 4.8 MDBK cells persistently infected with ncp NADLJiv90^{-} are not protected from cp NADL-induced CPE 108

Figure 4.9 The loss of superinfection exclusion in BVDV persistently infected cells correlates with a decrease in primary viral RNA replication 111

Figure 4.10 Scheme for analysis of HCV superinfection exclusion 113

Figure 4.11 Cells harboring HCV do not support HCVcc Superinfection 114

Figure 4.12 HCV subgenomic replicon cells treated with an HCV-specific protease inhibitor become permissive for HCVcc infection 119

Figure 4.13 The HCVpp system 121

Figure 4.14 J6/JFH-acutely infected cells, but not cells harboring a stable J6/JFH-FLneo replicon, are permissive for HCVpp infection 123

Figure 4.15 JFH-SGneo cells exhibit a post-entry superinfection block 126

Figure 4.16 Stable J6/JFH-FLneo replicon cells have decreased CD81 protein and RNA levels 129

Figure 4.17 Ectopic expression of CD81 renders stable J6/JFH-FLneo replicon cells permissive for HCVpp infection 131

Figure 4.18 BILN 2061 treated J6/JFH-FLneo replicon cells have increased CD81 surface expression and are permissive for HCVpp infection 133

Figure 4.19 Time course of superinfection with HCVpp 134

Figure 4.20 J6/JFH-infection of Huh-7.5 cells promotes the emergence of a $CD81_{low}$ cell population 137

Chapter 5

Figure 5.1 BVDV entry is pH-dependent 149

Figure 5.2 BVDV infectivity is acid-resistant 151

Figure 5.3 Schematic illustration of entry in the presence of bafilomycin A1 152

Figure 5.4 Bound BVDV virions cannot enter a bafilomycin A1 treated cell upon exposure to low pH 153

Figure 5.5 Characterization of HCVcc-Rluc 155

Figure 5.6 HCV entry is sensitive to bafilomycin A1 157

Figure 5.7 HCV entry is sensitive to concanamycin A and NH_4Cl 159

Figure 5.8 HCV infectivity is resistant to acidic pH 161

Figure 5.9 HCV is unaffected by inhibitors of CatB and CatL 165

Figure 5.10 Schematic illustration of entry in the presence of bafilomycin A1 with prior incubation at 37 ºC 166

Figure 5.11 Incubation at 37 ºC allows HCV to enter bafilomycin A1-treated cells 167

Figure 5.12 HCV entry is moderately inhibited by a dominant-negative inhibitor of clathrin-mediated endocytosis 170

Figure 5.13 HCVcc binds to CHO cells expressing SR-BI 172

Figure 5.14 Schematic illustration of cell fusion assay 174

Figure 5.15 CLDN1 enhances HCV glycoprotein-mediated fusion in 293T cells 176

Chapter 1. Introduction

1.1 Introduction to the family *Flaviviridae*

The family *Flaviviridae,* including important human and animal pathogens, is comprised of small enveloped viruses with a single-stranded, positive-sense RNA genome (reviewed in 126). This family is currently divided into three genera, the classical flaviviruses, the pestiviruses, and the hepaciviruses. The life cycle of the *Flaviviridae* commences with receptor-mediated endocytosis and low pH-mediated fusion (reviewed in 126) (Fig. 1.1). Following uncoating, the viral RNA is translated into viral proteins to initiate intracellular RNA replication, which takes place entirely in the host cell cytoplasm in association with intracellular membranes. Virions are thought to assemble in and acquire their envelope by budding into an intracellular, most likely endoplasmic reticulum (ER)-derived compartment, and exit the cell through the host secretory pathway. Although the three genera have similar virion morphology, genome organization and replication strategies, more common features especially in terms of translation mechanism and sequence homology are shared among the hepaci- and pestiviruses, than with the flaviviruses.

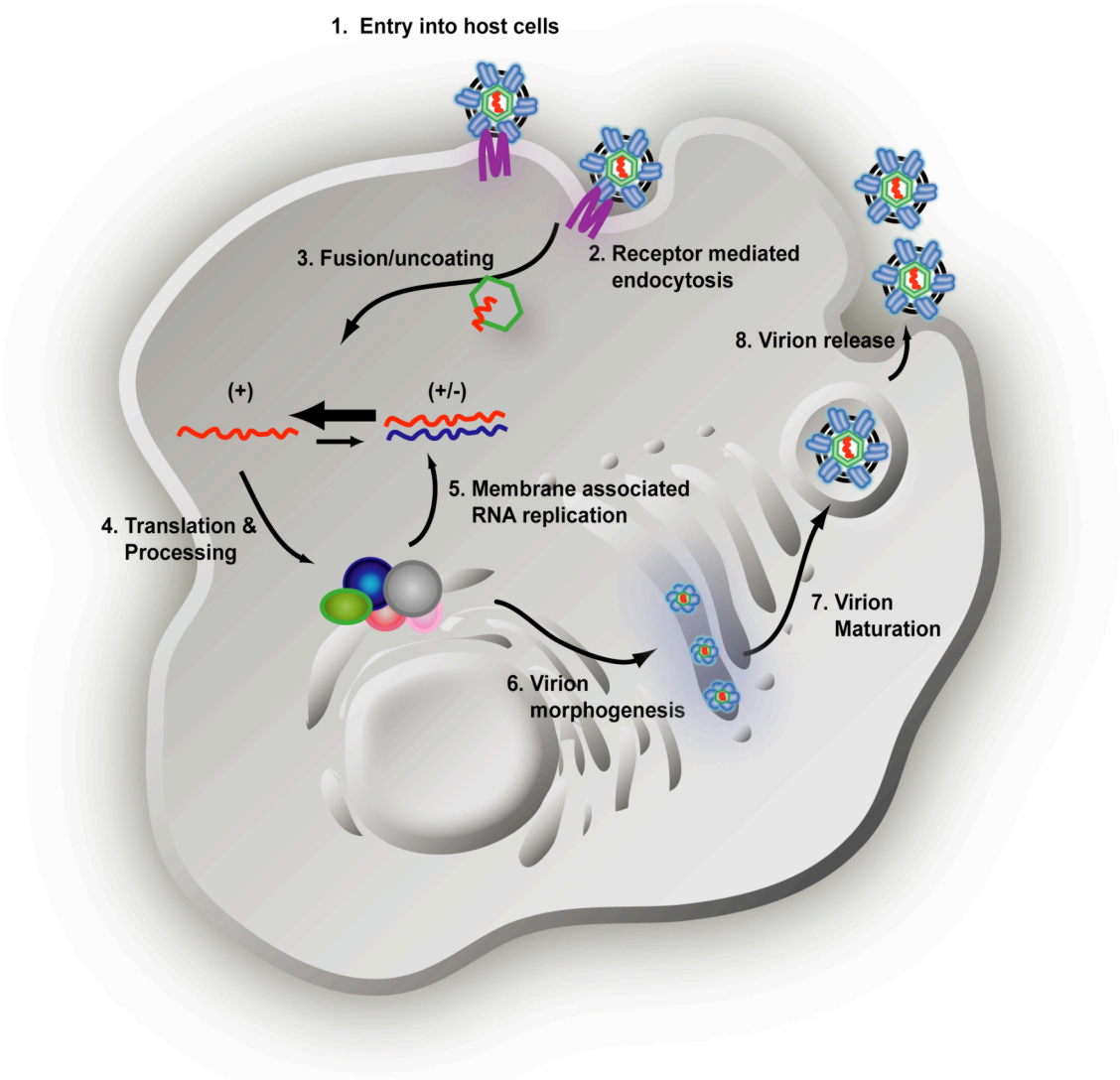

Fig. 1.1 The life cycle of the *Flaviviridae*. Virions enter the target cell by receptor-mediated endocytosis. Following uncoating, the viral genome is translated and the polyprotein processed into the individual viral proteins. RNA replication occurs in association with intracellular membranes and proceeds asymmetrically, favoring replication of positive-sense, genome-length RNAs. Virions mature within intracellular vesicles and are thought to acquire their envelope by budding into these vesicles. Nascent virions are transported out of the cell through the host secretory pathway. Adapted from (126).

1.2 Features of bovine viral diarrhea virus

Pestiviruses, including bovine viral diarrhea virus (BVDV), border disease virus (BDV) and classical swine fever virus (CSFV), cause economically important diseases in livestock leading to substantial financial losses within the industry each year (reviewed in 126). BVDV infection can result in a wide range of clinical symptoms from acute self-limiting disease to a sporadic, fatal mucosal disease (MD) (194). Transmission of BVDV *in utero* has a number of detrimental outcomes including fetal death, as well as immunotolerance in newborn calves leading to persistent life-long BVDV infection, which can progress to MD. Though vaccines are available for immunization against BVDV (149), there is a need to improve their safety and efficacy, especially to prevent transmission *in utero*.

BVDV genome organization and encoded proteins

BVDV harbors an RNA genome of approximately 12.5 kb, which contains a large open reading frame (ORF) flanked by both 5' and 3' non-translated regions (NTRs) (Fig. 1.2) (reviewed in 126). Within the 5'NTR is an internal ribosome entry site (IRES), which drives cap-independent translation of the viral ORF, generating a polyprotein of approximately 4000 amino acids. The polyprotein is co- and post- translationally processed into

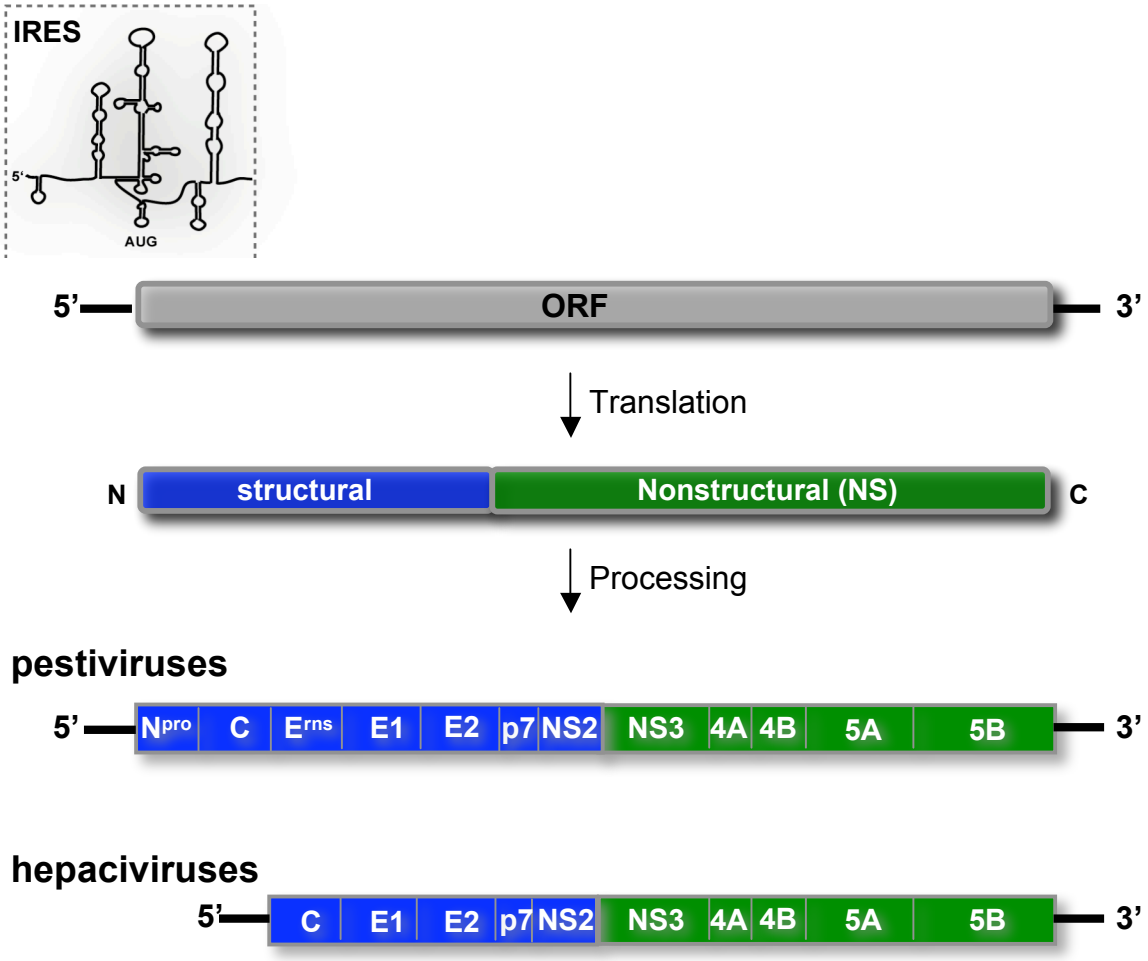

Fig. 1.2 Genome organization of pestiviruses and hepaciviruses. The genomes of pestiviruses and the hepaciviruses contain a large open reading frame (ORF), flanked by 5' and 3' nontranslated regions (NTR). The 5'NTR contains an IRES element that directs translation of the ORF generating a polyprotein. The polyprotein is processed into structural proteins (blue) and nonstrucutral (NS) proteins (green) by a combination of viral and host-encoded proteases.

mature proteins by a combination of viral and host proteases to produce the viral proteins: N^{pro}, C, E^{rns}, E1, E2, p7, NS2, NS3, NS4A, NS4B, NS5A, and NS5B.

Within the virion, BVDV genomic RNA is complexed with multiple copies of capsid protein forming the viral nucleocapsid. The nucleocapsid is surrounded by a lipid envelope decorated with the three envelope glycoproteins, E^{rns}, E1, and E2 (171, 195). E^{rns} is both secreted from infected cells and present as disulfide-linked homodimers on the surface of virions (55, 116, 172, 202). The E^{rns} glycoprotein exhibits ribonuclease activity, but the role of this activity although apparently important for BVDV infection and pathogenesis remains ambiguous (78, 177). E2 forms disulfide linked homo- and heterodimers with E1 and has been implicated in receptor binding as major neutralizing antibodies are directed against the E2 protein in an infected host (46, 159, 196). p7 is a small, hydrophobic protein that may function as an ion channel. Although p7 is not found within BVDV particles, it is essential for production of infectious virus (51, 73, 76).

The remainder of the polyprotein is composed of non-structural (NS) proteins, which, likely partnered with cellular factors, are responsible for assembly or function of the viral replication complex. NS2 is an autoprotease responsible for cleavage at the NS2/3 junction (111). The

efficiency of cleavage between NS2-3 modulates levels of RNA replication and differs between BVDV biotypes (described below) (112). In addition, uncleaved NS2-3 protein is required for infectious virus production (2). NS3 contains a serine protease motif at its N-terminus (17, 67) that cleaves between NS3/NS4A, NS4A/NS4B, NS4B/NS5A, and NS5A/NS5B (191, 211, 215). NS4A functions as an NS3 protease cofactor for cleavage between NS4B/NS5A and NS5A/NS5B (191, 215). Additionally, NS3 contains NTPase and helicase sequence motifs, and these enzymatic activities have been demonstrated *in vitro* (67, 71, 75, 190). NS5B is the viral RNA-dependent RNA polymerase (RdRp) (113, 222). Autonomous BVDV RNA replication in transfected cells does not require viral structural proteins (C, E^{rns}, E1, E2), N^{pro}, p7 or NS2 (18, 154, 192).

BVDV entry and cellular entry factors

After interaction with one or more cellular receptors, BVDV enters the target cell by clathrin-mediated endocytosis in a pH-dependent manner (109, 118). CD46, a regulator of complement activation, has been identified as a cellular receptor for BVDV (137). CD46 contains four extracellular complement control protein (CCP) repeats (CCP1 to 4), an O-glycosylated STP region, a transmembrane domain, and a cytosolic tail (127, 128) (Fig.

1.3). The extent of glycosylation in the STP region (127) and the length of the cytosolic tail (137) is determined by differential splicing of CD46 transcripts. The viral glycoprotein, which acts as a ligand for CD46, has not yet been determined, although it is likely E2 based on inhibition studies using CSFV recombinant E2 protein (86) and the observation that E2 determines the cell culture tropism of BVDV (122, 169). BVDV binding has been mapped to CD46 CCP1, the domain most distal from the plasma membrane, and this region is necessary for BVDV infection (107). However, the requirement for additional BVDV entry factors is likely, given that BVDV enters cells by receptor-mediated endocytosis and CD46 is excluded from endosomes due to a sorting signal in its C-terminal tail. In addition, expression of CD46 cannot render certain cell types permissive for BVDV entry despite efficient virus binding (137). Interactions with highly sulfated heparin, mediated by the E^{rns} protein, have also been shown to be important for entry of cell-culture adapted strains of BVDV (89). The increased affinity for heparin is due to a point mutation within the C terminus of E^{rns} (90). There has also been some evidence that low density lipoprotein receptor (LDL-R) has a role in BVDV entry (3), although a recent study strongly refutes this hypothesis (108).

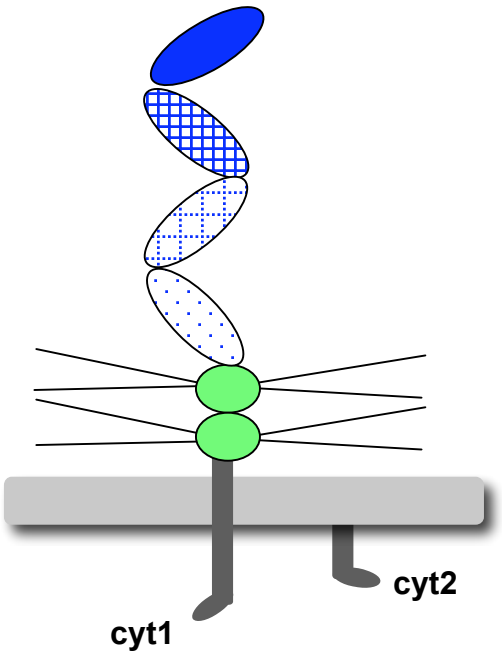

Fig. 1.3 Structure of CD46. Ovals = complement control protein (CCP) repeats. Small green ovals = STP (serine, threonine, proline-rich) motifs. Thin lines = O-glycosylation sites. Gray bar = plasma membrane. cyt1, cyt2 = alternative cytoplasmic tails. Adapted from (32).

BVDV pathogenesis and isogenic infectious clones

Cows suffering from fatal MD harbor two BVDV biotypes, noncytopathic (ncp) and cytopathic (cp), as described by their respective effects on tissue culture cells (140, 146). In the infected animal, cp BVDV develops from mutation of the ncp BVDV parental strain and as a result the cp and ncp strains are genetically closely related. Further evidence for this hypothesis is that experimental superinfection of persistently infected animals with a closely related cp virus can result in MD (25, 148). Many of the cp BVDV variants that have been isolated contain genome rearrangements, point mutations or insertions leading to increased NS2-3 autoprotease activity (reviewed in 194). In cell culture, this is manifested by the accumulation of free NS3 protein and increased RNA replication, both of which are associated with cytopathogenicity. Although the mechanism of the BVDV-induced cytopathic effect is still unclear, it appears that higher levels of RNA replication may activate cellular pathways leading to apoptosis (95).

ncp BVDV NADLJiv90^{-} and cp BVDV NADL are an isogenic pair of infectious viral cDNA clones, the former harboring a cellular insertion, Jiv90, upstream of the cleavage site between the NS2/3 proteins, which renders this virus cp (143). Jiv90 is a 90 amino acid domain of Jiv (J-domain protein interacting with viral protein), which is a cellular chaperone

for the NS2-3 autoprotease. *Cis* or *trans* over expression of Jiv during BVDV infection has been shown to increase cleavage at the NS2/3 site (112). Additional cp and ncp pairs with an insertion in NS2 have also been characterized including, strain CP7 which contains a smaller insertion of Jiv (193), and strain Osloss which has a ubiquitin sequence just upstream of NS3 (145).

1.3 Features of hepatitis C virus

Hepatitis C virus (HCV) is the type member of the *Hepacivirus* genus, which has recently been expanded to include GBV-B (reviewed in 126). First identified as the causative agent of non-A, non-B hepatitis in 1989, HCV is an important human pathogen establishing a chronic infection in approximately 70-80% of cases. Persistent HCV infection is associated with the development of severe liver disease, most notably, liver cirrhosis and hepatocellular carcinoma (135). A daunting 120 million people worldwide are infected with HCV and at present there is no HCV vaccine available. Moreover, antiviral therapy has limited efficacy, being successful in only about 50% of patients. HCV is currently the primary indication for liver transplantation in both the United States and Europe (29) and contributing to

public health concerns, extrahepatic disease associated with chronic HCV infection affects nearly 40% of patients (138).

HCV genome organization and encoded proteins

Similar to BVDV, the HCV genome is a single-stranded RNA molecule of approximately 9.6 kb, containing a large ORF flanked by 5' and 3' NTRs (reviewed in 126) (Fig. 1.2). Translation of the viral ORF, driven by a cap-independent mechanism via an IRES element within the 5'NTR, generates a polyprotein of 3011 amino acids that is processed by host and viral encoded proteases into structural and nonstructural proteins: C, E1, E2, p7, NS2, NS3, NS4A, NS4B, NS5A, NS5B. An additional protein, termed ARF or F for alternative reading frame or frameshift protein, respectively, resulting from ribosomal frameshifting within the core region, has also been described (26). However, a recent study suggests that the ARF/F-encoded protein is dispensable for replication and conservation of the ARF coding region is due to the presence of a functional RNA element (142).

The structural proteins, core (C), E1, and E2, form the physical virion. The viral nucleocapsid, composed of C protein and genomic RNA, is encapsidated in a lipid envelope studded with non-covalently linked heterodimers of the E1 and E2 glycoproteins (156). Both E1 and E2 are type

I integral membrane proteins and have been shown to accumulate in the ER where particles are thought to assemble (156). The E2 glycoprotein likely mediates receptor binding of HCV to the host cell, given its ability to bind multiple putative HCV receptors (38, 82, 162, 166, 176). The role of E1 is less clearly defined, although it has been proposed to contain the putative fusion peptide (58). Analogous to the BVDV p7 protein, HCV p7 protein is essential for viral infectivity and can form ion channels (73, 160, 167, 174). Downstream from p7, NS2 encodes a C-terminal autoprotease, which cleaves at the junction between NS2/3 and requires the N-terminal domain of NS3 to function (70, 83, 132). The remainder of the polyprotein encodes NS3-NS4A-NS4B-NS5A-NS5B that form the viral replication complex and are capable of autonomous HCV RNA replication (131). The catalytic activities of NS3, encoding protease, helicase, and RNA-stimulated NTPase activities, and NS5B, encoding the RdRp, explained above for BVDV are maintained in HCV. The NS4B protein is necessary and sufficient for membranous web formation, which has been observed in cells harboring HCV replication complexes (50, 69).

Evolution of model systems for HCV research

HCV research in the laboratory has been hampered by the absence of a small animal model and cell culture systems capable of supporting the complete viral life cycle (reviewed in 8, 126). The identification of the first full-length, infectious clone, H77, a genotype 1a isolate, which is infectious in chimpanzees, was a significant advance in the early study of HCV (105, 216). Soon after, additional HCV genomes derived from various genotypes were also constructed (reviewed in 8, 10). Although infectious *in vivo*, all of these HCV genomes exhibited little to no replication in cell culture. This obstacle was overcome when it was reported that transfection of a subgenomic replicon, expressing the HCV NS3-NS5B coding region and a dominant selectable marker, *neomycin phosphotransferase* (*neo*), in the place of the viral structural proteins, allowed the selection of rare, successful HCV RNA replication events (131). It was later determined that the ability to replicate efficiently in cultured cells is due to the presence of adaptive mutations acquired in the viral genome (reviewed in 8, 10). The use of highly permissive cells, such as the Huh-7.5 human hepatoma cell line, allowed even more efficient RNA replication in culture (9). Building on these advances, full-length replicons were generated that replicated to high levels in cell culture. However, cells harboring these genome-length

replicons produced little to no infectious virus (23, 88, 165). Nevertheless, studies using HCV full-length and subgenomic replicons have established much of our current understanding of HCV translation and replication events, identified essential HCV-host factor interactions, and provided a system to screen possible antiviral agents. In the absence of an authentic infectious system, examination of HCV entry was based on retroviral pseudoparticles bearing HCV E1 and E2 glycoproteins (HCVpp) (13, 47, 85), which provided the first insights into putative cellular receptors, as well as the pathway of virus entry (see below).

A breakthrough in the study of HCV was the development of an HCV infectious cell culture system (HCVcc) based on the HCV genotype 2a JFH-1 isolate from a patient in Japan suffering from fulminant hepatitis (101). JFH-1 is distinct from previously described genomes in its efficient replication in cell culture independent of adaptive mutations (100). Moreover, the full-length JFH-1 genome and a chimeric genome expressing the JFH-1 replicase in the context of the genotype 2a J6 isolate structural proteins (J6/JFH) are capable of producing viral particles in cell culture (123, 203, 221). These particles, termed HCV cell culture derived virus (HCVcc), are infectious both *in vitro* (123, 203, 221) and *in vivo* (123, 203). Recently, additional chimeric genomes capable of virus production,

harboring the genotype 1a, H77 isolate or the genotype 1b, Con1 isolate, have been generated (164). The HCVcc infectious system therefore enables study of the complete viral life cycle, including entry and assembly events, in the context of cell culture.

HCV entry and cellular entry factors

HCV entry is a multi-step process requiring specific interactions between the E1 and E2 glycoproteins and a number of cellular receptors/coreceptors. HCV enters cells by clathrin-mediated endocytosis (21). Productive infection requires a low pH compartment (13, 47, 85, 123, 203, 221) and depends on the presence of cholesterol in the target cell membrane (97). Using the HCVpp and HCVcc systems, several cellular factors have been implicated in HCV entry, including CD81, SR-BI, CLDN1, and highly sulfated glycosoaminoglycans (GAGs) (Fig. 1.4). Although the list of candidate receptors is extensive, certain cell lines remain nonpermissive for HCV entry despite expression of all of these molecules, suggesting that they act in conjunction with an additional, as yet unidentified entry factor(s). It is also possible, however, that these cell lines are resistant to HCV entry due to a host restriction factor that acts downstream from the receptor level.

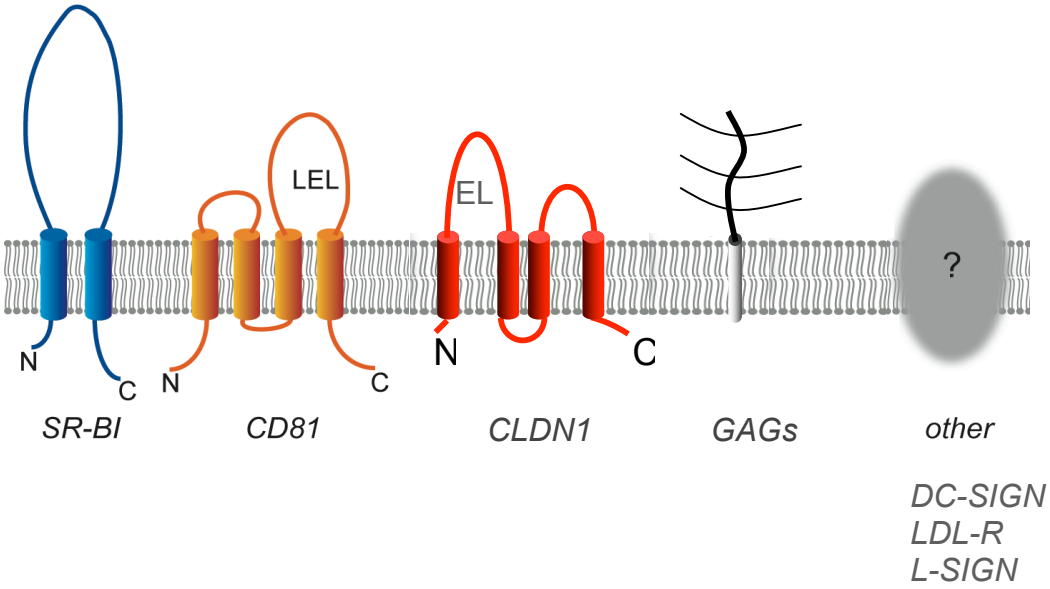

Fig. 1.4 Cellular factors for HCV entry. HCV cell entry is thought to require interaction of the HCV glycoproteins E1 and E2 with cellular entry factors that likely include CD81, scavenger receptor class B type I (SR-BI), claudin-1 (CLDN1), glycosoaminoglycans (GAGs), and other as yet unidentified molecules.

The tetraspanin CD81, first demonstrated to be an E2 binding protein, has now been clearly established as an essential HCV entry factor (15, 41, 166, 220). CD81 has short N- and C-terminal cytoplasmic tails, four transmembrane domains, and small and large extracellular loops (120, 121). The CD81 large extracellular loop (LEL) confers interaction with E2 (57, 166) and is a critical determinant of HCV entry (59, 220). CD81 LEL also contains two disulfide bonds important for the interaction with E2 (82, 102, 162). HCVcc and HCVpp entry is inhibited by anti-CD81 antibodies (13, 85, 123, 203, 221), RNAi targeting of CD81 (220), and protein fragments of CD81 (59, 123). In addition, the CD81-deficient, human hepatoma cell line HepG2 is HCV resistant, but becomes competent for HCV entry upon transduction with CD81 (15, 123, 220). CD81 is expressed on most cell types except platelets and red blood cells and is therefore unlikely to determine HCV's liver tropism. Consistent with this idea, recent studies suggest that the role of CD81 in HCV entry is downstream from primary attachment (41, 53, 106).

SR-BI also binds HCV E2 and is expressed highly on hepatocytes, where it mediates the selective uptake of cholesterol and cholesterol esters from high-density lipoprotein (HDL) particles (176). Although to a lesser extent than for CD81, HCV infection is inhibited by SR-BI antibodies and

RNAi targeting (15, 117). As further evidence supporting a role for SR-BI in productive HCV entry, the presence of HDL enhances HCVpp infectivity in an SR-BI dependent manner (14, 144, 155, 200) and infection is inhibited by the SR-BI ligand, oxidized LDL (201). It is also possible that SR-BII, a splice variant differing from SR-BI only in its C-terminal tail (205), may also have a role in HCV entry.

CLDN1, an integral membrane protein and component of the tight junction, was recently identified as a required HCV entry factor by expression cloning of cDNAs derived from the highly permissive Huh-7.5 cell line (53). 293T cells express CD81, as well as SR-BI, and become fully permissive for HCVpp and HCVcc infection upon CLDN1 transduction. CLDN1 is highly expressed in the liver and has four transmembrane domains and two extracellular loops (reviewed in 199). HCV entry requires residues within extracellular loop 1 and is unaffected by disruption of intracellular protein-protein interaction motifs in the CLDN1 C-terminal tail. HCVpp infection of 293T cells expressing CLDN1 remains CD81-dependent, further supporting the model that no one factor is sufficient for HCV entry.

The presence of highly sulfated glycosoaminoglycans (GAGs), such as heparin, on the target cell membrane has also been shown to contribute to

HCV entry (11, 106). HCV infection is inhibited in the presence of increasing amounts of soluble heparin, as well as by treatment of cells with heparinase I or III prior to infection (106). Although not certain, GAGs are thought to increase the efficiency of HCV entry possibly by facilitating primary attachment to the target cell.

Other candidate receptors include the dendritic cell- and liver-specific intracellular adhesion molecule 3-grabbing nonintegrins (DC-SIGN and L-SIGN) and LDL-R. DC- and L-SIGN do not appear to mediate productive HCV infection, but can bind HCVpp and transmit the virus to permissive cells in co-culture (40, 133). A similar mechanism may occur *in vivo*, where DC- and L-SIGN could pick up viral particles and transfer them onto hepatocytes, although this hypothesis has yet to be validated. LDL-R can bind plasma derived-HCV and appears to allow cellular uptake of HCV RNA (3, 150, 214). It is unclear, however, whether LDL-R can mediate productive HCV uptake, given that HCVpp do not require LDL-R in the target cell membrane (13, 85).

1.4 Objectives

During my graduate studies I have explored two complementary subjects – the pathways of BVDV and HCV entry and the phenomenon of superinfection exclusion. My initial objective was to establish a screen for BVDV genome fragments that could act as transdominant inhibitors of BVDV replication. This work led to the identification of the E2 glycoprotein as a BVDV inhibitor and further study demonstrated that E2 expression acted to prevent BVDV entry into MDBK cells. We connected these observations with previous studies of BVDV superinfection exclusion and hypothesized that the E2 protein was mediating a superinfection block at the level of BVDV entry. I also sought to determine if superinfection exclusion was established in HCV-infected and replicon-containing cells. Like BVDV, HCV superinfection was inhibited, but the main mechanism of exclusion was downstream from virus entry. With the advent of the HCV infectious system, I attempted to further define the HCV entry pathway using cell-culture derived virus. I also pursued similar studies with BVDV, finding that both HCV and BVDV require an activation step to trigger pH-dependent entry. My hope is that this body of work will provide insights into the basic virology of HCV and BVDV and the control and effective treatment of these two medically and financially important pathogens.

Chapter 2. Materials and methods

Cells

Huh-7.5 (24) and 293T cells were maintained in Dulbecco's modified Eagle's medium (DMEM) supplemented with 10% heat-inactivated fetal bovine serum (FBS) and 100 nM nonessential amino acids. Gamma-irradiated FBS was used for 293T cells when packaging the BVDV cDNA library. Huh-7.5 cells harboring HCV replicons were maintained DMEM with 10% FBS, 100 nM nonessential amino acids, and 0.5 mg/ml G418. Vero cells were grown in DMEM with 10% FBS. MDBK cells were maintained in DMEM with 10% heat-inactivated horse serum. CHO cells were maintained in DMEM/F-12 with 10% FBS. BHK-J cells were maintained in minimal essential medium (MEM) with 7.5% FBS. Media and reagents for cell culture were purchased from Gibco-BRL, Life Technologies Ltd.

Chemicals

Bafilomycin A1 (stock solution is 50 μM in DMSO), concanamycin A (stock solution is 25 μM in ethanol), and CA-074 (stock solution is 10 mM in DMSO) were purchased from Sigma (St. Louis). FYdmk (*Z*-Phe-Tyr-(*t*Bu)-diazomethylketone) (stock solution is 10mM in DMSO) was purchased from Calbiochem (San Diego). BILN 2061 (114) and 2'-C-

methyladenosine (31) were resuspended at a concentration of 10 mM in DMSO.

BVDV RNA transcription, transfection, and virus stocks

For *in vitro* transcription, pBAC/NADL, pACNR/NADLJiv90$^-$, and pACNR/NADLJiv90$^-$/5'ubi-luc plasmids were linearized by digestion with *Sbf*I (Promega) and blunt-ended using a combination of T4 DNA polymerase and Klenow. After phenol extraction and precipitation with ethanol, 1-2 μg of template was transcribed using the T7 Megascript kit (Ambion), according to the manufacturers instructions. RNA was purified using an RNeasy Mini column (Qiagen) or by precipitation with 1/2 vol of 7.5 M NH_4Ac and analyzed by 1% agarose gel electrophoresis.

To generate stocks of BVDV strains NADL, NADLJiv90$^-$, and NADLJiv90$^-$*luc*, MDBK cells were trypsinized, harvested by centrifugation (500 x *g*, 5 min), washed twice and resuspended in ice-cold phosphate buffered saline (PBS) (Accugene) at 2.0 x 10^7 cells/ml. 5-10 μg of NADL, NADLJiv90$^-$, or NADLJiv90$^-$*luc* RNA was mixed with 0.4 ml of cells in a 0.2-cm gap cuvette and immediately pulsed using a BTX ElectroSquarePorator (900 V, 5 pulses, 99 μs/pulse) (143). Electroporated cells were allowed to recover for 10 min at room temperature prior to the

addition of complete media and then plated in a 100-mm diameter cell culture dish. Supernatants were harvested after 24-48 h. Virus stocks were aliquoted and stored at –80 ºC until use.

HCV replicons and cells harboring HCV replicons

pSGR-JFH1 has been described (100) and cells harboring this replicon (see below) will be referred to as JFH-SGneo cells. Con1-FLneo (I) and Con1-SGneo (I) are full-length and subgenomic genotype 1b (Con1 isolate) constructs, respectively, containing an S2204I mutation in NS5A that have been described (22, 24), and will be referred to here as Con1-FLneo and Con1-SGneo. H-FLneo and H-SGneo, are HCV genotype 1a (H77 isolate) full-length and subgenomic replicons, respectively, that contain the adaptive mutations P1496L, V1880A, A1940V, C1968R allowing for persistent replication of the H77 genome in Huh-7.5 cells. These adaptive mutations were identified after transfection of Huh-7.5 cells with H-SGneo (L) (23) and selection with G418 and subsequently reengineered into the H-SGneo (L) or H-FLneo (L) backbone (J. Fan and C. M. Rice, unpublished data).

J6/JFH-FLneo, JFH-SGneo, Con1-FLneo, Con1-SGneo, H-FLneo, and H-SGneo replicon cell populations were generated by electroporation of

Huh-7.5 cells with 1 μg of the corresponding *in vitro* transcribed RNA [see below and (123)]. Replicon-containing cells were selected and maintained with 0.5 mg/ml G418.

HCV RNA transcription, transfection, and virus stocks

For *in vitro* transcription, pFL-J6/JFH, pFL-J6/JFH-5'C19Rluc2AUbi, pJ6/JFH-FLneo, and pSGR-JFH1 plasmids were linearized by digestion with *Xba*I. pCon1-FLneo and pCon1-SGneo were linearized with *Sca*I and pH-FLneo and pH-SGneo plasmids were linearized with *Hpa*I. 1-2 μg of linearized template DNA was transcribed using the T7 Megascript kit (Ambion) according to the manufacturer's instructions, followed by purification using the RNeasy Mini Kit (Qiagen) with on column DNase treatment. The quality of the RNA was assessed using 1% agarose gel electrophoresis.

To generate stocks of J6/JFH and FL-J6/JFH-5'C19Rluc2AUbi (HCVcc-Rluc), Huh-7.5 cells were trypsinized, harvested by centrifugation (500 x *g*, 5 min), washed twice and resuspended in ice-cold PBS (Accugene) at 1.5 x 10^7 cells/ml. 1-2 μg of J6/JFH or FL-J6/JFH-5'C19Rluc2AUbi RNA was mixed with 0.4 ml of cells in a 0.2-cm gap cuvette and immediately pulsed using a BTX ElectroSquarePorator (820 V, 5 pulses, 99 μs/pulse)

(123). Electroporated cells were allowed to recover for 10 min at room temperature prior to the addition of complete media and plated in a 150-mm diameter cell culture dish. After 72 h, electroporated cells were trypsinized and replated in complete media. Virus containing supernatant from replated cells was then harvested after an additional 3-4 d post electroporation. Virus stocks were aliquoted and stored at –80 ºC until use.

For HCVcc-Rluc infections, cells were incubated with undiluted virus [multiplicity of infection (MOI) ~0.01, 200 μl/well for 24-well plate] for 1-3 h at 37 ºC or 2 h at 4 ºC where indicated. Cells were washed twice with media, incubated for the indicated time (usually 24 h) at 37 ºC, and harvested for luciferase assays. All infections of G418-resistant cell populations were performed in the absence of G418. For infections including 2'-C-methyladenosine, drug (1.35 μM) was added to the media at the time of infection and maintained during the 24 h incubation. At each time point, cells (untreated or treated with inhibitor) were harvested from triplicate wells for luciferase assays, and cells from duplicate wells were analyzed for HCV RNA levels.

Generation of HCVpp stocks and HCVpp infection

HCV pseudoparticles expressing firefly luciferase (HCVpp-Luc), and VSVGpp-Luc and no envelope control viruses were generated in 293T cells as described (85) by co-transfection of an envelope-deficient HIV genome (pNL4-3.Luc.R^-.E^-) and a plasmid expressing HCV H77 (56) or J6 (141) viral glycoproteins E1 and E2, vesicular stomatitis virus G protein (VSV G), or an empty vector (no envelope). For infection, Huh-7.5 cells, seeded in a 96-well plate (1 x 10^4/well), were incubated with HCVpp, VSVGpp, or no envelope pp in the presence of polybrene (4 μg/ml) for 6-12 h at 37 ºC. Luciferase activity was determined at 72 h postinfection (h.p.i.). HCVpp RLU values were normalized to VSVGpp values for each sample. Infections of G418-resistant cell populations were performed in the absence of G418. To generate HCVpp expressing a GFP reporter (HCVpp-GFP) and control VSVGpp-GFP, 293T cells were co-transfected as above with the CSGW HIV provirus encoding only GFP (44), a plasmid expressing the HIV gag-pol genes, and either an HCV H77 E1 and E2 or the VSV G-protein expression plasmid. Infections were performed as above and cells were harvested for flow cytometry at 48 h.p.i. (see below).

Vesicular stomatitis virus, Sindbis virus, and herpes simplex virus-1 stocks

Vesicular stomatitis virus (VSV), San Juan strain, stocks were generated by infection (MOI 0.01) of BHK-J cells (125), and collection of cell supernatants at approximately 17 h.p.i. For plaque assays, cells were seeded in 6-well plates and infected in duplicate with dilutions of virus. Cells were overlaid with 0.6% SeaKem LE agarose (Cambrex) in MEM containing 2.5% FBS, and incubated for 16 h when they were fixed with 7% formaldehyde and stained with crystal violet (1.25% crystal violet in 20% ethanol). Plaques were enumerated and titers were expressed as plaque forming units/ml (pfu/ml).

Stocks of Toto1101/Luc (20), a Sindbis virus (SIN) expressing firefly luciferase, were generated by electroporation of *in vitro* transcribed RNA into BHK-J cells. For *in vitro* transcription, pToto1101/Luc was linearized with *Xho*I and transcribed using the SP6 Megascript Kit (Ambion) in the presence of cap analog.

Stocks of KOS*dluxori*L (188), herpes simplex virus-1 (HSV-1) expressing firefly luciferase, were generated by infection of Vero cells at an MOI of 0.01. After infected cells had detached from the plate (~48-72 h.p.i.), culture media (containing detached cells) was harvested and clarified by centrifugation (5 k rpm, 15 min). The supernatant was transferred to a

new bottle and centrifuged at 9 k rpm for 1 h (*A*). The pellet from the first centrifugation was resuspended in medium, freeze-thawed 1x, and sonicated 2x (30 s/cycle) (*B*). *B* was then used to resuspend the pellet from *A*. The solution was sonicated (45 s) and centrifuged at 1.5 k rpm for 10 min. The supernatant was aliquoted and stored at –80 ºC until use.

BVDV plaque and focus forming assays

MDBK cells, seeded in 6-well dishes, were infected with 10-fold dilutions of virus for 1 h at 37 ºC. The cells were overlaid with 1% SeaKem LE agarose in MEM containing 5% horse serum and penicillin/streptomycin and incubated at 37 ºC for 3 d. Monolayers were fixed with 7% formaldehyde and the agarose overlays were removed. For plaque assays, the monolayer was stained with crystal violet as previously described (143). For focus-forming assays, the monolayer was permeabilized with 0.25% Triton X-100 in PBS and stained with anti-BVDV polyclonal antibody B224 (diluted 1:500 in PBS/0.25% Triton X-100) (kindly provided by Kenny Brock, Auburn University) and peroxidase-conjugated anti-bovine IgG (diluted 1:1000 in PBS/0.25% Triton X-100) (Sigma) (168). BVDV positive foci were visualized using the DAB peroxidase substrate (Vector Laboratories).

Construction of random BVDV cDNA library

The random BVDV cDNA library was generated by Matthew Evans (Rockefeller University). To prepare BVDV random cDNA fragments, 10-20 μg of pBAC/NADL in 1 ml TM buffer (50 mM Tris pH 8, 15 mM $MgCl_2$) was nebulized in a chamber (Invitrogen) by application of 40 psi N_2 gas for 3 min. The fragments were cleaned using a QIAquick PCR purification kit (Qiagen) and eluted in 50 μl TM buffer. To create blunt ends, the fragments were incubated with 9 U T4 DNA polymerase and 10 U Klenow in the presence of dNTPs for 15 min at room temperature. The enzymes were heat inactivated at 75 ºC for 10 min. The fragments were then phosphorylated using 10 U T4 polynucleotide kinase for 10 min at 37 ºC. The fragments were run on a 0.7% agarose gel and size fractionated into two groups containing 100-500 bp or 500-2000 bp fragments. Each group of fragments was gel purification using the Qiaquick gel purification kit (Qiagen).

pBabeHAZSrfcI is an Moloney murine leukemia virus (MLV) expression vector which is derived from pBabeHAZ (63) and modified to contain a unique *Srf*I restriction site for cloning blunt-ended inserts. Inserts are expressed from a simian virus 40 (SV40) promoter, as fusion proteins with an influenza hemagglutinin (HA) epitope tag (YPYDVPDYA) at the N

terminus and a zeocin resistance protein (Zeo) at the C terminus. In this vector, Zeo is out of frame with the start site of the HA tag and is not expressed unless there is a stop codon-free insert in the cloning site.

To prepare the vector for insertion of the BVDV fragments, 1 μg pBabeHAZSrfcI was digested to completion with *Srf*I and gel purified to remove any contaminating uncut vector. Linearized vector was eluted in 100 μl shrimp alkaline phosphatase (SAP) buffer and phosphatased by two rounds of treatment with 10 U SAP. For library construction, 20 ng *Srf*I-digested pBabeHAZSrfcI vector was ligated with 60 ng BVDV cDNA fragments in a total volume of 30 μl. Ligation products were purified using the Qiaquick PCR purification kit and eluted in 10 μl H_2O. 5 μl of the purified ligation was added to 60 μl DH10B ElectroMAX cells (Gibco BRL) and divided equally into two cuvettes. Cells were electroporated using a BioRad Gene Pulser 2 and plated on Luria Bertani (LB) agar plates supplemented with 100 μg/ml ampicillin (Amp). Colonies were scraped into LB broth containing Amp and grown for 5 h at 37 ºC. Plasmid DNA was isolated using a Qiagen Plasmid Maxi Kit (Qiagen).

Packaging and screening of the random BVDV library

For packaging of the BVDV library, 293T cells, grown in gamma-irradiated serum to eliminate contaminating BVDV, were seeded in 100-mm plates (2 x 10^6 cells/plate) and incubated overnight. 1.5 μg of BVDV library in pBabeHAZSrfcI was mixed with 1 μg MLV-gagpol and 1 μg VSV G envelope expression plasmids (63) in a total of 15 μl TE (10 mM Tris, 1 mM EDTA). The mixture was added to a tube containing 18 μl Fugene-6 (Roche) in 200 μl OptiMEM (Gibco). Complexes were allowed to form for 15 min at room temperature and then added to 293T cells in fresh medium. At 48 h post transfection, supernatants were harvested and filtered through a 0.45-μm syringe filter. For transduction, media from MDBK cells, seeded in a 6-well plate ($5x10^5$/well), was replaced with the retrovirus containing supernatant, and the cells were spun in a centrifuge (1150 x *g*) for 30 min at room temperature. The plates were transferred to a 37 ºC incubator for an additional 1.5 h, after which the inoculum was removed and culture media was added. At 48 h post transduction, selective media containing 400 μg/ml zeocin was added to each well. Cells were maintained in selective media for the duration of the experiments. A control cell population was also created by transduction with pBabeHAZ vector (63), where HA and Zeo are in frame, followed by zeocin selection. Zeo resistant cells expressing the

BVDV library or the empty vector, pBabeHAZ, were expanded and infected with BVDV NADL at an MOI of 5. Colonies that developed after infection were expanded and reinfected with NADL. Colonies that survived secondary infection were further analyzed.

Analysis of resistant MDBK clones

The genomic DNA from $2.5x10^6$ cells of each resistant clone was harvested using the DNeasy Tissue Kit (Qiagen), based on the manufacturer's protocol, and eluted in 200 μl elution buffer. 10 μl of the isolated genomic DNA was mixed with the primers 5'-gcttatccatatgatgtt ccagatt-3' and 5'-gcaccggaacggcactggtcaactt-3'. The viral insert was amplified with the Expand High Fidelity PCR system (Roche) using 10 cycles of 94 ºC for 15 s, 60 ºC for 30 s, 72 ºC for 1.5 min and 20 cycles of 94 ºC for 15 s, 60 ºC for 30 s, and 72 ºC for 1 min (adding 5 s/cycle). PCR products were gel purified and sequenced. To test if the library inserts could provide resistance to naïve cells, the PCR products were cloned into pBabeHAZSrfcI using *Eco*RI and *Not*I restriction sites. The pBabeHAZSrfcI clones were packaged and used to transduce MDBK cells as above.

*Construction of pLenti6-EGFP, pLenti6-E1*E2p7*, pLenti6-Sig-E2, and pLenti6-Sig-E2**

pLenti6-EGFP is a derivative of pLenti6/GW-V5/LacZ (Invitrogen). The EGFP sequence was amplified from pEGFP (Invitrogen) using the EGFP-specific primers, 5'-cgggatccaccaccatggggcgcgccggcggaagcggcgg aagcatggtgagcaagggcgaggagctgttcac-3' and 5'-ggctcgagttacttgtacagctcgtc catgccgagagtgatc-3', which added *Bam*HI and *Xho*I restriction sites, to the 5' and 3' ends of the EGFP sequence, respectively. The *Bam*HI-EGFP-*Xho*I cassette was cloned into pLenti6/GW-V5/LacZ, which had been digested with *Bam*HI and *Xho*I. To generate pLenti6-E1*E2p7*, nucleotides 2312-3598 from the BVDV NADL genome were PCR amplified. The forward primer added a *Bam*HI restriction site, a *Kozack* consensus sequence, and an ATG nucleotide sequence (5'-ggggatccgccaccatggtgaagttagtgttgagggcac-3'). The reverse primer added a stop codon followed by a *Xho*I restriction site (5'-ggggctcgagttatgatccatactgaatccctaa-3'). The *Bam*HI- E1*E2p7*-*Xho*I cassette was inserted into the pLenti6 backbone that had been digested with *Bam*HI and *Xho*I. To generate pLenti6-Sig-E2, the full-length E2 sequence (nucleotides 2462-3583) was amplified using the forward primer 5'-cgggatc cgccaccatgaagactatcattgctttgagctacattttctgtctggttctcg-3' that added a *Bam*HI restriction site, a *Kozack* consensus sequence and ATG, followed by the HA signal sequence (MKTIIALSYIFCLVLG), and a short linker region

containing unique *Nhe*I and *Asc*I restriction sites. The reverse primer, 5'-ctcgagttaccctaaggcctt-3', added a stop codon and *Xho*I restriction site. The *Bam*HI-Sig-E2-*Xho*I cassette was inserted into the pLenti6 backbone that had been digested with *Bam*HI and *Xho*I. For pLenti6-Sig-E2*, nucleotides 3148-3490 were PCR amplified using 5'-gaacgagactggttacaggcta-3' and 5'-ggctcgagttaggact cagcgaagtaatcccg-3'. The reverse primer added a stop codon and *Xho*I restriction site. The PCR product was digested with *Bsr*GI and *Xho*I and cloned into pLenti6-Sig-E2 that had been digested with *Bsr*GI and *Xho*I.

For packaging, 1.5 μg lentiviral vector was packaged by cotransfection of 293T cells with 1 μg HIV-gagpol and 1 μg VSV G expression constructs (Invitrogen) using Fugene-6. MDBK cells were transduced as described above for the BVDV library. Transduced MDBK cells were selected with blasticidin (4 μg/ml) for 3 d, and infected with NADLJiv90^{-}*luc*.

BVDV Binding Assay

MDBK-E1*E2p7* and pBabe cells, seeded in 12-well plates (2.5 x 10^5/well), were cooled on ice for 5 min and triplicate wells were infected with BVDV NADLJiv90^{-} (MOI 10) for 1 h at 4 °C. Cell monolayers were washed 7x with cold culture media, freeze-thawed 3x, and mixed with 450

μl TRIzol to extract RNA for real-time quantitative RT-PCR (qRT-PCR). BVDV RNA levels were quantified by qRT-PCR (see below) and the average amount of BVDV bound to MDBK-pBabe cells over three independent experiments was set at 100%.

For antibody blocking experiments, cells were preincubated with hybridoma supernatant from a mixture of monoclonal antibodies (MAb) (BVD/CA 17, 26, and 27, kindly provided by Till Rümenapf, Justus-Liebig University) for 2 h at 37 ºC. Cells were chilled on ice and infected in the presence of antibody with BVDV NADLJiv90^{-} at 4 ºC as above. After infection, monolayers were washed and RNA extracted using the RNeasy Mini Kit (Qiagen). BVDV RNA was quantified using qRT-PCR (see below).

Immunoblotting

To detect the BVDV E2 protein in MDBK cells, cells were lysed in SDS lysis buffer (0.5% SDS, 50 mM Tris-Cl, pH 7.5, 1mM EDTA). Proteins were separated by 8% SDS-PAGE, transferred to a nitrocellulose membrane, and detected using α-E2 MAb 214 (Veterinary Laboratories Agency, Weybridge, United Kingdom) and a horseradish peroxidase (HRP)-conjugated α-mouse secondary antibody (Sigma). Detection was performed

with the SuperSignal West Femto Maximum Sensitivity Substrate (Pierce), according to the manufacturer's instructions.

To detect CD46 protein in MDBK cells, cells were lysed as above in SDS lysis buffer. Proteins were separated by 10% SDS-PAGE, transferred to a nitrocellulose membrane, and detected using CD46 polyclonal antiserum (diluted 1:200 in Tris buffered saline with 10% horse serum, kindly provided by Till Rümenapf, Justus-Liebig University) and horseradish peroxidase (HRP)-conjugated α-rabbit secondary antibody (Sigma). Detection was performed with the SuperSignal West Pico chemiluminescent substrate (Pierce).

To detect CD81 from Huh-7.5 cell lysates, cells were lysed in SDS loading buffer (2% SDS, 100 mM Tris-Cl pH 6.8, 20% glycerol). Proteins were separated by 12% SDS-PAGE under nonreducing conditions, transferred to a nitrocellulose membrane, and detected using α-CD81 MAb JS-81 (BD Pharmingen), followed by HRP-conjugated α-mouse secondary antibody (Pierce). β-actin was detected with MAb AC-15 (Sigma) and an α-mouse secondary as above. Detection was performed with the SuperSignal West Pico chemiluminescent substrate (Pierce).

Immunostaining and flow cytometry

For live cell surface staining of CD46, cells were detached with PBS-0.5 mM EDTA and resuspended in 5% goat serum, 0.1% sodium azide in DPBS. Cells were incubated with primary antibody, α-CD46 (kindly provided by Till Rümenapf, Justus-Liebig University) diluted in 0.5% BSA, 0.1% sodium azide (SB), washed with SB, then incubated with Alexa Fluor 488 or 633 goat α-mouse IgG secondary antibody (Molecular Probes, Eugene, OR). Cells were washed with SB, fixed with 2% paraformaldehyde, and analyzed by flow cytometry on a FACSCalibur (Becton Dickinson), counting 10^4 cells.

For live cell surface staining of CD81, cells were detached by a brief treatment with trypsin and resuspended in 3% FBS-0.05% sodium azide in PBS (WB1). Cells were incubated with α-CD81 1.3.3.22 (Santa Cruz Biotechnology, Santa Cruz, CA) or purified mouse IgG_1 (BD Pharmingen, Franklin Lakes, NJ) primary antibodies, washed with WB1, then incubated with Alexa Fluor 488 goat α-mouse IgG secondary antibody (Molecular Probes, Carlsbad, CA). Alternatively, cells were incubated with phycoerythrin-conjugated CD81 antibody (MAb JS-81, BD Pharmingen). Cells were washed with WB1, fixed in 0.5% paraformaldehyde, and analyzed by flow cytometry as above. For total cell staining, cells were

detached, fixed in 0.5% paraformaldehyde, and permeabilized with 0.5% FBS-0.1% saponin in PBS (WB2). Fixed cells were then incubated with CD81 or isotype control primary antibody, followed by Alexa Fluor 488 goat α-mouse IgG secondary antibody, and analyzed by flow cytometry.

For CD81/NS5A co-staining, live cells were detached and stained with phycoerythrin-conjugated CD81 antibody (MAb JS-81, BD Pharmingen) as described above, fixed with 0.5% paraformaldehyde, permeabilized with WB2, and stained for NS5A, using α-NS5A primary antibody (MAb 9E10) (123), followed by Alexa Fluor 647 goat α-mouse IgG_{2a} specific secondary antibody (Invitrogen). Cells were then analyzed by flow cytometry.

Luciferase assays

For *Renilla* (HCVcc-Rluc) and firefly luciferase assays (BVDV NADLJiv90-*luc*, KOS*dluxori*L, Toto1101/Luc, HCVpp-Luc, VSVGpp-Luc), cells were washed 1x with DPBS and lysed with *Renilla* or Cell Culture lysis buffer (Promega), respectively (100 µl/well for 24-well plate, 50 µl/well for 96-well plate). Lysates were harvested by scraping and mixed with 50-100 µl Luciferase Assay Substrate (Promega), as suggested by the manufacturer. Luciferase activity was measured using a Lumat LB9507 or a

Centro LB960 luminometer (Berthold Technologies, Bad Wildbad, Germany).

For HCVcc-Rluc infections in the HCV superinfection exclusion study, relative luciferase units (RLU) values were normalized for the number of viable cells in each sample by quantifying total cellular ATP levels using the CellTiter-Glo Luminescent Cell Viability Assay (Promega) according to the manufacturer's instructions. The normalization step was performed to control for differences in cell size or viability that might exist among the various cell populations used in the HCV superinfection exclusion study.

Real-time quantitative reverse transcription PCR (qRT-PCR)

For BVDV qRT-PCR, total RNA was extracted from cells using either TRIzol reagent (Invitrogen) or the RNeasy Mini Kit (Qiagen). RNA was mixed with primers and probe specific for the BVDV 5'NTR as well as for bovine β-actin to normalize total RNA levels. BVDV-specific RNA and bovine β-actin RNA were amplified using the Platinum Quantitative RT-PCR ThermoScript One-Step System (Invitrogen) and detected using the ABI Prism 7700 sequence detection system (PE Applied Biosystems, Foster City, Calif.). BVDV and bovine β-actin cDNAs were generated by reverse transcription at 60 ºC for 30 min, followed by inactivation of the RT at 95 ºC

for 10 min. cDNAs were then amplified with 40 cycles of 95 ºC for 15 s and 60 ºC for 1 min. The BVDV forward and reverse primers are 5'-ggt gactgcaggtcgggtag-3' and 5'-ggtaaaatagtggccctggctt-3', respectively. The probe sequence is 5'-6FAM-cagaggacctgtgagcgggatctacct-TAMRA-3' (Eli Lilly and Co.). The forward and reverse primers for bovine β-actin are 5'-atgtggatcagcaagcaggagta-3' and 5'-aagcatttgcggtggacaa-3' respectively. The probe sequence is 5'-VIC-cgagtctggcccctc-MGBNFQ-3' (Applied Biosystems). BVDV RNA levels were normalized to levels of bovine β-actin RNA.

To amplify CD81 RNA, total RNA was harvested using the RNeasy Mini Kit (Qiagen). 50-150 ng of total cellular RNA was mixed with primers and probe specific for CD81 or glyceraldehyde-3-phosphate dehydrogenase (GAPDH) RNA. The CD81-specific primers and FAM-labeled probe were purchased from Applied Biosystems using a TaqMan inventoried gene expression assay for CD81 (Assay ID: Hs00174717_m1). GAPDH-specific primers and VIC-labeled probe were purchased from Applied Biosystems (Catalog # 4326317E). RNAs were amplified using the Platinum Quantitative reverse-transcription PCR ThermoScript One-Step System (Invitrogen) and detected with the ABI Prism 7700 sequence detection system (PE Applied Biosystems, Foster City, Calif.). cDNAs were generated

by reverse transcription at 50 ºC for 30 min, followed by inactivation of the reverse transcriptase at 95 ºC for 5 min. cDNAs were amplified with 40 cycles of 95 ºC for 15 s and 60 ºC for 1 min. CD81 RNA levels were normalized to levels of GAPDH RNA.

HCV RNA was amplified from 50 ng of total RNA using the 3'NTR MultiCode RT-qPCR System (EraGen) and detected as above with the ABI Prism 7700. cDNA was generated by reverse transcription at 45-60 ºC, for 15 min, 1 min per degree, and amplified with 40 cycles of 95 ºC for 20 s, 60 ºC for 30 s, and 72 ºC for 30 s. The sequence of the forward primer, labeled with 5' 6FAM-isoC (2'-deoxy-5-methyl-isocytidine), was 5'-ggctccatcttagccctagtc-3' and the sequence of the reverse primer was 5'-agtatcggcactctctctgcagt-3' (Biosearch Technologies, Inc.).

Bafilomycin A1, concanamycin A, and NH_4Cl inhibitor experiments

Huh-7.5 cells were seeded in a 24-well plate (5 x 10^4/well). Cells were pretreated with drug (bafilomycin A1, concanamycin A, or NH_4Cl) diluted in medium for 1 h at 37 ºC. The cells were then chilled on ice for 5 min and infected with HCV (FL-J6/JFH-5'C19Rluc2AUbi), SIN (Toto1101/Luc), or HSV-1 (KOS*dluxoriL*) for 2 h at 4 ºC. Once added to a particular well, the drug was present for the duration of the experiment. After binding, the cells

were washed twice with cold DPBS and then warm media with or without drug was added. For postinfection drug addition, the drug was added directly to the media in the well. SIN and HSV-1 samples were harvested at 12 h.p.i. HCV samples were harvested at 24 h.p.i.

Low pH treatment

HCV or SIN stocks, in media containing 20 mM HEPES, (4-1-piperazine ethanesulfonic acid) were diluted 1:5 in a citric acid buffer at pH 4.1 or 7.0 (15 mM citric acid, 150 mM NaCl). The final pHs of the solutions were pH 5.0 or 7.0 ± 0.1. For experiments with reducing agent, 10 mM dithiothreitol (DTT) was included in the citric acid buffer. The buffers containing the diluted virus were incubated in a 37 ºC water bath for 10 min. After incubation, to neutralize the pH, a tenth volume of DMEM containing 150 mM HEPES was added. Each sample was then diluted 1:10 in medium containing 20 mM HEPES. Huh-7.5 cells, seeded in a 24-well plate, were infected with 200 µl of the diluted HCV or SIN sample per well for 2 h at 37 ºC. The monolayers were washed twice with DPBS and fresh media was added. SIN samples were harvested at 24 h.p.i. and HCV samples at 48 h.p.i.

HCV, BVDV, and SIN entry at the plasma membrane

Huh-7.5 (HCV, SIN) or MDBK (BVDV) cells were treated with bafilomycin A1 (25 nM) diluted in media for 1 h at 37 ºC. The cells were infected with HCV, BVDV or SIN in the presence of bafilomycin A1 for 1 h (BVDV) or 2 h (HCV, SIN) at 4 º C. After incubation, cells were sequentially washed with cold DPBS, warm citric acid buffer (pH 7.0 or 5.0), and medium. Medium containing bafilomycin A1 was replaced and cells were incubated at 37 ºC. Samples were harvested at 24 h.p.i. For experiments with reducing agent, 10 mM DTT was included in the citric acid buffer. For HCV-infected cells that were shifted to 37 ºC prior to the low pH wash, after 1 h at 37 ºC, cells were removed from the incubator, washed as indicated above with DPBS, citric acid buffer (pH 7.0 or 5.0), and medium. Medium containing bafilomycin A1 was replaced and cells were incubated at 37 ºC. Samples were harvested at 24 h.p.i.

Cathepsin B/L inhibitor experiments

Huh-7.5 cells, seeded in a 24-well plate (5 x 10^4/well), were pretreated with CA-074 (100 μM) or FYdmk (0.1 μM) for 3.5 h at 37 ºC. Cells were infected for 2 h at 37 ºC with HCV, HIV expressing firefly luciferase pseudotyped with VSV G (HIV-VSVG), or VSV expressing GFP

pseudotyped with Ebola virus glycoprotein (VSV-EboV GP) (35) (a generous gift from James Cunningham, Harvard University). Cells were washed and incubated for 24 h at 37 ºC. Drug was present in treated wells for the duration of the experiment. At 24 h.p.i., cells were harvested for luciferase assays (HCV/HIV-VSV-G) or flow cytometry (VSV-EboV GP). Flow cytometry was performed on a FACSCalibur (Becton Dickinson), counting 10^4 cells.

Transduction of J6/JFH-FLneo cells with TRIP-CD81 or TRIP-CD9

The lentiviral vector expressing wild-type human CD81 (TRIP-CD81) or CD9 (TRIP-CD9) protein has been described (220). For transduction, J6/JFH-FLneo cells were incubated overnight with undiluted TRIP-CD81 or TRIP-CD9 lentivirus in the presence of polybrene (4 μg/ml). 48 h post transduction, CD81 surface expression was confirmed by immunostaining and flow cytometry as above, and cells were infected with HCVpp-Luc (H77).

Treatment of HCV replicon-containing cells with BILN 2061

HCV subgenomic replicon cell populations containing H-SGneo, Con1-SGneo, and JFH-SGneo replicons were treated with 40 nM (H-SGneo

and Con1-SGneo cells) or 5 μM BILN 2061 (JFH-SGneo cells) in DMSO, 10 or 20x the EC_{50} determined in (123), respectively, in the absence of G418. The media was changed every 2-3 d. HCV RNA levels were determined in BILN 2061- or DMSO-treated cells at 4 and 9 d post treatment at which point the cells were challenged with HCVcc-Rluc. The RLU values from each cell population on day 4 or 9 were expressed as the percentage of the DMSO-treated Huh-7.5 RLU on day 4 or 9, respectively. J6/JFH-FLneo replicon cells were treated with 5 μM BILN 2061 or DMSO for 9 d, after which the concentration of drug was raised to 20 μM. HCV RNA levels were determined at 4, 9, and 23 d post treatment when they were analyzed for CD81 surface expression and HCV RNA levels, and challenged with HCVpp-Luc (H77).

Construction of VEE-AP180c-GFP and inhibition of clathrin-mediated endocytosis

The GFP-AP180c sequence was amplified from pGFP-AP180c (a generous gift from Ian Mills, Cambridge Research Institute) using a GFP-specific forward primer (5'-ggaacccctgcaggatggtgagcaagggcgagga-3') and an AP180c-specific reverse primer (5'-ggaacccctgcaggttacaagaaatccttgatgt taaga-3'). Both primers added an *Sbf*I site to the 5' and 3' end of PCR

product, generating an *Sbf*I-GFP-AP180c-*Sbf*I cassette, which was cloned into a likewise digested VEE-*Sap*I-puro plasmid. VEE-*Sap*I-puro is a derivative of VEE-GFP-puro (163) in which the GFP sequence was deleted and replaced with an insertion flanked by *Sap*I restriction sites, generating a unique *Sbf*I restriction site (C. T. Jones, *in preparation*).

For *in vitro* transcription of VEE-AP180c-GFP and VEE-GFP-puro, plasmids were linearized with *Mlu*I and 1 μg of template was transcribed in the presence of cap analog using the SP6 Megascript Kit (Ambion), DNase-treated and purified using the RNeasy Mini Kit (Qiagen). 2.5 μg of VEE-AP180c-GFP or VEE-GFP-puro RNA was electroporated into Huh-7.5 cells using a BTX ElectroSquarePorator (820 V, 5 pulses, 99 μs/pulse) as described above. Cells were seeded into a 24-well plate and incubated for 24 h, when they were infected with HCVcc-Rluc or HSV-1 (KOS*dluxori*L) for 2 h at 37 ºC. Infected cells were harvested for luciferase assays at 24 h.p.i.

HCVcc binding assay

To create the CHO cell populations for the HCVcc binding experiment, cells were mock transduced or incubated overnight with TRIP lentiviral vectors expressing human CD81, CLDN, or SR-BI in the presence of polybrene (4 μg/ml). Expression was confirmed by immunostaining for

the appropriate receptors and flow cytometry. These CHO cell populations were created by Thomas von Hahn (Rockefeller University).

CHO cells, mock transduced, or transduced with human CD81, CLDN1, or SR-BI, seeded in triplicate wells, were preincubated with α-SR-BI (C167) or α-human IgG antibodies (1 μg/ml) for 1 h at 37 ºC, then incubated with J6/JFH HCVcc (MOI ~0.5) in the presence of antibody for 2 h at 37 ºC. After binding, the cells were washed extensively with DPBS and total RNA was harvested using the RNeasy Mini kit (Qiagen). HCV RNA was amplified from 100 ng total RNA using the LightCycler RNA Amplification kit (Roche) and detected using a LightCycler 480 (Roche). The forward and reverse primer sequences are 5'-cttcacgcagaaagcgtcta-3' and 5'-caagcaccctatcaggcagt-3', respectively (Applied Biosystems). The probe sequence is 5'-6FAM-tatgagtgtcgtgcagcctc-MGBNFQ-3' (Applied Biosystems).

HCV glycoprotein-mediated cell fusion assay

The cell fusion assay was performed as described (53). Briefly, to create acceptor cells capable of responding to fusion with a HIV-1 transactivator of transcription (Tat) expressing cell, 293T cells were transduced with V1dTat-GFP VSVGpp. From this population, cell clones

were isolated that had little to no GFP expression in the absence of Tat, but had a high reporter signal when infected with V1 VSVGpp, which expresses Tat. GFP expression was quantified by FACS as described above. To test the effects of CLDN1 in this assay, the acceptor cell clones were transduced with TRIP-mCherryCLDN1 VSVGpp, which renders 293T cells susceptible to HCVpp-Luc (53).

To create donor cell populations, 293T cells were seeded in 6-well plates (8 x 10^5/well) that had been coated with poly-L-lysine (100 μg/ml, Sigma), to prevent cells from detaching. The cells were transfected with either 1.5 μg of mock protein, V1 vector, to provide Tat expression, a glycoprotein expression vector, either H77 HCV E1E2 or VSV G (1.5 μg), or V1 vector plus glycoprotein (0.75 μg each) using Fugene-6. Briefly, the DNA in TE buffer, was added to 200 μl OptiMEM containing 18 μl Fugene-6. The mixture was incubated and added to the 293T cells in fresh media. The culture media was changed approximately 6-12 h post transfection. At 36 h post transfection, combinations of donor and acceptor cells were co-seeded (1.5x10^6 cells each/well) in poly-L-lysine-coated 2-well chamber slides (BD Falcon). 12 h later, cells were washed with citric acid buffer at either pH 5.0 or pH 7.0 (15 mM citric acid, 150 mM NaCl), followed by media to neutralize the pH, and incubated for an additional 48 h. Cells were

fixed with 2% paraformaldehyde and mounted with 80% glycerol. The total number of green foci on the slide for each co-culture was enumerated by eye using a Nikon Eclipse TE300 fluorescent microscope.

Chapter 3. A transdominant screen of bovine viral diarrhea virus reveals an inhibitor of virus entry

3.1 Introduction

Viruses are obligate parasites and hence host factor interactions, in addition to those between viral proteins and RNA, are essential to the BVDV life cycle. One caveat of certain biochemical techniques that use the viral protein of interest as bait is that interacting factors are pulled out with little hint to their function or relevance. Alternatively, functional genomics is a powerful approach to identify virus-virus and virus-cell factor interactions. One technique is based on the isolation of genetic suppressor elements, sequences derived from a gene or genome of interest that can act as transdominant inhibitors of a particular biological function, for example by binding to and blocking an essential interaction surface (48, 84). This type of approach allows selective inhibition of specific RNA or protein interactions and identifies a probe to further study the targeted process. Libraries of sequences derived from viral genomes have been used to study various processes, including the phage lambda life cycle (84) and HIV-1 latency (48). Cellular processes have also been examined by screening for cellular cDNA fragments that inhibit mammalian cell growth or provide resistance to cytotoxic drugs (134, 161, 210).

In this study, using a random fragment BVDV cDNA library, I identified a fragment of the BVDV genome, the C-terminus of E1, E2, and

the N-terminus of p7, that acts as a transdominant inhibitor of BVDV replication. MDBK cells expressing the fragment, called MDBK-E1*E2p7* cells, were defective at the level of BVDV entry, although CD46 receptor expression and binding of BVDV to the cells were normal. Analysis of the MDBK-E1*E2p7* cell population has application for defining the molecules required for BVDV entry into MDBK cells.

3.2 BVDV E2 as a transdominant inhibitor of BVDV entry

A functional genomics approach to identify essential interactions in the BVDV life cycle

Throughout the life cycle of an RNA virus, viral RNAs and proteins are closely associated and presumably interact intimately with cellular factors. To identify interactions required for BVDV replication, a random cDNA library of the BVDV genome was constructed. A plasmid encoding the BVDV NADL genome was sheared into fragments, which were cloned into the retroviral vector pBabeHAZSrfcI. Inserts were flanked by the coding sequence for an HA epitope prefaced by a start codon and by a zeocin resistance gene, 5'and 3' to the fragments respectively (Fig. 3.1A). The final library encoded approximately 40,000 BVDV clones, with inserts ranging in size from 0.2 - 2 kb, averaging approximately 0.7 kb.

Fig. 3.1 Scheme for BVDV library screening. (**A**) Schematic illustration of the library expression cassette within the pBabeHAZSrfcI retroviral vector. An SV40 promoter (gray) drives expression of the BVDV cDNA library fragment (red) fused to an HA tag (light green) at the N terminus and a zeocin selectable marker (green) at the C terminus. (**B**) To package the library, 293T cells were transfected with the BVDV library in pBabeHAZSrfcI, as well as Gag-pol and VSV G-protein expression constructs, and supernatants were harvested. MDBK cells were transduced with the packaged library and selected with zeocin. To screen the library, Zeo-resistant (Zeo^r) MDBK cells were infected with cp BVDV NADL. Colonies that developed following the infection were harvested and expanded.

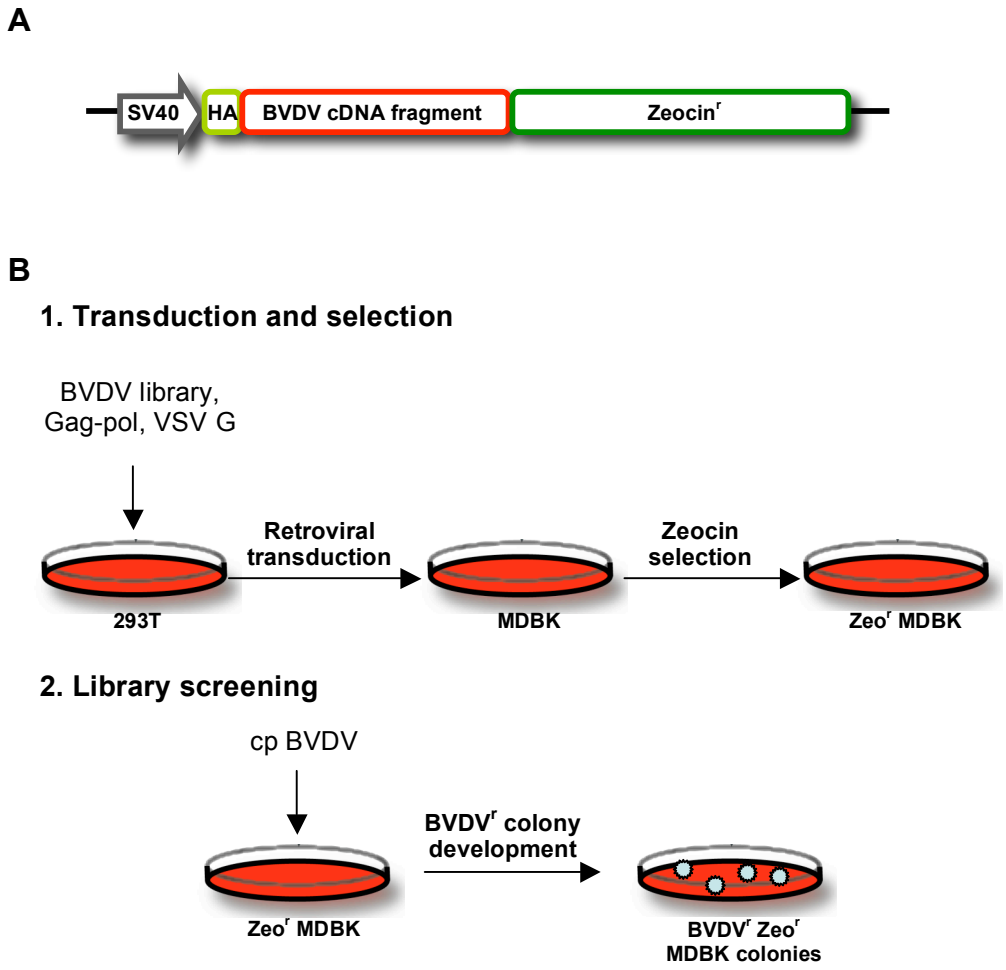
A
SV40
HA
BVDV cDNA fragment
Zeocin^r
B
1. Transduction and selection
BVDV library,
Gag-pol, VSV G
Retroviral
transduction
Zeocin
selection
293T
MDBK
Zeo^r MDBK
2. Library screening
cp BVDV
BVDV^r colony
development
Zeo^r MDBK
BVDV^r Zeo^r
MDBK colonies

Fig. 3.1

To screen the library for transdominant inhibitors of BVDV replication, Zeo-resistant MDBK cells expressing the BVDV library or the empty vector, pBabeHAZ, were infected with cp BVDV NADL to isolate cells able to survive BVDV-induced cytopathic effect (CPE) (Fig. 3.1B). Of the 20 resistant colonies that survived BVDV challenge, 11 survived expansion, and only three remained resistant after reinfection with BVDV NADL. To determine the identity of the library inserts contained in the resistant clones, I harvested genomic DNA from these cells and amplified the retroviral insertion by PCR. Two of the three clones contained an insertion of approximately 1.2 kb, which encoded 150 bases of BVDV E1, the entire E2 gene, and 15 bases of p7, and was named E1*E2p7* (Fig. 3.2). In one of these cell clones, a 0.7-kb library fragment, derived from the BVDV NS5A gene, but cloned into pBabeHAZSrfcI in the reverse orientation with respect to the BVDV genome, was found in addition to the E1*E2p7* fragment, likely a result of coinfection with two library clones. The same 0.7-kb insertion was also found in the third resistant clone. This sequence, however, could not protect naïve cells from BVDV infection (data not shown) and was therefore eliminated from further analysis.

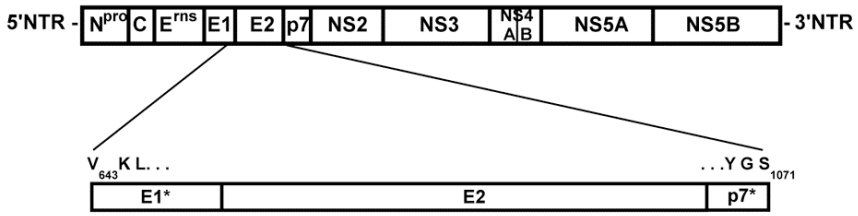

Fig. 3.2 A genetic screen identifies the BVDV E1*E2p7* sequence as a transdominant inhibitor of BVDV replication. Sequence alignment of the E1*E2p7* library insertion with the BVDV genome. The brackets descending from the pictured BVDV genome highlight the BVDV sequence present in the resistant clones. The amino acid and its position relative to the BVDV NADL polyprotein are indicated.

*Naïve cells expressing E1*E2p7* are resistant to homologous BVDV infection*

To test if E1*E2p7* could provide resistance to naïve cells, the sequence was re-cloned into pBabeHAZSrfcI, packaged into pseudoparticles, and used to transduce naïve MDBK cells. After selection with zeocin, the resulting cell population was called MDBK-E1*E2p7*. As a control, an MDBK-pBabe population, transduced with the empty vector pBabeHAZ, was generated.

MDBK-E1*E2p7* and pBabe cells were infected with BVDV NADL and cell supernatants were harvested at various time points to determine viral titer. Over time, the BVDV titers obtained from MDBK-E1*E2p7* cells were 10-1000-fold lower than from pBabe control cells (Fig. 3.3A). In addition, while total CPE was observed in the pBabe cells, there was minimal CPE in the E1*E2p7* cells (data not shown). A similar 1000-fold difference in infectivity between the control and E1*E2p7* cells was observed with noncytopathic (ncp) BVDV NADLJiv90^{-} (Fig. 3.3B). Even a high MOI infection (MOI 10) could not overcome the inhibition to BVDV replication in the E1*E2p7* cells (Fig. 3.3C). These data demonstrate that the E1*E2p7* insert was responsible for the resistance observed in the original MDBK clones.

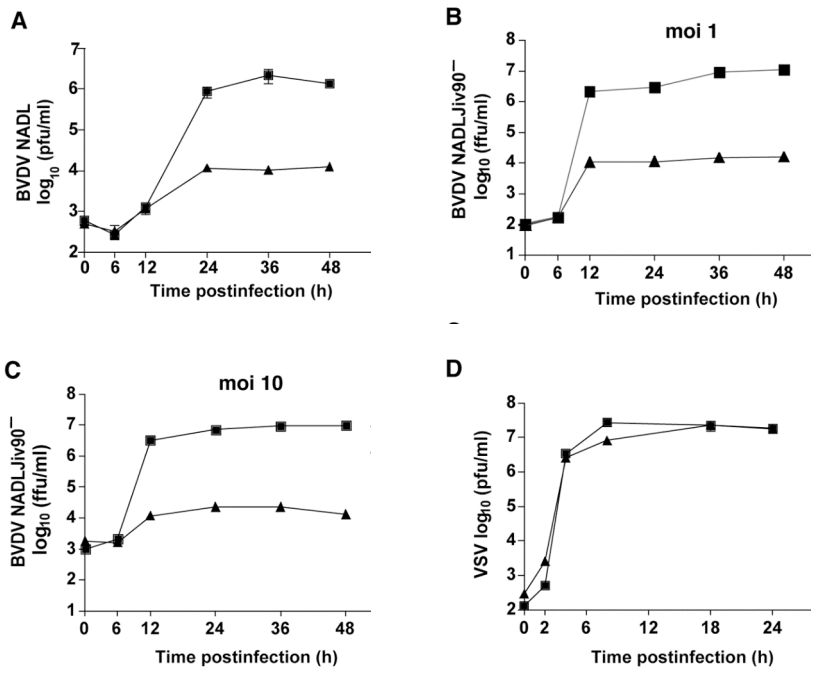

Fig. 3.3 Cells expressing BVDV E1*E2p7* are resistant to homologous BVDV infection. (**A**) Cells transduced with a retroviral vector expressing the E1*E2p7* sequence, MDBK-E1*E2p7* cells (triangles), and MDBK-pBabe control (squares) cells were infected with BVDV NADL. Each point represents the mean titer of virus present in the supernatants of duplicate wells at the indicated time point p.i. This graph is representative data from at least 2 independent experiments. Error bars show the standard errors of the means. (**B, C**) MDBK-E1*E2p7* (triangles) and pBabe (squares) cells were infected with ncp BVDV NADLJiv90^{-} at an MOI of 1 (B) or 10 (C) and supernatants were harvested as above. Titers were determined by focus forming assays in duplicate. Error bars show the standard errors of the means. (**D**) MDBK-E1*E2p7* cells are permissive for heterologous VSV infection. MDBK-E1*E2p7*(triangles) and pBabe (squares) cells were infected with VSV and supernatants were harvested as above and titered in duplicate by plaque assay. Error bars show the standard errors of the means.

To determine if the phenotype observed in the MDBK-E1*E2p7* cells was a BVDV-specific effect or a general virus inhibition, the E1*E2p7* and pBabe cells were infected with the interferon-sensitive rhabdovirus, vesicular stomatitis virus (VSV). VSV was equally able to grow and form plaques on the E1*E2p7* and pBabe cells (Fig. 3.3D and data not shown). Therefore, the resistance in the MDBK-E1*E2p7* cells was not due to a general antiviral mechanism.

A small amount of virus could be detected in the supernatants of MDBK-E1*E2p7* cells after infection with either cp or ncp BVDV (Fig. 3.3A, B, C). This could be due to a low level of virus infection in all of the E1*E2p7* cells or to infection of a subset of permissive cells in the population. To examine this further, I infected the E1*E2p7* and pBabe cells with NADLJiv90^{-}GFP, an ncp BVDV that expresses GFP, and harvested the cells for flow cytometry. At 48 h.p.i., only 4-5% of E1*E2p7* cells were GFP positive compared to more than 70% of pBabe cells (Fig. 3.4A). This result indicates that the majority of cells in the MDBK-E1*E2p7* cell population cannot support BVDV replication. Moreover, BVDV NADL could not form plaques on E1*E2p7* cell monolayers (Fig. 3.4B), suggesting that although some cells were infected, virus spread was inefficient due to a large number of non-permissive cells.

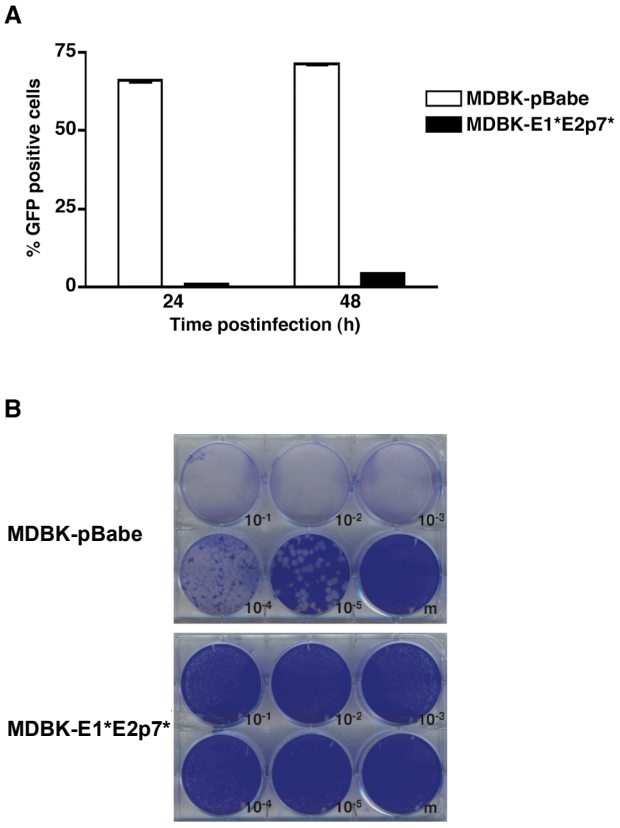

Fig. 3.4 The MDBK-E1*E2p7* cell population contains a small subset of permissive cells. (**A**) MDBK-E1*E2p7* and pBabe cells were infected with NADLJiv90-GFP. At 24 and 48 h.p.i., cells were harvested for FACS analysis to determine the number of GFP positive cells. Values are the average of duplicate samples; error bars show the standard errors of the means. (**B**) Serial dilutions of BVDV NADL were used to infect monolayers of MDBK-E1*E2p7* or pBabe cells. The cells were then overlayed with agarose, incubated for 3 d and stained with crystal violet.

BVDV E2 is a heavily glycosylated, ER-resident, integral membrane protein, which is cleaved from the BVDV polyprotein by host signal peptidase (76, 206) (Fig. 3.5). To further characterize the MDBK-E1*E2p7* cells, I compared E2 protein expression in MDBK-E1*E2p7* cells to that from BVDV-infected MDBK cells by western blotting with an α-E2 antibody. BVDV-infected cell lysates displayed a dominant band between 50 and 60 kDa, corresponding to the molecular weight of the mature E2 protein, and a minor species migrating slightly slower, most likely due to the stable E2-p7 product in BVDV infected cells (76) (Fig. 3.6). Two bands were also detected from MDBK-E1*E2p7* cell lysates, although the major band detected in these cells was of a greater molecular weight compared to BVDV-infected cell lysates (Fig. 3.6), and is likely an E2p7*-Zeo fusion protein. The presence of a minor species in MDBK-E1*E2p7* cells, migrating similarly to the molecular weight of the dominant band within the infected cell lysates, suggests that there is some processing of E2 at its C-terminus from the E1*E2p7* protein (Fig. 3.6). In addition, the localization of E2 protein in E1*E2p7* cells was analogous to E2 expressed after BVDV infection, as judged by indirect immunofluoresence using an α-E2 antibody and sensitivity of immunoprecipitated E2 to Endoglycosidase H or PNGase F, respectively (data not shown).

Fig. 3.5 Putative membrane topology of BVDV E2. The E2 glycoprotein is an ER-resident protein with a C-terminal transmembrane anchor (orange) and a short C-terminal tail (green). Arrows indicate sites of cleavage by host signal peptidase. Adapted from (172).

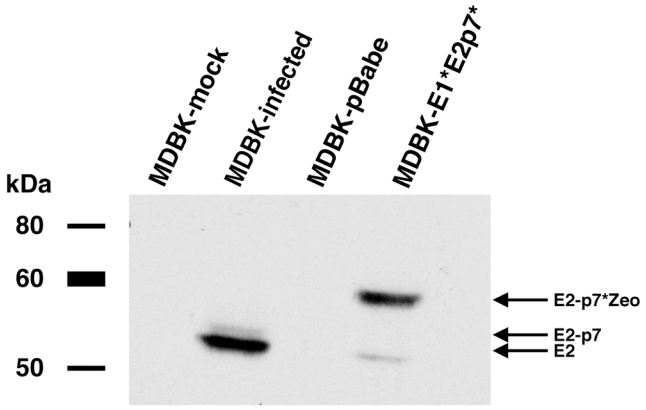

Fig. 3.6 E2 expression in MDBK-E1*E2p7* cells. Lysates from MDBK-E1*E2p7* and BVDV NADL infected-MDBK cells were assayed by western blot using an antibody against BVDV E2 (MAb 214). Lysates from mock-infected MDBK cells and pBabe cells were used as negative controls. Arrows indicate the expected identity of the protein in each band based on molecular weight.

Expression of the BVDV E2 ectodomain is sufficient for BVDV inhibition

I sought to determine if E2 expression alone, in the absence of the E1* and p7* flanking sequences present in the MDBK-E1*E2p7* cells, was sufficient for BVDV inhibition. MDBK cells were infected with a packaged lentivirus expressing either the original construct, E1*E2p7* (pLenti6-E1*E2p7*), or the E2 coding region alone, preceded by the signal sequence from influenza HA to direct E2 into the ER lumen and followed by a stop codon (pLenti6-Sig-E2) (Fig. 3.7). MDBK cells transduced with a lentivirus expressing EGFP (pLenti6-EGFP) were used as a control. Transduced MDBK cells were infected with NADLJiv90^{-}*luc* (119), a bicistronic ncp BVDV that expresses a luciferase reporter gene driven by the BVDV IRES and the BVDV polyprotein via the EMCV IRES (Fig. 3.8A). The ubiquitin gene (*ubi*) was inserted upstream of the *luc* gene, to create the correct N terminus of Luc upon cleavage of Ubi. After infection with NADLJiv90^{-}*luc,* cells expressing E1*E2p7* or E2 alone had a similar reduction in luciferase activity compared to the EGFP control cells (Fig. 3.8B). These results indicate that the flanking E1* and p7* sequences did not contribute to the BVDV inhibition observed using the original E1*E2p7* construct.

To determine if the E2 ectodomain alone was responsible for BVDV inhibition, pLenti6-Sig-E2*, expressing the E2 ectodomain with no

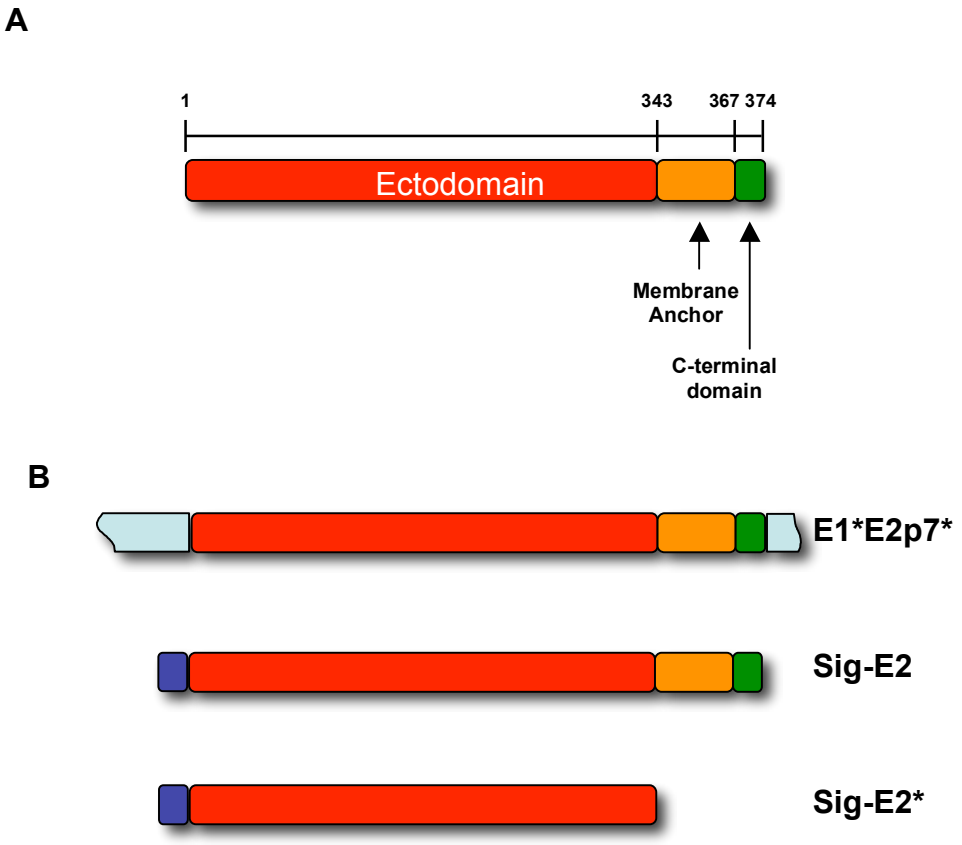

Fig. 3.7 E2 expression constructs. (**A**) Organization of the E2 protein. Numbers indicate the amino acid number within E2 corresponding to the start of a particular domain (104). (**B**) E2 expression constructs cloned into the pLenti6 lentiviral vector. The light blue fragments correspond to the E1* and p7* sequence of E1*E2p7*. Red, orange and green boxes represent domains of the E2 protein as indicated in A. The dark blue box in Sig-E2 and Sig-E2* corresponds to the HA signal sequence inserted upstream of the first amino acid of the E2 protein.

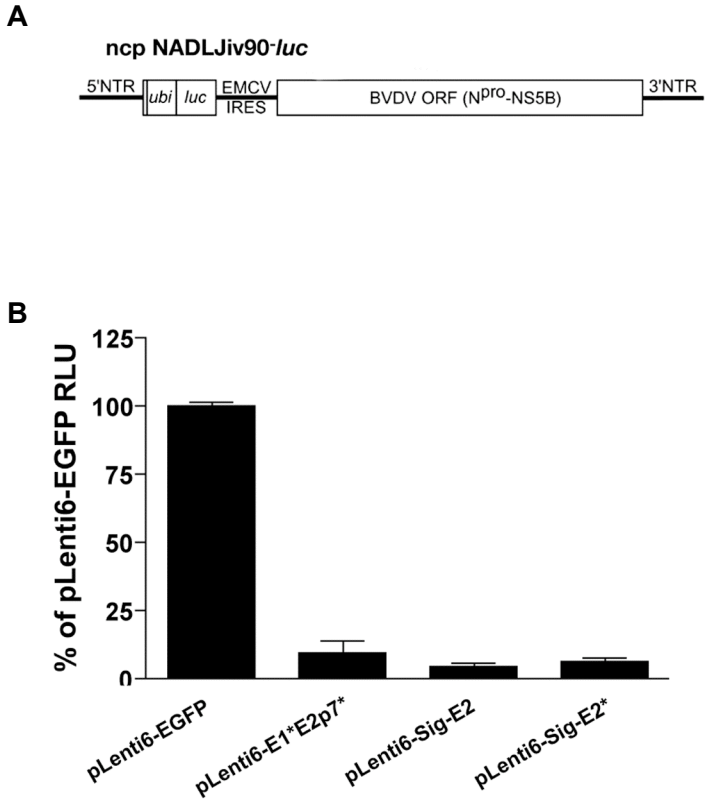

Fig. 3.8 The E2 ectodomain is sufficient for BVDV inhibition. (**A**) Schematic diagram of ncp NADLJiv90-*luc* viral RNA. (**B**) MDBK cells were transduced with packaged lentiviral vectors expressing EGFP, E1*E2p7*, Sig-E2, or Sig-E2*. After blasticidin selection, each cell population was infected with NADLJiv90-*luc*. At 48 h.p.i., cells from triplicate wells were harvested for luciferase assays. The graph shows the average of the 2 independent experiments done in triplicate; error bars show the standard errors of the means.

transmembrane or C terminal domain, was constructed (Fig. 3.7). MDBK cells were infected with packaged pLenti6-Sig-E2* lentivirus and challenged with NADLJiv90^{-}*luc*. Luciferase activity from the Sig-E2* cells was similar to that from E1*E2p7* and Sig-E2 cells and more than 1 log lower than from the negative control-EGFP expressing cells (Fig. 3.8B). Immunofluorescence staining for E2 within the Sig-E2* cells showed a significant amount of E2 within the cell, possibly in the ER and secretory pathway (data not shown). Although, it is not clear whether ER retention provided by the E2 transmembrane domain is required for BVDV inhibition, this data demonstrates that the E2 ectodomain is sufficient to obtain the BVDV inhibition observed from E1*E2p7*.

*BVDV is blocked prior to translation in MDBK-E1*E2p7* cells*

To examine the block to BVDV infection in the original MDBK-E1*E2p7* cells, I again used NADLJiv90^{-}*luc*, which provided a sensitive assay to monitor BVDV translation and replication. Similar to the above titration experiments, a 100-1000-fold decrease in luciferase activity was observed after NADLJiv90^{-}*luc* infection of MDBK-E1*E2p7* cells compared to pBabe cells (data not shown).

I examined translation of the incoming NADLJiv90^{-}*luc* genome in the absence of viral RNA replication using a BVDV-specific polymerase inhibitor (6). After infection with NADLJiv90^{-}*luc*, the luciferase activity within the pBabe cells peaked at 6 h and steadily decreased as expected due to the polymerase inhibitor. At the 6 h time point, the luciferase activity on the E1*E2p7* cells was approximately 10-fold less than on pBabe cells (Fig. 3.9A), which could be due a defect in translation or in the ability of BVDV to enter the cells and deliver its genome to the cytoplasm. To distinguish between these options, I tested whether bypassing the virus entry steps by transfection could overcome the block to BVDV replication in E1*E2p7* cells. Virus titer in the supernatants of MDBK-E1*E2p7* and pBabe cells was examined after electroporation of *in vitro* transcribed BVDV NADL RNA. Over a 48 h period there was no difference in the titer of BVDV from MDBK-E1*E2p7* compared to the pBabe control cells (Fig. 3.9B). Because BVDV could be efficiently translated and replicated if allowed to bypass the entry steps into MDBK-E1*E2p7* cells, the block to BVDV replication is presumably at the level of virus entry, defined here as a step that occurs prior to translation.

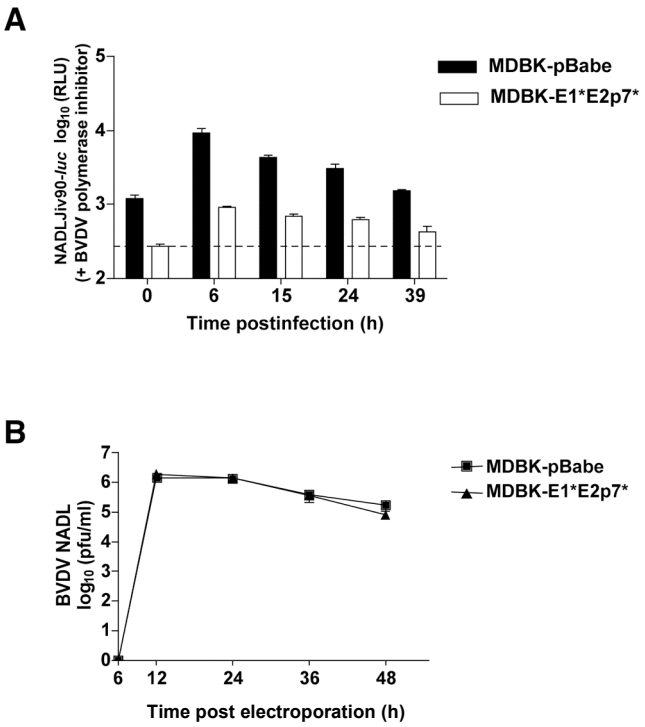

Fig. 3.9 MDBK-E1*E2p7* cells have a defect at the level of BVDV entry. (**A**) MDBK-E1*E2p7* and pBabe cells were infected with NADLJiv90-*luc* in the presence of a BVDV polymerase inhibitor (6). At each time point, cells were harvested for luciferase assays. Each bar represents the mean value of duplicate wells; error bars show the standard errors of the means. The dashed line indicates the background level of the assay from naïve MDBK cells. (**B**) MDBK-E1*E2p7* and pBabe cells were electroporated with *in vitro* transcribed BVDV NADLJiv90-*luc* RNA. At each time point, supernatants from electroporated cells were harvested and titered on MDBK cells. Each point represents the mean titer of duplicate wells; error bars show the standard errors of the means.

*CD46 expression and BVDV binding on MDBK-E1*E2p7* cells is similar to control cells*

I hypothesized that the resistance to BVDV entry in MDBK-E1*E2p7* cells may be at the level of the viral receptor, CD46 (137). MDBK-E1*E2p7* and pBabe cells were analyzed for CD46 expression using flow cytometry and found to have similar levels on their surfaces (Fig. 3.10A). Western blot of total cell lysates also revealed comparable levels of total CD46 in the two cell types (Fig. 3.10B). Taken together, these results suggest that down regulation of CD46 from the cell surface is not responsible for the BVDV inhibition seen in cells expressing the E1*E2p7* insertion.

Although surface levels of CD46 were apparently similar between MDBK-pBabe and E1*E2p7* cells, it remained possible that E1*E2p7* cells could have a functional defect in cell surface binding of BVDV. To investigate this possibility, cells were chilled to 4 ºC and infected with ncp BVDV NADLJiv90^{-} at an MOI of 10. Cell-associated BVDV RNA was quantified by real-time quantitative RT-PCR analysis. The assay revealed similar levels of BVDV binding on the surface of both MDBK-pBabe and E1*E2p7* cells (Fig. 3.11A). Preincubation with an α-CD46 antibody reduced cell associated BVDV RNA levels in both cell types by approximately 50% (Fig. 3.11B), indicating that much of the detected

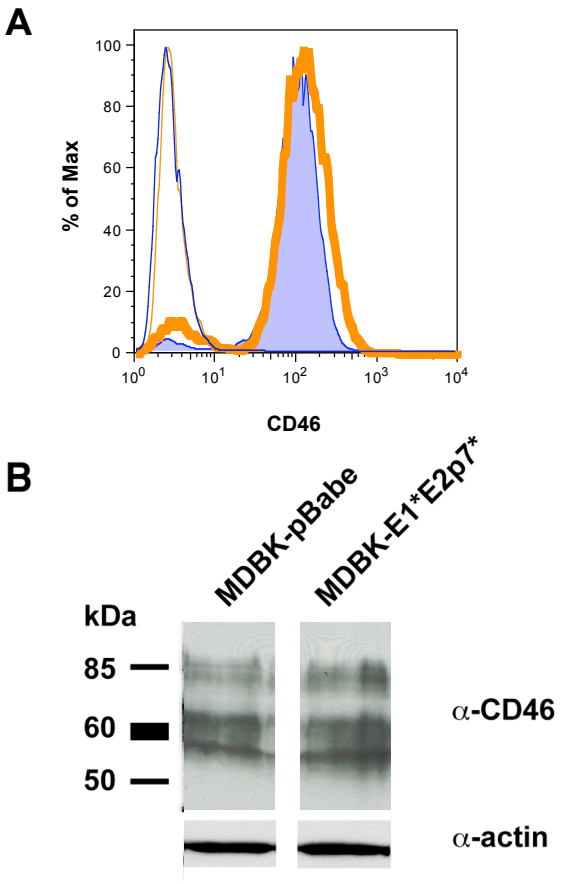

Fig. 3.10 CD46 expression on MDBK-E1*E2p7* cells is similar to control pBabe cells. (**A**) To analyze CD46 expression on the cell surface, cells were detached and stained with a polyclonal antibody against bovine CD46. Cells were stained in the absence of detergent to selectively stain only the surface of the cells. CD46 expression on MDBK-E1*E2p7* (thick, orange line) and pBabe cells (tinted, blue curve) was analyzed by FACS after gating on live cells. Cells stained with preimmune sera are indicated as thin solid lines. (**B**) To examine total CD46 expression, lysates from MDBK-E1*E2p7* and pBabe cells were western blotted with an antibody against bovine CD46 (α-CD46) or actin (α-actin). The presence of multiple bands in the α-CD46 blot is due to multiple spliced isoforms of CD46 in the cell.

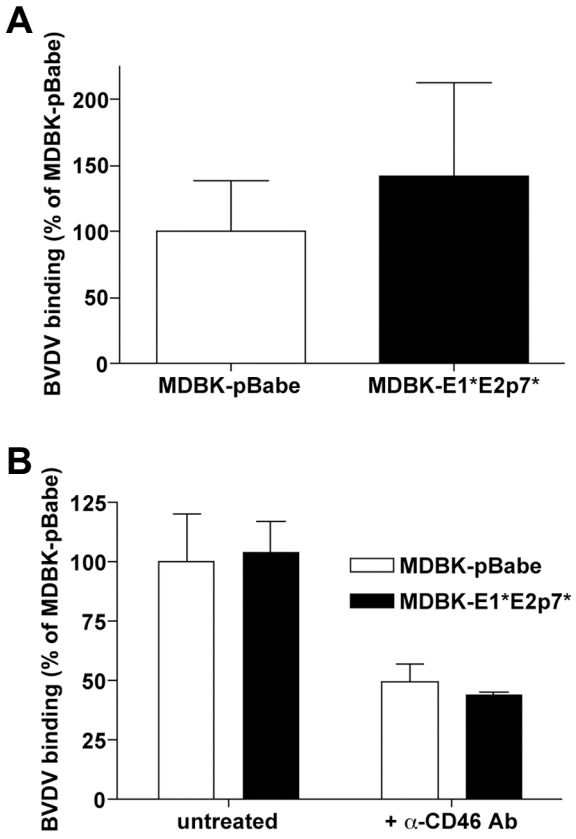

Fig. 3.11 BVDV binding to MDBK-E1*E2p7* cells is similar to control pBabe cells. (**A**) Cells were incubated for 1 h at 4 ºC with BVDV NADLJiv90^{-} at an MOI of 10. Cells were washed extensively and RNA was harvested for quantitative RT-PCR to determine cell associated BVDV RNA levels. Values are expressed as the percent of MDBK-pBabe BVDV binding. Each bar is the average value of 3 independent experiments done in triplicate; error bars show the standard errors of the means. (**B**) Cells were treated with an α-CD46 antibody prior to infection with BVDV as described above. RNA was harvested for quantitative RT-PCR to determine cell associated BVDV RNA levels. Values are expressed as the percent of untreated MDBK-pBabe BVDV binding and are the average of at least duplicate samples; error bars show the standard deviations.

binding was dependent on CD46. These results indicate that the block to BVDV infection in MDBK-E1*E2p7* cells lies downstream of BVDV binding to the cell surface.

3.3 Discussion

To identify essential interactions in the BVDV life cycle, I took a functional genomics approach using a random genomic cDNA library of the BVDV genome and screening it for genome fragments that could act as transdominant inhibitors of viral replication. Two unique BVDV sequences were identified within resistant colonies that developed after cp BVDV infection – one aligning with the E2 protein in the BVDV structural region and another within the NS5A protein. Only the former insertion, which expressed the C-terminal end of E1, E2, and the N terminus of p7 (E1*E2p7*), could provide resistance to naïve cells. Further experiments demonstrated that BVDV was blocked at the level of entry in the MDBK-E1*E2p7* cells. However, if allowed to bypass the entry block, BVDV replication was unaffected by expression of the E1*E2p7* insertion.

The role of the BVDV structural proteins in preventing BVDV infection is supported by previously published data. A cell line expressing the BVDV C through E2 proteins was shown to be non-permissive for

BVDV replication (170). Additionally, Harada *et al*. described an MDBK cell line expressing BVDV E2 and p7 separated by an IRES that was similarly inhibited in BVDV infection (76). My work described here, further maps the BVDV structural region necessary for BVDV inhibition to the ectodomain of the E2 protein and suggests that this inhibition is CD46-independent. Sig-E2*-expressing cells, encoding the signal sequence of the HA protein, and the E2 ectodomain followed by a stop codon, were as resistant to BVDV entry as those expressing the original E1*E2p7* construct. Therefore, the E1 and p7 flanking sequences, as well as the E2 transmembrane and C terminal domains are not required for BVDV inhibition. Moreover, the signal sequence for E2, normally provided by E1, acting to direct the E2 ectodomain into the ER lumen, could be replaced by a heterologous signal sequence to provide similar inhibition as the original insertion. Hence, the ectodomain of E2, independent from the transmembrane and C-terminal domain, can act as a transdominant inhibitor of BVDV entry.

BVDV inhibition provided by the E1*E2p7* insertion may be due to a number of possible mechanisms. BVDV entry could be inhibited as a result of E2 interfering directly with the activity of a particular BVDV entry factor, or indirectly by antagonizing a host signaling pathway required for

virus uptake. Expression of BVDV E2 may prevent BVDV from entering the cell by a similar mechanism as superinfection exclusion observed in acutely infected cells (119). We and others have examined the phenomenon of BVDV superinfection exclusion in MDBK cells and shown that superinfecting BVDV encounters superinfection blocks both at the levels of entry and replication [Sections 4.2, 4.3 and (119, 147)]. For the entry block, it was found that cells harboring a BVDV genome lacking the E2 gene fail to exclude superinfecting BVDV at the level of entry. In light of this data, it is possible that expression of E2 within MDBK cells may mimic the phenomenon of superinfection exclusion at the level of viral entry.

Superinfection exclusion has been observed for a number of viruses including HIV (1, 42, 92, 186), alphaviruses (1, 93), and VSV (180, 209). Envelope protein-mediated receptor down regulation and interference with the activity of a cellular receptor are well-documented mechanisms of viral superinfection exclusion. For example, the down regulation of CD4 from the surface of HIV infected cells by the viral envelope precursor gp160 (42, 92, 186) or the removal of sialic acid by influenza neuraminidase from the glycoproteins within the secretory pathway and the surface of infected cells (4, 115, 158) prevents superinfection of these viruses. Additionally, the Env protein of the retrovirus foamy virus (FV) was shown to be sufficient for

mediating superinfection exclusion in FV-infected cells (19). Interference with a cellular receptor has also been observed for mouse gammaretroviruses. Mouse cells harboring certain integrated proviruses, ecotropic *Fv4* or polytropic *Rmcf* or *Rmcf2,* which express murine leukemia virus (MLV)-envelope genes, are resistant to exogenous ecotropic or polytropic MLV infection, respectively (16, 77, 87, 213).

The entry pathway for BVDV is CD46-dependent (137), although I found that CD46 expression in MDBK-E1*E2p7* cells did not differ from pBabe control cells. Consistent with this result, BVDV binding, which is mediated by CD46 (109, 137), was also equivalent between MDBK-E1*E2p7* and the control cells. It remains possible that E2 could be interfering with a specific molecular form or localization of CD46 that is expressed on the cell surface and required for BVDV to be internalized into MDBK cells, yet our experiments suggest that the block to BVDV entry lies downstream of the CD46-dependent step.

Screening a random genomic library to identify transdominant inhibitors has a number of advantages over simply screening ORFs from the BVDV genome. First, a random approach is inherently unbiased and thus allows the identification of functional domains or regions that may not be tested by a rationally designed approach. In addition, simply based on the

number of different sequences being screened, a library approach increases the likelihood of identifying functional interactions required for viral replication. Moreover, because the random library represents the entire BVDV genome, there is the potential to characterize interactions, which may occur between sequences that lie distal from each other within the viral genome.

Functional genomics is a powerful approach to examine essential interactions between individual viral components, as well as between viral and cellular factors. Viral protein or RNA components associate and recruit cellular cofactors for processes such as viral translation and replication, and for host defense evasion and pathogenesis. Screening of a random fragment library derived from the HIV-1 genome identified inhibitors of productive HIV-1 infection and latency, which aligned with 7 regions of the virus genome (48). In our study, screening of a random fragment library of the BVDV genome identified a viral sequence capable of preventing BVDV entry into MDBK cells. The advantage of this approach over other *in vitro* techniques is that the BVDV inhibitor was identified in a functional context where it prevented viral infection, directly demonstrating the relevance of an E2-mediated interaction in BVDV replication. Notably, only one cDNA, spanning the full-length E2 gene, out the 40,000 cDNA clones included in

the random BVDV library, was pulled out of our screen and conferred resistance to naïve cells. This suggests that expression of the E1*E2p7* insertion in MDBK cells provides a strong, inhibitory mechanism against BVDV. Although the minimal region required for BVDV inhibition was the E2 ectodomain, the larger insertion could have provided some advantage in stability or expression level during screening in MDBK cells. In future studies, I may consider less stringent screening methods compared to cell death, which could allow selection for cDNA insertions offering intermediate levels of BVDV resistance to MDBK cells. This approach has potential to further identify essential interactions that occur with components of the full-length BVDV genome.

Chapter 4. The mechanisms of BVDV and HCV superinfection exclusion

4.1 Introduction

Superinfection exclusion, or homologous interference, is the ability of an established virus infection to interfere with secondary virus infection. Multiple mechanisms that contribute to superinfection exclusion have been demonstrated for various viruses, including interference with receptor-mediated attachment (27, 28, 184, 185) and penetration into cells (180, 181, 209), as well as downstream replication events (1, 66, 99). In this Chapter, superinfection exclusion in BVDV and HCV infected cells was examined.

Superinfection exclusion has been described for pestiviruses (147), but the molecular mechanisms responsible for this phenomenon remain unclear. It was found that MDBK cells acutely infected with ncp BVDV are protected from cytopathic effect (CPE) following superinfection with cp BVDV, but not with an unrelated cp virus, VSV. Dual mechanisms of BVDV superinfection exclusion were observed; one occurred at the level of viral entry and another at the level of viral replication. It was determined that superinfecting BVDV fails to enter acutely infected cells and that the structural protein E2 was responsible for this block. If the viral entry steps were bypassed by transfection of the viral RNA, the RNA could be translated but failed to replicate in cells acutely infected with BVDV. The second mechanism of superinfection exclusion at viral RNA replication was

dependent on the level of primary RNA replication and was not influenced by expression of the viral structural proteins (C, E^{rns}, E1, and E2).

The recent development of an HCV infectious system that permits the growth of virus in cell culture (HCVcc) has enabled study of the complete virus lifecycle (123, 203, 221). In this study, I observed that cells acutely infected with genotype 2a HCV chimeric strain J6/JFH and cells harboring HCV RNAs from a range of genotypes were resistant to HCVcc superinfection. Further analysis revealed that superinfection was blocked downstream of viral entry. Unlike cells acutely infected with J6/JFH and cells supporting Con1 and H77 full-length, and Con1, H77, and JFH subgenomic replicons, cells containing a persistent, full-length J6/JFH replicon were nonpermissive for HCVpp. Study of this HCVpp-resistant, stable J6/JFH replicon population suggested that J6/JFH replication/infection applies a strong negative selection for CD81-expressing cells. This observation could be mimicked at later time points after infection with J6/JFH HCVcc.

4.2 Background information for BVDV superinfection exclusion

Sections 4.2 and 4.3 encompass a comprehensive study of BVDV superinfection exclusion. This section (4.2) explains previous results

obtained by Young-Min Lee (Washington University). The following section (4.3) describes an additional set of experiments to further analyze the observations that BVDV superinfection exclusion is lost upon passaging and that the level of exclusion correlates with the level of primary RNA replication. All of these data have been reported in reference (119).

MDBK cells acutely infected with ncp BVDV are protected from CPE when superinfected with cp BVDV, but not with VSV

To examine whether ncp BVDV-infected MDBK cells are protected from subsequent BVDV infection, MDBK cells were infected with ncp NADLJiv90^{-} at an MOI of 10 and challenged at 12 h.p.i. with cp NADL. As a control, naïve MDBK cells were infected in parallel with cp BVDV. CPE caused by cp BVDV replication was monitored quantitatively by plaque assay or qualitatively by incubating infected monolayers in liquid medium.

Plaques were formed on cell monolayers in plaque assays and no viable cells were observed for cultures incubated in liquid medium following infection of naïve MDBK cells with cp BVDV (Fig. 4.1A, plates 4 and 8). In contrast, neither plaques nor recognizable CPE resulted from superinfection of acutely ncp BVDV-infected cells with cp BVDV (Fig. 4.1A, plates 3 and 7), even 5 d post superinfection when naïve MDBK cells began to die due to

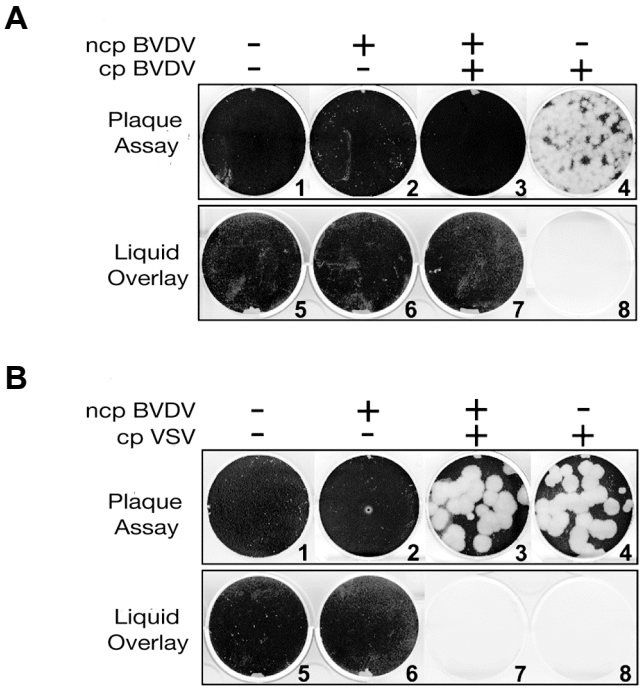

Fig. 4.1 MDBK cells acutely infected with ncp BVDV are protected from CPE when superinfected with homologous cp BVDV, but not with VSV. (**A** and **B**) Naïve MDBK cells were first mock-infected, or infected with ncp NADLJiv90^{-} BVDV. At 12 h.p.i, ncp NADLJiv90^{-}-infected cells were washed three times with media, and either mock-superinfected or superinfected with cp NADL BVDV or cp VSV for 1 h. + or – above each column of plates indicates infection or mock-infection, respectively, with the particular virus shown at the top left. The cells were overlaid with agarose (**A** and **B**, plates 1-4) or incubated in liquid culture media (**A** and **B**, plates 5-8). The cells were fixed and stained with crystal violet to visualize live cells surviving CPE after 5 d (**A**) or 3 d (**B**).

overgrowth. Primary ncp BVDV-infected cells did not show any signs of CPE (Fig. 4.1A, plates 2 and 6). In addition to ncp NADLJiv90$^-$ virus, MDBK cells infected with a heterologous ncp strain of BVDV, SD-1 (45), were also protected from CPE upon superinfection with cp NADL (data not shown).

Next it was determined if ncp BVDV-infected MDBK cells are generally protected from virus-induced CPE, including that induced by a heterologous virus. To do so, VSV, a negative-sense interferon-sensitive rhabdovirus, was used to challenge the ncp BVDV-infected MDBK cells. CPE induced by VSV infection of BVDV-infected cells was indistinguishable from that of VSV-infected naïve MDBK cells as determined by plaque assays (Fig. 4.1B, compare plates 3 and 4) and observing infected monolayers overlaid with liquid media (Fig. 4.1B, compare plates 7 and 8). Thus, MDBK cells infected with ncp BVDV, either ncp NADLJiv90$^-$ or ncp SD-1 BVDV, were protected from CPE when superinfected with homologous cp BVDV, but not with heterologous cp VSV. This suggests that the block may be virus-specific and not mediated by a general cellular antiviral defense pathway such as interferon or a block in the ability of the cells to undergo virus-induced cell death.

To address whether the lack of CPE was due to a block in the ability of superinfecting virus to replicate in acutely infected cells, MDBK cells acutely infected with ncp NADLJiv90^{-} were superinfected with ncp NADLJiv90^{-}*pac*, which expresses a dominant selectable marker, the puromycin N-acetyltransferase (*pac*) gene (see Fig. 4.3A). After selection with puromycin, neither foci nor surviving cells were observed in superinfected monolayers whereas naïve MDBK cells infected with ncp NADLJiv90^{-}*pac* were transduced to puromycin resistance with high efficiency (data not shown). These results indicate that the lack of CPE observed in the first experiments was likely due to the failure of the superinfecting cp BVDV to replicate efficiently in cells acutely infected with ncp BVDV (rather than inhibition of CPE despite replication of the cp virus).

Superinfection exclusion is established rapidly

To determine the kinetics with which superinfection exclusion is established, we infected with ncp NADLJiv90^{-}*luc* (Fig. 3.8A). The level of luciferase activity from ncp NADLJiv90^{-}*luc* after superinfection of ncp NADLJiv90^{-} -infected cells was used as a measure of the degree of superinfection exclusion.

Naïve MDBK cells were infected with ncp NADLJiv90^{-} virus for 0, 0.25, 0.50, 1, 2, 4, 8, or 12 h prior to superinfection with ncp NADLJiv90^{-} *luc*. At 24 h post superinfection, the luciferase activity was determined. Cells preincubated with ncp NADLJiv90^{-} for at least 30-60 min prior to superinfection with ncp NADLJiv90^{-}*luc* had dramatically reduced luciferase activity compared to cells simultaneously coinfected with the two viruses (Fig. 4.2). Beyond 4 h preincubation, little luciferase activity was detected. Thus, superinfection exclusion of BVDV is efficiently established within 30-60 min after primary BVDV infection.

BVDV persistently infected cells lose the ability to exclude superinfecting virus

To determine if superinfection exclusion is maintained during persistent infection, individual persistently infected cells were examined. Cells were infected with ncp NADLJiv90^{-}*pac* and maintained under puromycin selection (Fig. 4.3A). At 1, 2, 3, 4, and 5 d after acute infection, cells were superinfected with cp NADL. Two days later, supernatants were harvested and titered by plaque assay to measure the yield of cp NADL. Over the 5 d period, the decrease in virus production from the puromycin selected cells directly correlated with the increase in cp NADL titer from these cells (Fig. 4.3B). The fact that the cells were maintained under

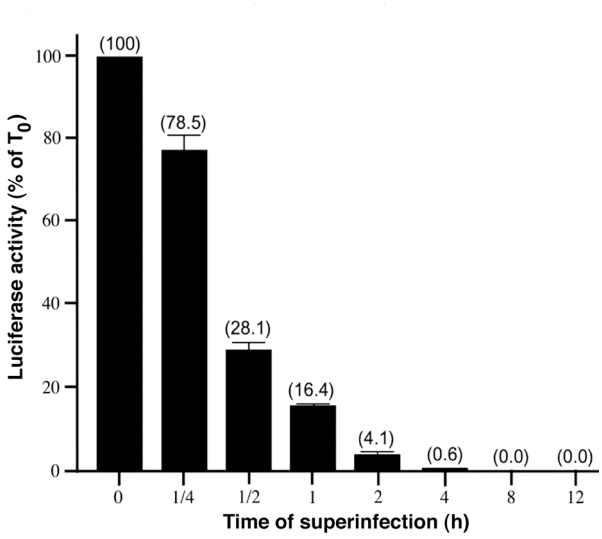

Fig. 4.2 Superinfection exclusion is established within 30-60 minutes of primary BVDV infection. Naïve MDBK cells were infected with ncp NADLJiv90$^-$ for 0.25, 0.5, 1, 2, 4, 8, or 12 h prior to superinfection. The cells were then superinfected with ncp NADLJiv90$^-$*luc* virus. In parallel, naïve MDBK cells were coinfected with ncp NADLJiv90$^-$ and ncp NADLJiv90$^-$*luc* viruses, indicated as time point 0. After 24 h incubation, the cells were lysed and assayed for luciferase activity.

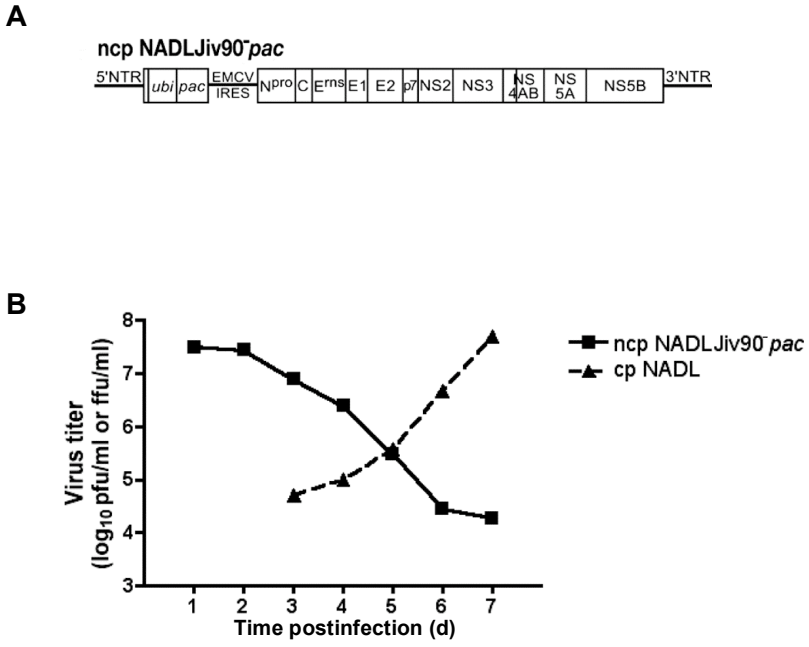

Fig. 4.3 Superinfection exclusion is transient and lost upon passaging. (**A**) Schematic diagram of ncp NADLJiv90-*pac* viral RNA. (**B**) MDBK cells were infected with ncp NADLJiv90-*pac* and maintained under puromycin selection. At 1, 2, 3, 4, and 5 d after acute infection, supernatants were harvested from the infected cells to determine ncp NADLJiv90-*pac* titer by focus forming assay and also superinfected with cp NADL. Two days later, supernatants were harvested and titered by plaque assay to measure the yield of cp NADL. Plaque and focus forming assays were incubated for 3 d under overlaid agarose and then fixed and stained with crystal violet or α-BVDV antibody respectively. The titers of ncp NADLJiv90-*pac* and cp NADL are expressed as focus forming units per ml (ffu/ml) or pfu/ml, respectively.

puromycin selection throughout the course of the experiment ensured that cells superinfected with cp BVDV harbored replicating ncp BVDV, albeit at decreasing titers. These experiments strongly suggest that the loss of superinfection exclusion over time seen in persistently infected cells is due to an alteration occurring in the cells that remained persistently infected with BVDV rather than to a subpopulation of uninfected cells. Additional experiments regarding this point are shown below in Section 4.3.

Superinfecting BVDV is blocked at the level of viral entry

The lack of BVDV replication could be due to the inability of superinfecting BVDV particles to efficiently enter a BVDV-infected cell and/or the inability of the superinfecting viral genome to be translated and replicated after entry. To examine these two options, ncp NADLJiv90^{-}-infected cells were challenged with NADLJiv90^{-}*luc*. To assay primary translation of incoming genome RNA, luciferase activity was measured at 6 h.p.i. with ncp NADLJiv90^{-}*luc*. The 6 h time point was chosen by two criteria. First, infection with NADLJiv90^{-}*luc* in the absence or presence of a potent BVDV-specific RdRp inhibitor (6), resulted in luciferase activities differing by approximately 2.5-fold at 6 h, as compared to a greater than 500-fold difference by 15 h due to replication in the absence of the inhibitor

(data not shown). Second, transfection experiments showed no significant difference in luciferase levels between replication competent and replication defective BVDV replicons at the 6 h time point (see below).

Superinfection of ncp NADLJiv90^{-}-infected cells with ncp NADLJiv90^{-}*luc* virus resulted in luciferase activity almost 100-fold lower than that from naïve MDBK cells infected with ncp NADLJiv90^{-}*luc* (Fig. 4.4A, Infection). Transfection of this construct into ncp NADLJiv90^{-} infected cells showed that the superinfecting genome could be efficiently translated (Fig. 4.4A, Transfection; and below). Therefore, superinfecting ncp NADLJiv90^{-}*luc* was unable to deliver its translation competent RNA genome into ncp NADLJiv90^{-}-infected MDBK cells, indicating a block at the level of entry. Entry is loosely defined here to encompass all of the pre-translation steps.

To investigate the importance of the BVDV structural proteins, an MDBK cell line expressing only the BVDV nonstructural proteins was generated by transfection of a subgenomic ncp NADLJiv90^{-}ΔS-*pac* replicon and selection with puromycin (Fig. 4.4B). An MDBK cell line expressing all of the viral proteins was also generated using full-length ncp NADLJiv90^{-} *pac* RNA (Fig. 4.4B). Both puromycin-selected cell populations were challenged with ncp NADLJiv90^{-}*luc* and the luciferase activity was

Fig. 4.4 Homologous BVDV superinfecting particles are blocked at the level of viral entry. (**A**) Naïve (uninfected) or ncp NADLJiv90^{-}-infected (infected) cells were superinfected (Infection) or transfected (Transfection) with ncp NADLJiv90^{-}*luc*. At 6 h post superinfection or transfection, the cells were lysed and luciferase activity determined. The dashed line represents the background level of the assay from naïve MDBK cells. (**B**) Schematic diagram of ncp NADLJiv90^{-}*pac* and ncp NADLJiv90^{-}ΔS-*pac* viral RNAs. (**C**) ncp NADLJiv90^{-}*pac* (FL), ncp NADLJiv90^{-}ΔS-*pac* (ΔS), and naïve (N) cells were superinfected with ncp NADLJiv90^{-}*luc*. At 6 h.p.i., the cells were lysed and luciferase activity was determined. The dashed line represents the background level of the assay from naïve MDBK cells. (D) Naive (N), ncp NADLJiv90^{-}*pac* (FL), ncp NADLJiv90^{-}ΔC-*pac* (ΔC), ncp NADLJiv90^{-}ΔE^{rns}-*pac* (ΔE^{rns}), ncp NADLJiv90^{-}ΔE1-*pac* (ΔE1), and ncp NADLJiv90^{-}ΔE2-*pac* (ΔE2) selected MDBK cells were infected with ncp NADLJiv90^{-}*luc*. At 6 h.p.i., the cells were lysed and luciferase activity was determined.

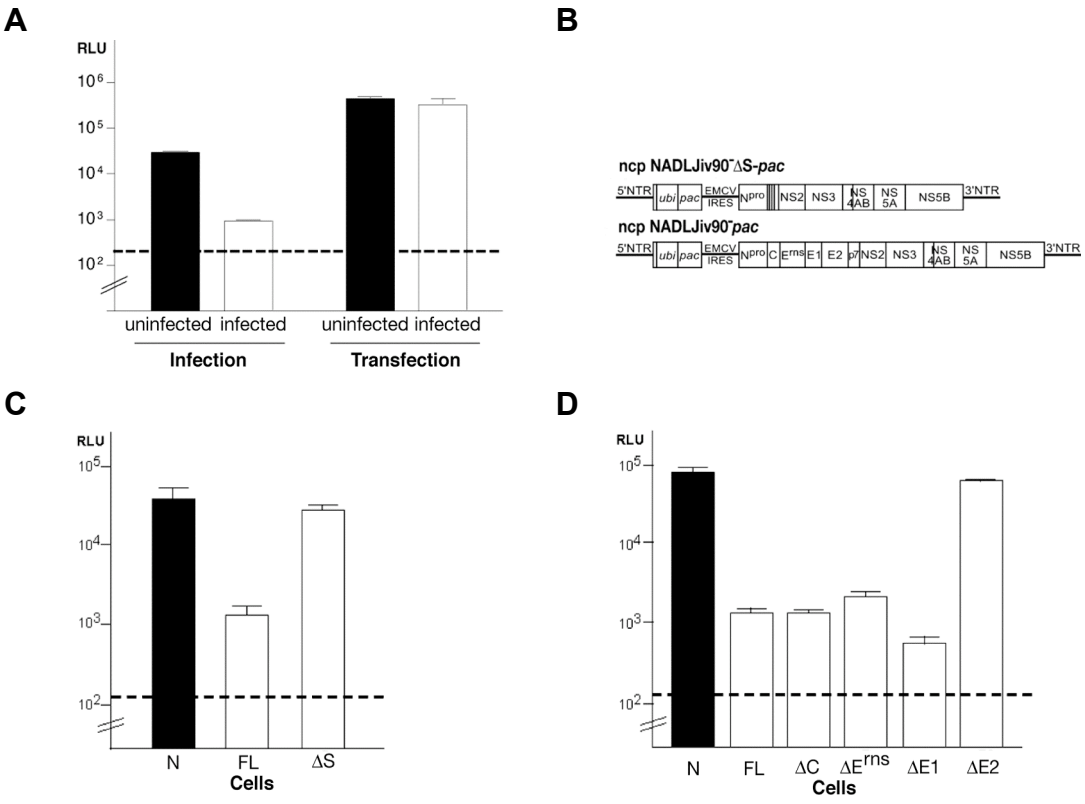
A
RLU
10^6
10^5
10^4
10^3
10^2
uninfected infected uninfected infected
Infection
Transfection
B
ncp NADLJiv90⁻ΔS-pac
5'NTR ubi pac EMCV IRES Npro NS2 NS3 NS 4AB NS 5A NS5B 3'NTR
ncp NADLJiv90⁻pac
5'NTR ubi pac EMCV IRES Npro C Erns E1 E2 p7 NS2 NS3 NS 4AB NS 5A NS5B 3'NTR
C
RLU
10^5
10^4
10^3
10^2
N FL ΔS
Cells
D
RLU
10^5
10^4
10^3
10^2
N FL ΔC ΔErns ΔE1 ΔE2
Cells

Fig. 4.4

determined at 6 h.p.i. In ncp NADLJiv90^{-}*pac* selected cells (Fig. 4.4C, FL) the luciferase activity after superinfection was more than 50-fold less than in naïve cells (Fig. 4.4C, N). In contrast, the ncp NADLJiv90^{-}ΔS-*pac* selected cells, were as susceptible as naïve cells for delivery and early translation of luciferase-expressing virion RNA (Fig. 4.4C, ΔS). These results demonstrate that expression of one or more BVDV structural proteins was required for superinfection exclusion at the level of viral entry.

To investigate which viral structural protein was responsible for exclusion during entry, four puromycin-selected MDBK cell lines were generated. Each harbored a recombinant viral RNA containing an in-frame deletion of each viral structural gene, designated as NADLJiv90^{-}ΔC-*pac*, NADLJiv90^{-}ΔE^{rns}-*pac*, NADLJiv90^{-}ΔE1-*pac*, and NADLJiv90^{-}ΔE2-*pac*. The selected cells appeared to express similar amounts of NS2-3 protein, measured by immunoblotting or radioimmunoprecipitation with an α-NS3 specific antiserum (data not shown). The MDBK cell lines were infected with ncp NADLJiv90^{-}*luc* viral particles and luciferase activity at 6 h.p.i. was determined. Luciferase activities obtained from ncp NADLJiv90^{-}ΔC-*pac*, ncp NADLJiv90^{-}ΔE^{rns}-*pac*, and ncp NADLJiv90^{-}ΔE1-*pac* mutant cell lines upon superinfection with ncp NADLJiv90^{-}*luc* virus (Fig. 4.4D, ΔC, ΔE^{rns}, ΔE1), were similar to cells expressing a full complement of structural

proteins (Fig. 4.4D, FL). These results suggest that the viral structural proteins C, E^{rns}, and E1 do not play a major role in exclusion at the level of viral entry. In contrast, ncp NADLJiv90^{-}*luc* infection of the ncp NADLJiv90^{-}ΔE2-*pac* selected cells resulted in similar luciferase activity (Fig. 4.4D, ΔE2) to that obtained from infection of naïve MDBK cells (Fig. 4.4D, N). Hence, these findings show that deletion of viral glycoprotein E2 was sufficient to abolish the exclusion at the level of viral entry. Interestingly, although ncp NADLJiv90^{-}*luc* could be efficiently translated in the ncp NADLJiv90^{-}ΔE2-*pac* selected cells there was no amplification of this genome, suggesting a second, internal block to superinfection might exist.

Transfection of BVDV RNA reveals a second block at replication, but not translation

To determine if superinfecting viral RNA would be competent for replication if it were allowed to bypass the viral entry steps, MDBK cells acutely infected with ncp NADLJiv90^{-} were transfected with ncp NADLJiv90^{-}*pac* RNA. These cells did not survive puromycin selection (Fig. 4.5, plate 8), indicating that the transfected ncp NADLJiv90^{-}*pac* RNA had failed to replicate. Naïve MDBK cells transfected with ncp NADLJiv90^{-}*pac* RNA transcripts were able to grow in media containing puromycin, and

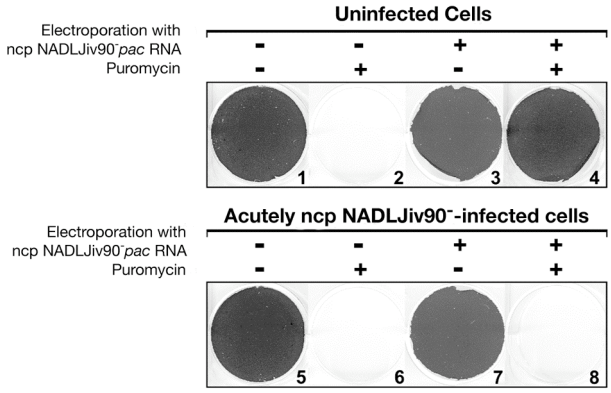

Fig. 4.5 Transfected ncp NADLJiv90^{-}*pac* RNA fails to replicate in ncp NADLJiv90^{-} infected cells. Naïve MDBK cells were either mock-infected (plates 1-4) or acutely infected with ncp NADLJiv90^{-} (plates 5-8). The cells were then mock-transfected or transfected with *in vitro* transcribed ncp NADLJiv90^{-}*pac* RNA. + or – above each column of plates indicates transfection or mock-transfection with ncp NADLJiv90^{-}*pac* RNA, respectively. Following transfection, the cells were incubated in culture media +/- 5 μg/ml of puromycin as indicated, and viable cells were fixed and stained with crystal violet after 5 d.

eventually became confluent (Fig. 4.5, plate 4). Whereas, MDBK cells infected with only ncp NADLJiv90$^-$ were unable to survive puromycin selection (Fig. 4.5, plate 6). Transfection of an alphavirus-based expression vector SINrep3-*lacZ* (61) indicated that there was no significant difference in transfection efficiency of naïve vs. BVDV-infected MDBK cells (data not shown). These findings demonstrate that the ncp NADLJiv90$^-$*pac* RNA transfected into MDBK cells acutely infected with ncp NADLJiv90$^-$ was unable to replicate to a level required for puromycin selection, and suggests an additional post-entry block to superinfection.

Since translation of the incoming genome is a prerequisite for RNA replication, additional experiments were performed (besides that described in Fig. 4.4A) to examine translation of BVDV RNA transfected into acutely BVDV-infected MDBK cells. To more clearly distinguish between translation of input RNA versus signal due to productive replication, a subgenomic ncp BVDV replicon, ncp NADLJiv90$^-$ΔS-*luc*, encoding the *luc* reporter with its isogenic replication-incompetent derivative, ncp NADLJiv90$^-$ΔS-*luc*-*pol*$^-$ (Fig. 4.6A), were compared. In naïve MDBK cells transfected with ncp NADLJiv90$^-$ΔS-*luc* RNA (Fig. 4.6B, solid circles), the luciferase activity at 6 h post transfection was similar to that observed with the *pol*$^-$ replicon (Fig. 4.6B, open circles), indicating (as mentioned earlier)

Fig. 4.6 ncp NADLJiv90$^-$ΔS-*luc* viral RNA transfected into ncp NADLJiv90$^-$-infected MDBK cells is competent for translation, but not for replication. (**A**) Schematic diagram of ncp NADLJiv90$^-$ΔS-*luc* and ncp NADLJiv90$^-$ΔS-*luc-pol*$^-$ viral RNAs. (**B**) Either 8 x 10^6 naïve (closed circles) or ncp NADLJiv90$^-$-infected MDBK cells (closed squares) were electroporated with 5 μg of ncp NADLJiv90$^-$ΔS-*luc* RNA. In parallel, 5 μg of ncp NADLJiv90$^-$ΔS-*luc-pol*$^-$ RNA was electroporated into naïve (open circles) and ncp NADLJiv90$^-$-infected (open squares) cells. The luciferase activity was measured at the indicated time. The dashed line indicates the background level of the assay from naïve MDBK cells. (**C**) Naïve MDBK cells were transfected with ncp NADLJiv90$^-$ΔS-*pac* or ncp NADLJiv90$^-$*pac* RNA and then selected with 5 μg/ml of puromycin. Both ncp NADLJiv90$^-$ΔS-*pac* selected (closed and open triangles) and ncp NADLJiv90$^-$*pac* selected cells (closed and open squares) were electroporated with either ncp NADLJiv90$^-$ΔS-*luc* RNA (closed triangles and squares) or ncp NADLJiv90$^-$ΔS-*luc-pol*$^-$ RNA (open triangles and squares). Naïve cells (closed and open circles) were also electroporated with ncp NADLJiv90$^-$ΔS-*luc* RNA (closed circles) or ncp NADLJiv90$^-$ΔS-*luc-pol*$^-$ RNA (open circles). After incubation for the indicated times, cell lysates were prepared and luciferase activity was determined.

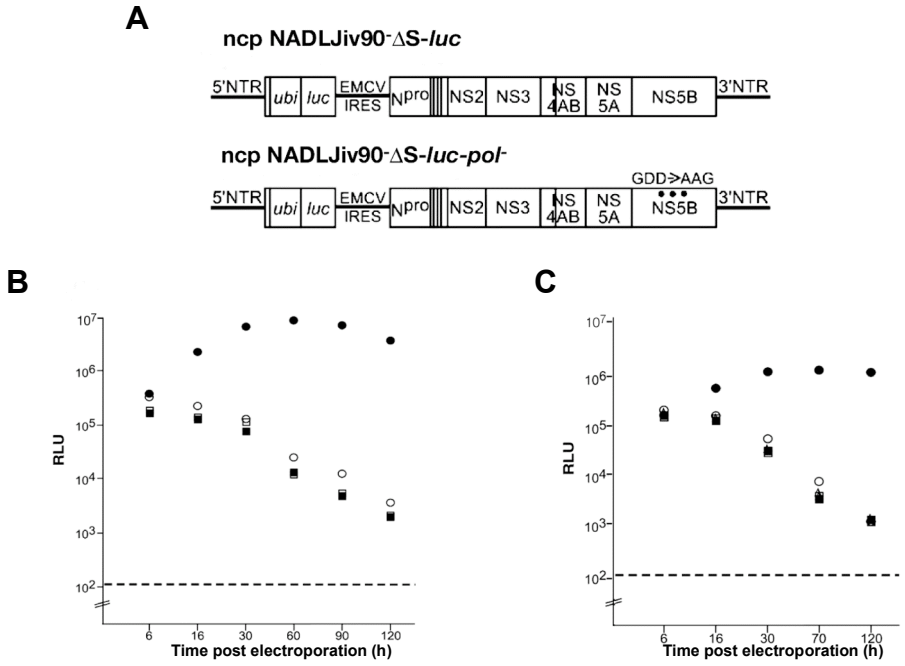
A
ncp NADLJiv90-ΔS-luc
5'NTR
ubi
luc
EMCV IRES
Npro
NS2
NS3
NS 4AB
NS 5A
NS5B
3'NTR
ncp NADLJiv90-ΔS-luc-pol-
GDD≫AAG
B
RLU
Time post electroporation (h)
C
RLU
Time post electroporation (h)

Fig. 4.6

that detectable RNA replication had not taken place at this early time point. Transfection of either ncp replicon into ncp NADLJiv90$^-$-infected MDBK cells resulted in similar luciferase levels at the 6 h time point (Fig. 4.6B, closed and open squares). Therefore, in ncp NADLJiv90$^-$-infected MDBK cells, transfected ncp NADLJiv90$^-$ΔS-*luc* viral RNA can be translated as efficiently as in uninfected cells.

After 6 h, the luciferase activity in naïve MDBK cells transfected with ncp NADLJiv90$^-$ΔS-*luc-pol*$^-$ RNA gradually decreased over time (Fig. 4.6B, open circles). In contrast, the luciferase activity from naïve cells transfected with ncp NADLJiv90$^-$ΔS-*luc* RNA dramatically increased at 16 h post transfection, and maintained this activity until the final time point at 120 h post transfection (Fig. 4.6B, solid circles). In contrast, in ncp NADLJiv90$^-$-infected MDBK cells, both initial activities decreased over time similarly to naïve MDBK cells transfected with ncp NADLJiv90$^-$ΔS-*luc-pol*$^-$ RNA (Fig. 4.6B, open circles). Therefore, in ncp NADLJiv90$^-$-infected MDBK cells viral RNA can be translated, but this RNA fails to replicate. These results demonstrate a second block at the level of BVDV RNA replication. The fact that there is no amplification of luciferase expression from the *pol*$^-$ genome after transfection of ncp NADLJiv90$^-$-infected cells indicated that lethal

mutations in the BVDV RdRp, NS5B, could not be trans-complemented, consistent with previous results (72).

To examine if the BVDV structural proteins were required for superinfection exclusion at the level of RNA replication, subgenomic ncp NADLJiv90^{-}ΔS-*pac* and full-length ncp NADLJiv90^{-}*pac* selected cells were transfected with NADLJiv90^{-}ΔS-*luc* (Fig. 4.6C, solid triangles) or NADLJiv90^{-}ΔS-*luc-pol*$^{-}$ (Fig. 4.6C, open triangles). In both cases, the luciferase activity decreased over time, and mirrored that of ncp NADLJiv90^{-}*pac* selected cells transfected with the *luc* replicons (Fig. 4.6C, solid and open squares). These results show that expression of the BVDV structural proteins is not required for exclusion at the level of viral RNA replication.

Level of RNA replication correlates with the extent of superinfection exclusion

A possible factor in the block at RNA replication could be the level of RNA replication in the infected cell. This hypothesis was supported by the observation that when puromycin-selected cells infected with ncp NADLJiv90^{-}*pac* were superinfected with cp NADL at various time points post primary infection, the increase in cp NADL titer over time on the

persistently infected cells directly correlated with a decrease in the ncp NADLJiv90^{-}*pac* titer (Fig. 4.3B).

To further examine this possible correlation, MDBK cell lines supporting different levels of viral RNA replication were generated by transfecting puromycin selectable replicons lacking the structural region to exclude structural protein effects. Since RNA replication of cp NADL has been shown to be higher than that of ncp NADLJiv90^{-} (143), both cp and ncp replicons were used. Naïve MDBK cells were transfected with either ncp NADLJiv90^{-}ΔS-*pac* or cp NADLΔS-*pac* viral RNAs and yielded puromycin resistant colonies that were picked and expanded into cell lines. As might be expected from previous work (168), the replicons within clones Cl.2, Cl.11 and Cl.10 were sequenced and found to contain adaptive mutations in the NS4B-5A region allowing persistent ncp replication. Some of these mutations have been previously characterized (168); others are the subject of ongoing work (M. Paulson, personal communication). Metabolic labeling of viral RNA using [^{32}P] orthophosphate showed the relatively low level of viral RNA replication in Cl.2 (<5%), harboring the ncp NADLJiv90^{-} ΔS-*pac* replicon, and higher levels in Cl.10 (50%), and Cl.11 (100%), harboring cp NADLΔS-*pac* replicons (Fig. 4.7A).

Fig. 4.7 The level of primary viral RNA replication correlates with the degree of superinfection exclusion at viral RNA replication. (**A**) Cell clones harboring different levels of BVDV RNA replication were generated by transfection of naïve MDBK cells with ncp NADLJiv90^{-}ΔS-*pac* or cp NADLΔS^{-}*pac* RNAs and selection with puromycin. Cl.2 was derived from ncp NADLJiv90^{-}ΔS-*pac* selected cells and Cl.10 and Cl.11 were derived from cp NADLΔS^{-}*pac* selected cells. The three cell clones were metabolically labeled for 6 h with [^{32}P] orthophosphate in the presence of dactinomycin. The viral RNAs were analyzed by gel electrophoresis and visualized by autoradiography. Labeled viral RNA was quantified by phosphoimage analysis. The relative levels of RNA replication are expressed in the bar graph as percent of replication in Cl.11, set at 100%. (**B**) Naïve MDBK cells (solid bar), Cl.2 (gray bar), Cl.10 (patterned bar), and Cl.11 (open bar) were infected with cp NADL. At a given time point, culture supernatants were collected and used to determine the virus titer. The extent of CPE caused by cp NADL viral replication was estimated under light microscopy and indicated by +/-. ∗ represents the absence of attached viable cells on culture dishes.

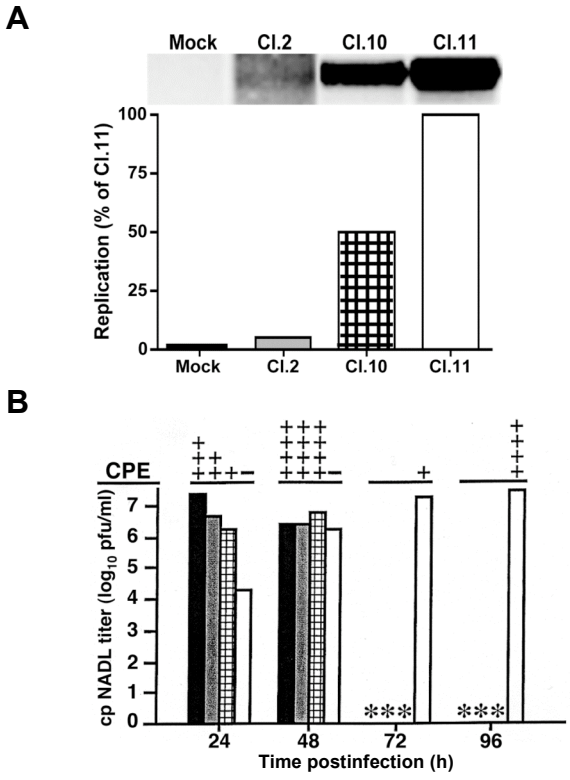
A
Mock
Cl.2
Cl.10
Cl.11
Replication (% of Cl.11)
100
75
50
25
0
Mock
Cl.2
Cl.10
Cl.11
B
CPE
+
++
+++
–
+++
+++
+++
–
+
+
+++
+
cp NADL titer (log10 pfu/ml)
7
6
5
4
3
2
1
0
***
***
24
48
72
96
Time postinfection (h)

Fig. 4.7

The cell clones were infected with cp NADL and observed for the extent of CPE and virus yield. At 24 h post transfection, maximum virus titer and clear CPE were observed in naïve MDBK cells (Fig. 4.7B, solid bar). In contrast, Cl.2 (Fig. 4.7B, gray bar) and Cl.10 (Fig. 4.7B, patterned bar) only displayed extensive CPE and reached maximum titer by 48 h post transfection. Cl.11, which had the highest level of ncp BVDV RNA replication, was protected from significant CPE until 72 h post transfection (Fig. 4.7B, open bar). Therefore, the level of ncp BVDV primary RNA replication strongly correlates with the extent of superinfection exclusion at the RNA replication level. An additional experiment supporting this hypothesis is described below (Section 4.3).

4.3 Additional studies of BVDV superinfection exclusion

BVDV superinfection exclusion is transient and lost upon passaging

To further examine the observation that superinfection exclusion may be lost during persistent infection, naïve MDBK cells were infected with ncp NADLJiv90^{-} and passaged every 2-3 d. At each passage, the ncp NADLJiv90^{-}-infected cells were superinfected with cp NADL and monitored for the ability to undergo CPE.

At passage 0 neither CPE nor visible plaques (Fig. 4.8A and data not shown) were found in the ncp NADLJiv90$^-$-infected cells upon superinfection with cp NADL. In contrast, upon superinfection of passage 1 cells, persistently infected for 3 d, major CPE and visible plaques were observed (Fig. 4.8A and data not shown). There was, however, an approximately 6-fold decrease in titer compared to cp NADL infection of naïve P1 cells (Fig. 4.8B). The extent of CPE and size of the plaques were also diminished compared to infection of the naïve P1 cells (Fig. 4.8A and data not shown). Superinfection of additional passages of persistently infected cells did not result in further changes to cp NADL titer, plaque size or the extent of CPE (Fig. 4.8B and data not shown). Thus, while persistently infected cells quickly lost the majority of the superinfection exclusion phenotype, their infectability was not fully restored even out to passage 20 and greater (data not shown). Nonetheless, the ability to efficiently exclude a superinfecting virus is primarily a transient phenotype associated with acutely infected cells.

Although it had been shown that the loss of superinfection exclusion was most likely not due to a mixed population of cells with only some infected by ncp NADLJiv90$^-$ (Section 4.2), to rigorously rule out this possibility, I examined the percentage of BVDV-positive cells at each

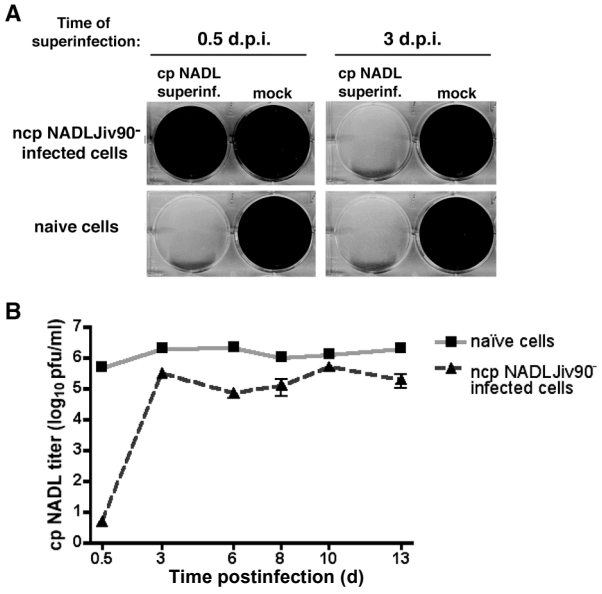

Fig. 4.8 MDBK cells persistently infected with ncp NADLJiv90$^-$ are not protected from cp NADL-induced CPE. (**A**) MDBK cells were infected with ncp NADLJiv90$^-$. At 0.5 and 3 d.p.i. the cells were superinfected with cp NADL or mock-superinfected as indicated above each column of plates. Naïve cells were also infected or mock-infected for comparison. The cells were incubated in liquid media for 3 d at which time they were fixed and stained with crystal violet to visualize live cells surviving CPE. (**B**) ncp NADLJiv90$^-$-infected and uninfected cells were maintained by passaging for a period of 13 d. Every 2-3 d, the cells were superinfected with cp NADL. Naïve cells were maintained over the same time period and infected in parallel. After superinfection, the cells were grown under overlaid agarose for 3 d and then fixed and stained with crystal violet. Plaques were enumerated and cp NADL titer on naïve cells or ncp NADLJiv90$^-$ infected cells was expressed as pfu/ml.

passage by flow cytometry using a BVDV α-NS3 antibody. Over a period of 5 passages, the majority of cells, 75.1 ± 13.0%, remained positive for BVDV antigen, although the ability to exclude superinfecting cp NADL was lost after 3 d of infection (passage 1) when at least 91% of cells were NS3 positive.

I also examined whether cells persistently infected with ncp BVDV lose the ability to exclude superinfecting ncp BVDV as well as cp BVDV. Persistently infected MDBK cells were infected with ncp NADLJiv90^{-}*luc* every 2-3 d over a period of 5 passages. At 24 h post superinfection, the cells were harvested to assay for luciferase activity. Although a small increase in luciferase activity was observed after superinfection of passage 2-5 persistently infected cells, the average luciferase activity on the persistently infected cells was only 0.69 ± 1.2% of that on the naïve cells, and never rose to more than 3% of the naïve cell luciferase activity (data not shown). Therefore, cells persistently infected with ncp BVDV remain efficient at excluding ncp BVDV over time as measured by this assay.

Decreased RNA levels during persistent ncp BVDV infection render cells susceptible to cp BVDV superinfection

To complement the experiments described in Section 4.2 regarding the level of BVDV RNA replication and its correlation with the degree of exclusion, I also looked directly at RNA levels in persistently infected cells. As superinfection exclusion of cp BVDV disappeared in persistently infected cells by approximately 3 d.p.i., the appearance of high titers of cp NADL correlated with a 6-fold decrease in ncp NADLJiv90$^-$ RNA levels as quantified by real-time quantitative RT-PCR (Fig. 4.9). In later passages the level of ncp NADLJiv90$^-$ RNA remained relatively constant, as did the titer of cp NADL on the persistently infected cell monolayers (Fig. 4.9). Hence, primary viral RNA levels decrease during persistent ncp BVDV infection and this correlates with the loss superinfection exclusion of cp BVDV.

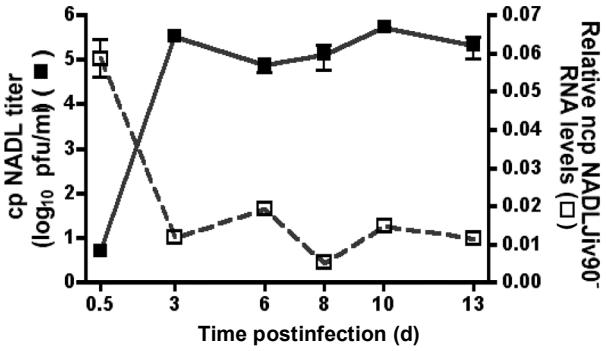

Fig. 4.9 The loss of superinfection exclusion in BVDV persistently infected cells correlates with a decrease in primary viral RNA replication. ncp NADLJiv90^{-}-infected cells were maintained by passaging for a period of 13 d. Every 2-3 d, the cells were superinfected with cp NADL and titers were determined by plaque assay as indicated on the left y-axis. The ncp NADLJiv90^{-}-infected cells were also analyzed for levels of ncp NADLJiv90^{-} RNA at each time point. Total cellular RNA was isolated and BVDV-specific RNA was quantified using real-time quantitative RT-PCR. The relative levels of ncp NADLJiv90^{-} RNA, indicated on the right y-axis, are expressed as the ratio of copies of BVDV RNA to copies of bovine β-actin RNA.

4.4 HCV superinfection exclusion

Superinfection exclusion in HCVcc-infected and replicon-containing Huh-7.5 cells

To determine if previous infection with HCV renders cells resistant to secondary HCV infection, Huh-7.5 cells were infected with J6/JFH genotype 2a chimeric virus (MOI 0.01) (123). At 4 d.p.i., when approximately 77% of cells stained positive for NS5A antigen (data not shown), the J6/JFH-acutely infected cells, in parallel with naïve Huh-7.5 cells, were challenged with the HCVcc *Renilla* luciferase reporter virus FL-J6/JFH-5'C19Rluc2AUbi (HCVcc-Rluc) (Fig. 4.10) (198). FL-J6/JFH-5'C19Rluc2AUbi encodes the first 19 residues of the HCV C protein fused to the N-terminus of *Renilla* luciferase (Rluc). The C-terminus of Rluc is fused to a 17-residue fragment from the self-cleaving foot and mouth disease virus 2A protein (2A), a ubiquitin monomer (Ubi) sequence, and finally the complete HCV polyprotein. Together, 2A and Ubi mediate removal of Rluc from the HCV polyprotein and generate the native N terminus of the HCV C protein. Luciferase activity resulting from HCVcc-Rluc superinfection of J6/JFH-infected cells was <10% of the Huh-7.5 luciferase signal, suggesting that superinfection exclusion is established in HCV-infected cells (Fig. 4.11A).

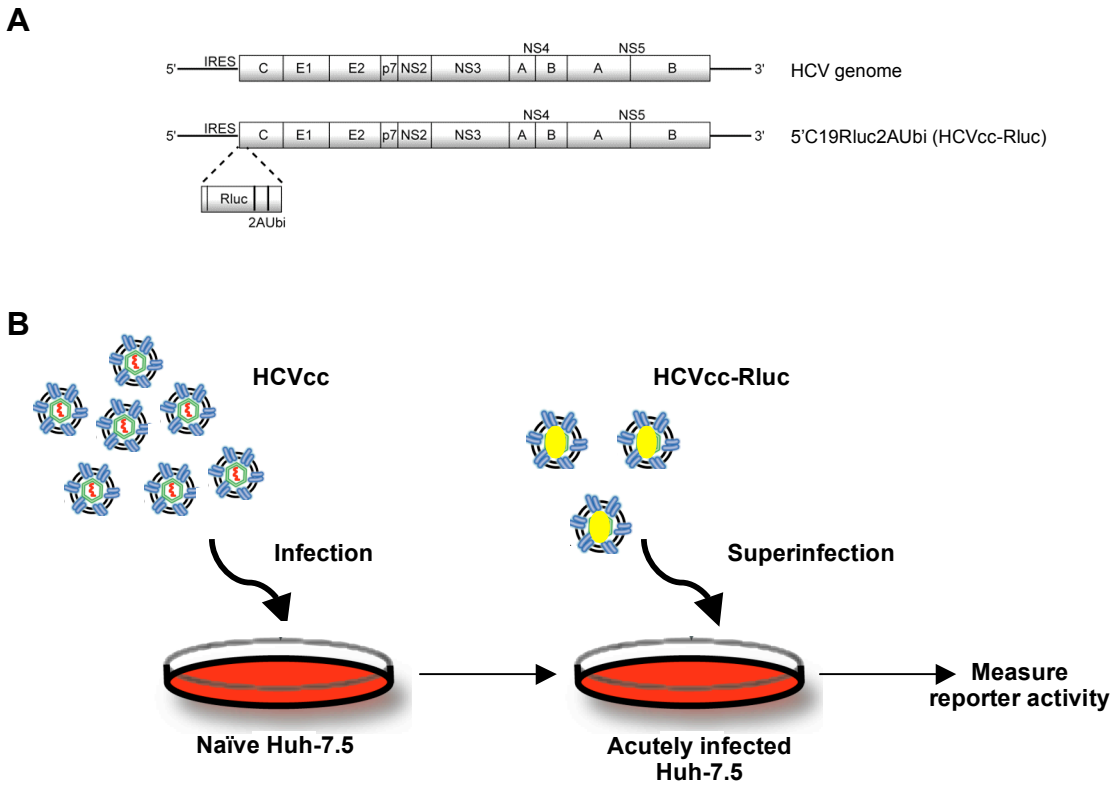

Fig. 4.10 Scheme for analysis of HCV superinfection exclusion. (A) Schematic of HCV and FL-J6/JFH-5'C19Rluc2AUbi (HCVcc-Rluc) genomes. The 5' NTR contains an internal ribosome entry site (IRES), which allows translation of the HCV polyprotein containing structural (C, E1, E2) and nonstructural proteins (p7, NS2, NS4A, NS4B, NS5A, and NS5B). FL-J6/JFH-5'C19Rluc2AUbi is a full-length HCV genome encoding the *Renilla* luciferase (Rluc), a foot and mouth disease virus (FMDV) 2A sequence (2A), and a ubiquitin monomer sequence (Ubi). The N-terminus of Rluc is fused to the first 19 residues of the HCV C protein. (**B**) Huh-7.5 cells were infected with HCVcc. After 4 d, these cells were superinfected with HCVcc-Rluc. Luciferase activity was measured at 24 h.p.i. as a readout for superinfection.

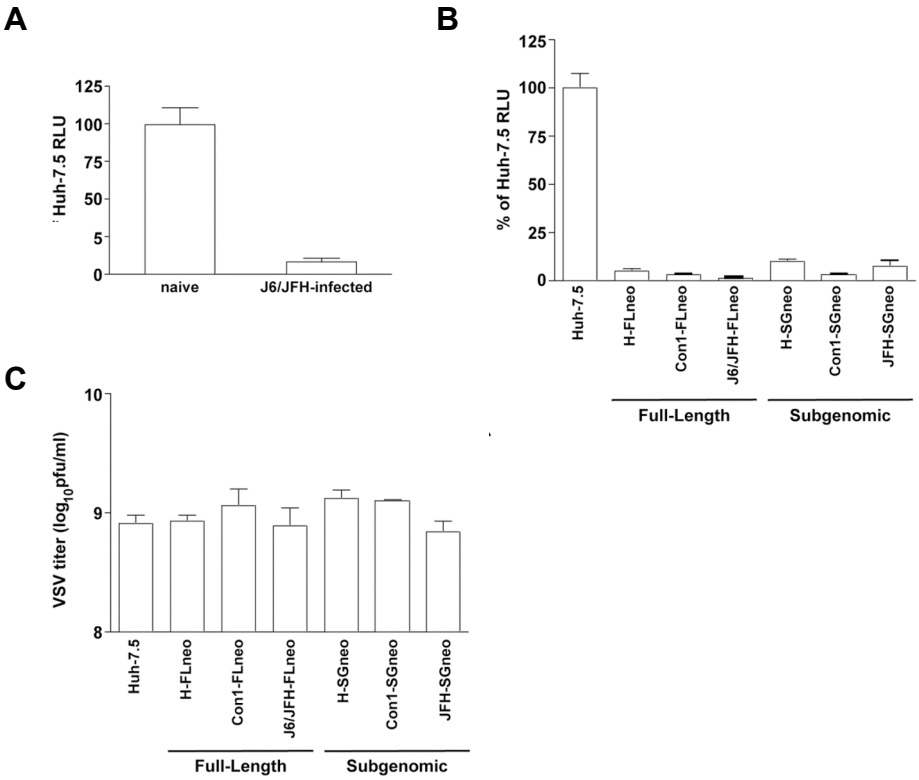

Fig. 4.11 Cells harboring HCV do not support HCVcc superinfection. (**A**) Huh-7.5 cells were infected with J6/JFH HCVcc and maintained in parallel with naïve cells. At 4 d.p.i., when approximately 77% of cells were NS5A positive, J6/JFH-acutely infected and naïve cells were superinfected with HCVcc-Rluc. Each bar, expressed as the percentage of the Huh-7.5 RLU, is the average value of triplicate wells; error bars show the standard deviations. RLU, relative light units. (**B**) Huh-7.5 and HCV full-length or subgenomic replicon-containing cells were infected with HCVcc-Rluc. Luciferase activity was measured at 24 h.p.i. Values, expressed as the percentage of Huh-7.5 RLU, are the combined data from two independent experiments done in triplicate; error bars represent the standard errors of the means. (**C**) Huh-7.5 and HCV replicon cells were infected with VSV and overlayed with agarose. After 16 h, cells were fixed with formaldehyde and stained with crystal violet to visualize plaques. Each bar is the mean titer from duplicate wells; error bars represent the standard errors of the means.

To determine if superinfection exclusion occurs across genotypes and in cells harboring long-term, persistent HCV replication, I generated HCV genotype 1a, 1b, and 2a full-length replicon-bearing cell populations. The bicistronic RNAs, H-FLneo (genotype 1a, H77), Con1-FLneo (genotype 1b, Con1), and J6/JFH-FLneo (genotype 2a, J6/JFH chimera), used to establish these replicon cells express the dominant selectable marker neomycin *N*-acetyltransferase (*neo*), which provides resistance to the drug G418 and thus allows stable maintenance of cells harboring replicating HCV RNA. The expression of *neo* is driven by the HCV IRES, while the EMCV IRES drives translation of the HCV polyprotein in the downstream cistron.

Following challenge of H-FLneo, Con1-FLneo, and J6/JFH-FLneo cells, as well as Huh-7.5 parental cells with HCVcc-Rluc (MOI 0.01), all of the replicon-containing cells were able to efficiently exclude HCVcc, yielding <10% of the luciferase activity of infected Huh-7.5 cells (Fig. 4.11B). This result indicates that cells harboring HCV genotypes 1a, 1b, or 2a, exhibit superinfection exclusion against genotype 2a HCVcc, similar to that observed in cells acutely infected with J6/JFH (Fig. 4.11A). To rule out that resistance to HCV infection was due to expression of the *neo* resistance gene by the HCV replicons, I challenged Huh-7.5 cells, which had been transiently transfected with a plasmid expressing *neo*, with HCVcc-Rluc.

Luciferase activity from the transfected cells was >80% of naïve Huh-7.5 cells, despite similar levels of NPTII expression compared to the HCV replicon-containing cells (data not shown).

To establish whether expression of the HCV structural-NS2 region was required for superinfection exclusion, I challenged Huh-7.5 cell populations selected for stable maintenance of H-SGneo, Con1-SGneo, or JFH-SGneo RNAs, the subgenomic counterparts of the full-length genomes described above. These genomes express *neo* and HCV NS3-NS5B via the HCV IRES and EMCV IRES, respectively. Similar to results observed with the full-length replicon cells, luciferase activity after infection of the HCV subgenomic replicon cell populations with HCVcc-Rluc was reduced to <15% compared to naïve Huh-7.5 cells (Fig. 4.11B).

Infection of replicon-containing cells with VSV yielded titers that were comparable to those observed on Huh-7.5 cells (Fig. 4.11C). This excludes the possibility that the observed HCVcc superinfection exclusion was due to the induction of a non-specific antiviral state.

Treatment with BILN 2061 restores HCV permissiveness

I treated the H-SGneo, Con1-SGneo, and JFH-SGneo replicon cells with the HCV-specific protease inhibitor BILN 2061 and subsequently

challenged with HCVcc-Rluc. At 4 d post treatment, HCVcc permissiveness was partially restored in H-SGneo, Con1-SGneo, and JFH-SGneo cells that had been treated with BILN 2061, as RLU values from these cells, and not from DMSO-treated cells, were at least 50% of Huh-7.5 control cells (Fig. 4.12A). The increase in HCVcc permissiveness in BILN 2061-treated cells coincided with an approximate 100-fold decrease in HCV RNA levels, compared to the DMSO-treated cells (Fig. 4.12B). By 9 d of BILN 2061 treatment, viral RNA levels had decreased further and the cells became fully permissive for HCVcc infection. A slight but unexpected decrease in luciferase activity was observed in BILN 2061-treated Huh-7.5 cells at the later time points. This was observed in several repetitions of the experiment (data not shown), suggesting that prolonged BILN 2061 treatment may create a cellular environment less favorable for HCV replication or select a subpopulation of less permissive cells. In any case, the dramatic increase in HCVcc permissiveness observed in BILN 2061-treated replicon cells indicates that superinfection exclusion requires the continuing presence of HCV RNA and/or proteins and is readily reversible by treatment with specific antivirals.

Fig. 4.12 HCV subgenomic replicon cells treated with an HCV-specific protease inhibitor become permissive for HCVcc infection. (**A**) Huh-7.5, JFH-SGneo, Con1-SGneo, and H-SGneo cells were treated with BILN 2061 or DMSO in the absence of G418 for 4 or 9 d. BILN 2061 (white and gray bars) or DMSO (black bars) -treated cells were infected with HCVcc-Rluc, in the absence of inhibitor, and samples were harvested for luciferase assays at 24 h.p.i. Black bars (DMSO-treated cells) represent the average RLU value over days 4 and 9 for each DMSO-treated cell population, compared to Huh-7.5 cells. RLU values from BILN 2061-treated cells (Gray and white bars) on day 4 or 9 are expressed as the percentage of the DMSO-treated Huh-7.5 RLU on day 4 or 9, respectively. Each bar is the average value of triplicate wells; error bars show the standard deviations. The data shown is representative of at least 2 independent experiments. (**B**) HCV RNA levels in DMSO (black bars) or BILN 2061-treated JFH-SGneo, Con1-SGneo, and H-SGneo replicon-containing cells at 4 (gray bars) or 9 d (white bars) post treatment were determined by real-time quantitative RT-PCR. Black bars (DMSO-treated cells) represent the average RNA level over days 4 and 9 for each DMSO-treated cell population. Error bars show the standard deviations.

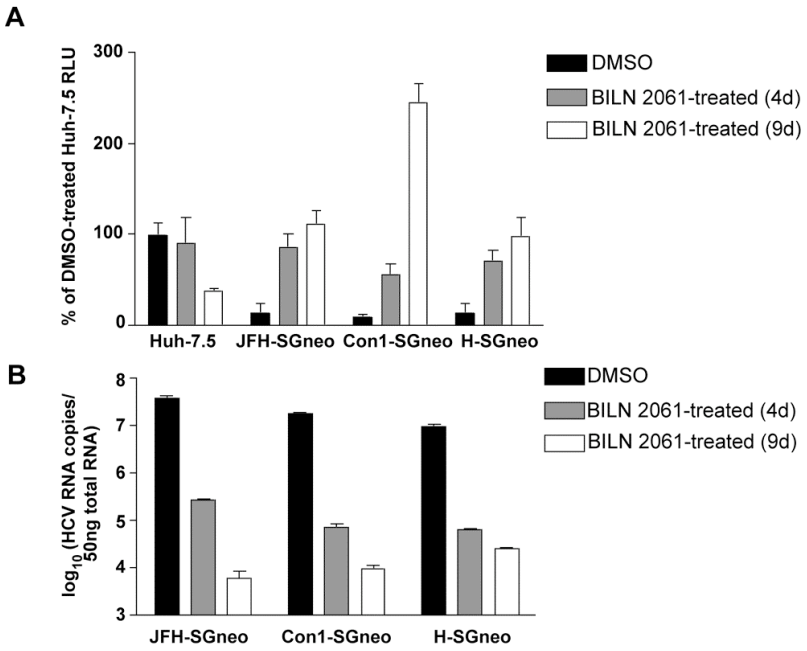
A
300
200
100
0
% of DMSO-treated Huh-7.5 RLU
DMSO
BILN 2061-treated (4d)
BILN 2061-treated (9d)
Huh-7.5
JFH-SGneo
Con1-SGneo
H-SGneo
B
8
7
6
5
4
3
log10 (HCV RNA copies/ 50ng total RNA)
DMSO
BILN 2061-treated (4d)
BILN 2061-treated (9d)
JFH-SGneo
Con1-SGneo
H-SGneo

Fig. 4.12

Superinfection exclusion occurs downstream of viral entry

Given that superinfection exclusion occurs at both entry and replication for BVDV [(119) and Sections 4.2, 4.3], I used lentiviral pseudoparticles bearing HCV glycoproteins (HCVpp) to examine HCV entry in acutely infected or stable replicon cell populations (Fig. 4.13). HCV glycoprotein-mediated HCVpp entry was monitored via expression of luciferase from the encapsidated HIV RNA genome (HCVpp-Luc) (13, 85). J6/JFH-acutely infected cells (4 d.p.i., 77% HCV NS5A positive; Fig. 4.11A) exhibited similar luciferase activity as naïve Huh-7.5 cells when infected with HCVpp-Luc bearing J6 glycoproteins (Fig. 4.14A). This suggested a block downstream of entry given the resistance of this cell population to HCVcc.

Full-length and subgenomic HCV replicon-containing cells were also challenged with HCVpp-Luc bearing J6 or H77 glycoproteins. With the exception of cells harboring the stable J6/JFH-FLneo replicon, all of the replicon-containing cells were fully permissive for HCVpp (Fig. 4.14B), suggesting that the dominant mechanism(s) of HCVcc exclusion in these selected cell populations was also post-entry.

Unexpectedly, HCVpp-expressed luciferase activity in the stable J6/JFH-FLneo replicon population was reduced 98% (J6 HCVpp) and 80%

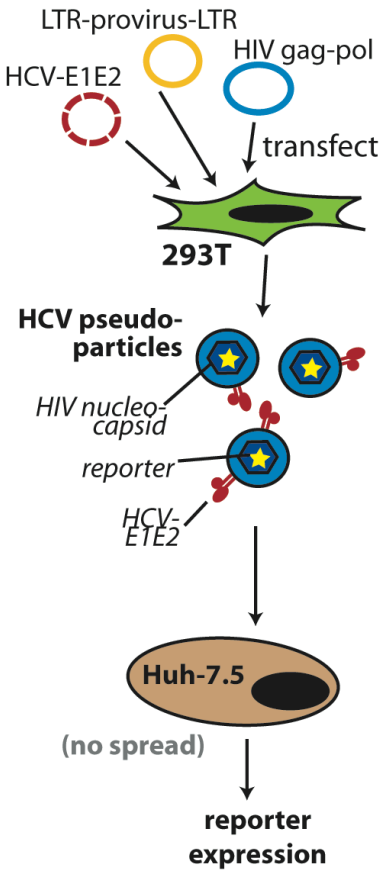

Fig. 4.13 The HCVpp system. 293T cells are cotransfected with an HIV-1 provirus expressing a luciferase or GFP reporter, a Gag-pol expression construct, and an HCV E1-E2 expression construct. HCVpp, secreted into the supernatants of the transfected cells, harbor an HIV-1 nucleocapsid expressing the reporter gene and HCV E1-E2 glycoproteins on their surface. HCVpp can be used to infect target cells, such as Huh-7.5, and give rise to reporter expression, but no spread of the virus throughout the culture.

Fig. 4.14 J6/JFH-acutely infected cells, but not cells harboring a stable J6/JFH-FLneo replicon, are permissive for HCVpp infection. (**A**) Huh-7.5 cells were infected with J6/JFH HCVcc and maintained in parallel with naïve cells. At 4 d.p.i., when approximately 77% of cells were NS5A positive, J6/JFH-acutely infected and naïve cells were superinfected with HCVpp-Luc bearing strain J6 glycoproteins. Each bar, expressed as the percentage of the Huh-7.5 RLU, is the average value of triplicate wells; error bars show the standard deviations. (**B**) Huh-7.5 and HCV full-length or subgenomic replicon-containing cells were infected with HCVpp-Luc bearing HCV genotype 1a, strain H77 (black bars) or genotype 2a, strain J6 (white bars) glycoproteins or with VSVGpp-Luc. Luciferase activity was measured at 72 h.p.i. HCVpp-Luc RLU were normalized to VSVGpp-Luc RLU and expressed as the percentage of the Huh-7.5 cell RLU. Each bar is the combined data from at least two independent experiments done in triplicate; error bars represent the standard errors of the means.

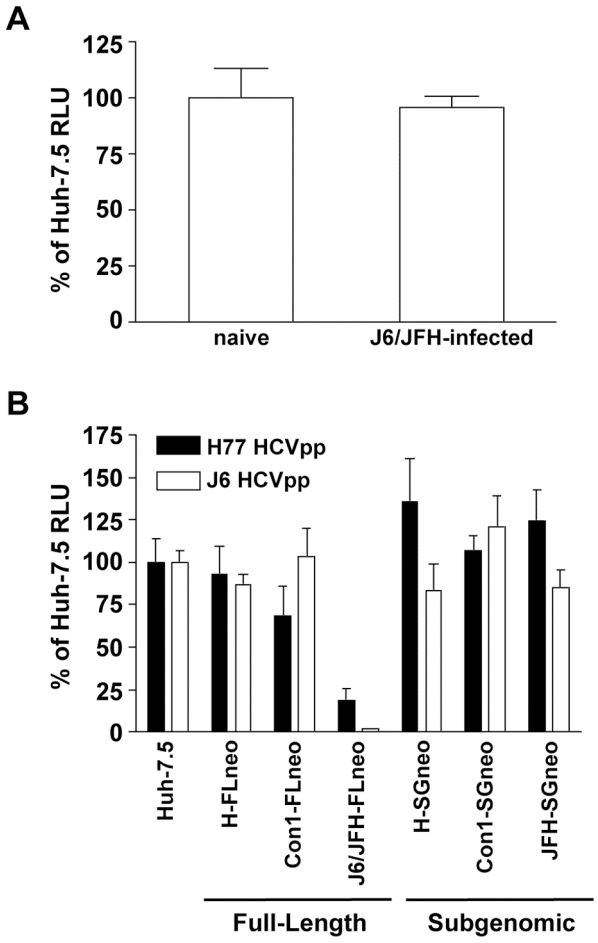
A
% of Huh-7.5 RLU
125
100
75
50
25
0
naive
J6/JFH-infected
B
% of Huh-7.5 RLU
175
150
125
100
75
50
25
0
H77 HCVpp
J6 HCVpp
Huh-7.5
H-FLneo
Con1-FLneo
J6/JFH-FLneo
H-SGneo
Con1-SGneo
JFH-SGneo
Full-Length
Subgenomic

Fig. 4.14

(H77 HCVpp) compared to control Huh-7.5 cells, in contrast to cells acutely infected with J6/JFH, which were fully permissive to HCVpp (Fig. 4.14A). These data suggest that in cells selected for long-term, persistent J6/JFH-FLneo replication, there is an additional block at the level of entry. I address this surprising observation in more detail below.

Examination of the post-entry superinfection block

To further define the superinfection block, I determined whether translation of incoming HCV RNA was inhibited. To monitor translation in the absence of viral replication, JFH-SGneo replicon and parental Huh-7.5 cells were infected with HCVcc-Rluc in the presence of 2'-C-methyladenosine a nucleoside inhibitor of the NS5B RNA-dependent RNA polymerase (31). 2'-C-methyladenosine was used at a 50-fold excess over the EC_{50} reported for HCV genotype 2a (123) and I confirmed that HCV RNA levels in HCVcc-infected Huh-7.5 and JFH-SGneo cells declined over the 24 h time course (data not shown).

In the absence of 2'-C-methyladenosine, luciferase activity in HCVcc-infected Huh-7.5 cells steadily increased and by 24 h was more than 10-fold greater than the level found in JFH-SGneo replicon cells (Fig.

4.15A). When 2'-C-methyladenosine was present during HCVcc-Rluc infection, luciferase activity was maximal at 6 h.p.i. and then decreased over 24 h in both Huh-7.5 and JFH-SGneo cells (Fig. 4.15B). During this time, luciferase activity was equivalent and even slightly greater in JFH-SGneo cells compared to Huh-7.5 cells (Fig. 4.15B), suggesting that entry, uncoating and primary translation were unaffected by the presence of the HCV replicon. Similar levels of luciferase activity were also observed after transfection of JFH-SGneo cells and Huh-7.5 cells with a polymerase defective luciferase reporter HCV RNA (data not shown). In addition, I compared HCVcc-Rluc primary translation in BILN 2061-cured JFH-SGneo cells to untreated JFH-SGneo cells. Similar to what I had observed above in the presence of 2'-C-methyladenosine, the two cell types had similar HCV translation capacities (Fig. 4.15C). Moreover, I also found that the BILN 2061-cured and untreated JFH-SGneo cells supported similar levels of translation after infection with a temperature-sensitive Sindbis mutant, Toto1101/Luc:ts110 (20), at the nonpermissive temperature, which allows translation, but is blocked for RNA replication (data not shown). Thus, these data indicate that the superinfection block in JFH-SGneo cells lies downstream from entry, uncoating, and primary translation.

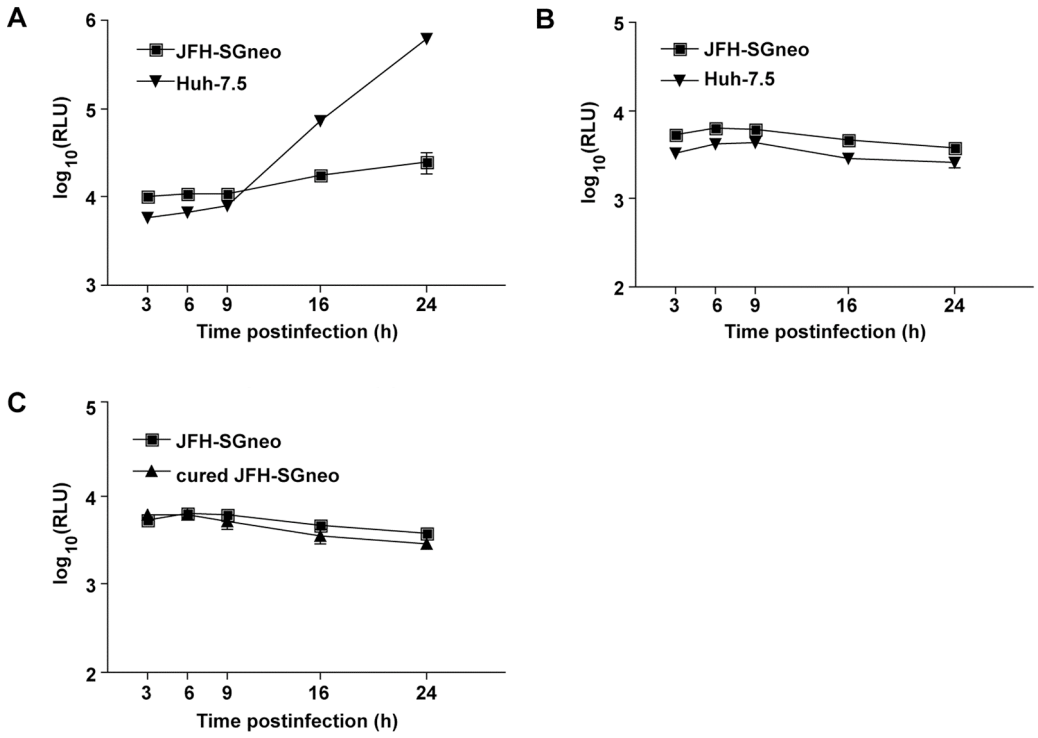

Fig. 4.15 JFH-SGneo cells exhibit a post-entry superinfection block. (**A**) Huh-7.5 and JFH-SGneo cells were infected with HCVcc-Rluc. At each time point, luciferase activity was determined from triplicate wells and normalized to the average cellular ATP content for each cell type at that time point. Each bar is the average value of triplicate wells; error bars show standard deviations. (**B** and **C**) Huh-7.5 (B) or BILN 2061-cured JFH-SGneo (C) and JFH-SGneo cells were infected with HCVcc-Rluc in the presence of 2'C-methyladenosine. At each time point, luciferase activity was determined from triplicate wells and normalized to the average cellular ATP content for each cell type at that time point. Each bar is the average value of triplicate wells; error bars show standard deviations.

An additional defect in J6/JFH-FLneo selected cells

I further investigated the surprising observation that HCVpp entry was blocked in the J6/JFH-FLneo cell population (Fig. 4.14B). A possible mechanism for restriction at the level of entry is down regulation or interference with an essential viral receptor or coreceptor. The tetraspanin CD81, originally identified as an HCV E2 binding protein (166), is an essential HCV coreceptor required for entry of HCVpp and HCVcc (reviewed in 12, 38). I examined CD81 surface expression on J6/JFH-FLneo, JFH-SGneo, and Huh-7.5 parental cell lines by flow cytometry. While JFH-SGneo and Huh-7.5 cells expressed similar levels of CD81 at the cell surface (Fig. 4.16A), levels were greatly reduced on the J6/JFH-FLneo cells (Fig. 4.16B). In addition, staining of permeabilized cells, western blot analysis of whole cell lysates, and real-time quantitative RT-PCR revealed that total cellular CD81 protein and RNA levels were also decreased in J6/JFH-FLneo cells compared to Huh-7.5 cells (Fig. 4.16C, D, E). In contrast, CD81 expression on the surface of HCV genotype 1a and 1b full-length and subgenomic replicon cell populations, as well as on cells acutely infected with J6/JFH was also examined and found to be similar to parental Huh-7.5 cells (data not shown), in keeping with the previous observation (Fig. 4.14) that these cells were permissive for HCVpp infection.

Fig. 4.16 Stable J6/JFH-FLneo replicon cells have decreased CD81 protein and RNA levels. (**A** and **B**) Huh-7.5 (tinted, blue curve), JFH-SGneo (A, thick, red line), and J6/JFH-FLneo (B, thick, orange line) cells were surface stained for CD81 and analyzed by flow cytometry. (**C**) Permeabilized Huh-7.5 (tinted, blue curve) and J6/JFH-FLneo (thick, orange line) cells were stained for total cell CD81 protein expression and analyzed by flow cytometry. Thin lines indicate the IgG isotype controls. (**D**) Western blot for CD81 or actin protein expression in lysates from J6/JFH-FLneo, Huh-7.5, and JFH-SGneo cells. (**E**) CD81 RNA was amplified using real-time quantitative RT-PCR from total RNA derived from Huh-7.5, J6/JFH-FLneo, and JFH-SGneo cells. Values were normalized to GAPDH RNA levels for each sample and are expressed as relative levels compared to Huh-7.5 cells. Values are the combined data from 3 independent experiments done in triplicate; error bars show standard errors of the means.

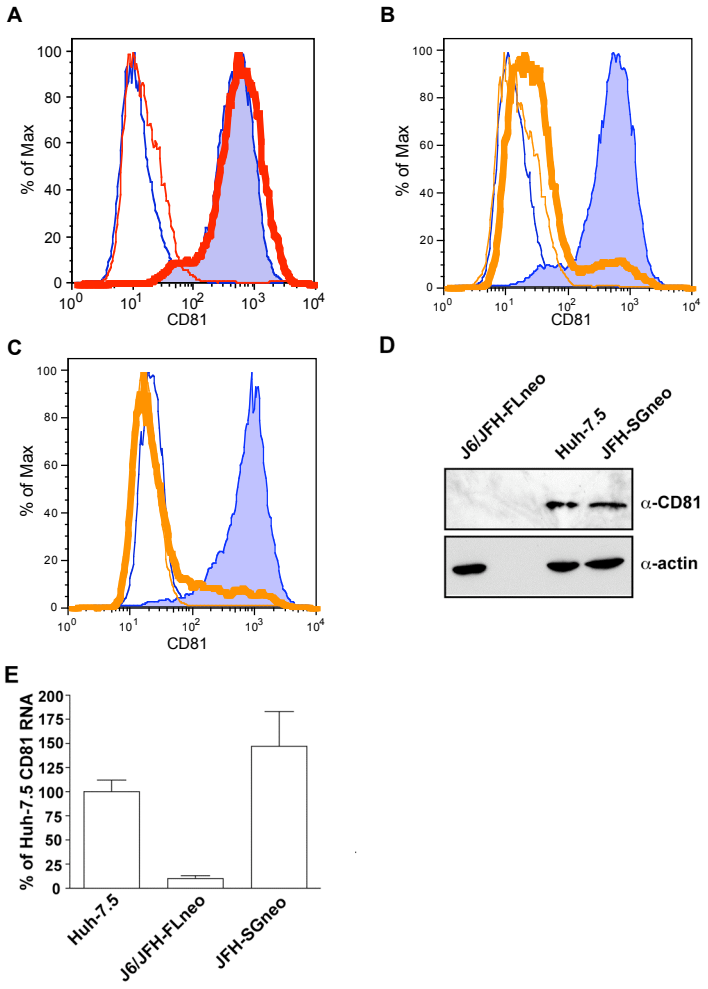
A
B
C
D
E
% of Max
CD81
J6/JFH-FLneo
Huh-7.5
JFH-SGneo
α-CD81
α-actin
% of Huh-7.5 CD81 RNA

Fig. 4.16

Additionally, levels of scavenger receptor BI, another proposed HCV entry factor (15, 176), were similar to Huh-7.5 parental cells in all of the replicon cells tested, including cells harboring the stable J6/JFH-FLneo replicon and J6/JFH-acutely infected cells (data not shown).

I next determined if reduced CD81 on J6/JFH-FLneo-containing cells was responsible for the entry defect by restoring CD81 expression. Transduction of the J6/JFH-FLneo cells with the lentiviral vector TRIP-CD81 (220) efficiently restored CD81 expression at the cell surface and permissiveness to HCVpp-Luc to a level of 150% of control Huh-7.5 cells (Fig. 4.17A and B, J6/JFH-FLneo-CD81). In contrast, J6/JFH-FLneo cells transduced with a lentivirus expressing the tetraspanin CD9 (TRIP-CD9), which does not bind E2 or support HCV entry, was less than 3% of Huh-7.5 cells (Fig. 4.17B). Thus, over-expression of CD81 rescues infection by HCVpp, indicating that reduced CD81 surface expression is responsible for the entry defect observed in J6/JFH-FLneo cells.

It was unclear if RNA replication and HCV protein expression by the J6/JFH-FLneo replicon was somehow down regulating CD81 mRNA and protein or whether G418 selection of the replicon-containing population was favoring cells with low or absent CD81. I first examined whether J6/JFH-FLneo cells would regain CD81 expression and HCVpp permissiveness after

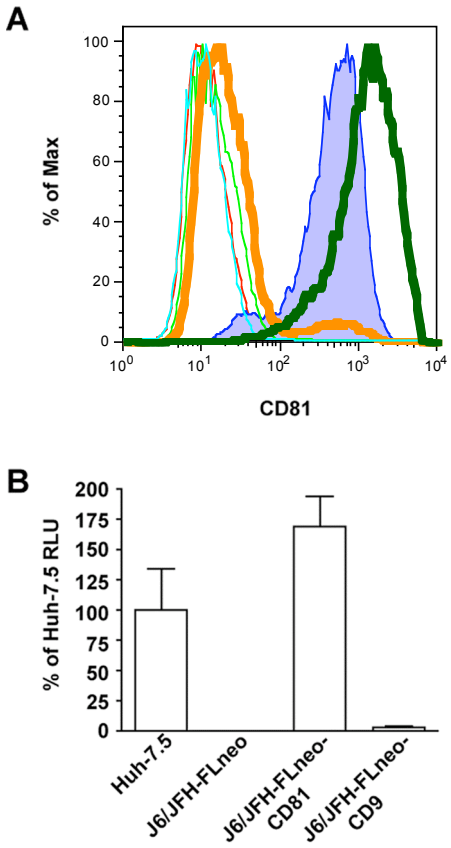

Fig. 4.17 Ectopic expression of CD81 renders stable J6/JFH-FLneo replicon cells permissive for HCVpp infection. (**A**) Transduction of J6/JFH-FLneo cells with TRIP-CD81 restores CD81 expression. J6/JFH-FLneo (orange line), J6/JFH-FLneo-CD81 (green line), and Huh-7.5 (tinted curve) cells were surface stained for CD81 and analyzed by flow cytometry. Thin lines indicate the IgG isotype controls. (**B**) Huh-7.5, J6/JFH-FLneo, J6/JFH-FLneo-CD81, and J6/JFH-FLneo-CD9 cells, transduced with TRIP-CD9, were infected with HCVpp-Luc (genotype 1a, strain H77) or VSVGpp-Luc and luciferase activity was measured at 72 h.p.i. HCVpp-Luc RLU were normalized to VSVGpp-Luc RLU. Each bar is the average value of triplicate wells; error bars show the standard deviations.

treatment with BILN 2061. Cells were treated with BILN 2061 at 20-50x the reported EC_{50} (123) over a period of 23 d in the absence of G418. Cell surface expression of CD81 and HCVpp-Luc permissiveness were assessed after 4 d, 9 d and 23 d of treatment. At 4 d, J6/JFH-FLneo cells remained resistant to HCVpp-Luc infection despite a 100-fold reduction in HCV RNA levels (Fig. 4.18A and data not shown). By 9 d, when HCV RNA levels had fallen 1000-fold, a small increase in luciferase signal was observed. After 23 d of BILN 2061 treatment, HCV RNA levels had fallen to background levels (< 0.005 RNAs/cell) and the cells became permissive for HCVpp-Luc infection with a concomitant increase in CD81 surface expression (Fig. 4.18B). These results indicate that permissive cells expressing CD81 can emerge after curing the population of replicating J6/JFH-FLneo.

I also examined this phenomenon during long-term J6/JFH infection of Huh-7.5 cells. Cells were infected at an MOI of approximately 0.3 (infected population) and maintained in parallel with naïve cells (naïve population) (Fig. 4.19). Both populations were analyzed for CD81 surface expression, NS5A expression, and permissiveness to HCVpp-GFP or as a control, VSVGpp-GFP. Pseudoparticle-challenged cells were harvested at 48 h.p.i., stained for NS5A, and analyzed by flow cytometry. The percentage of total GFP positive, *i.e*. HCVpp-infected cells, both NS5A positive and

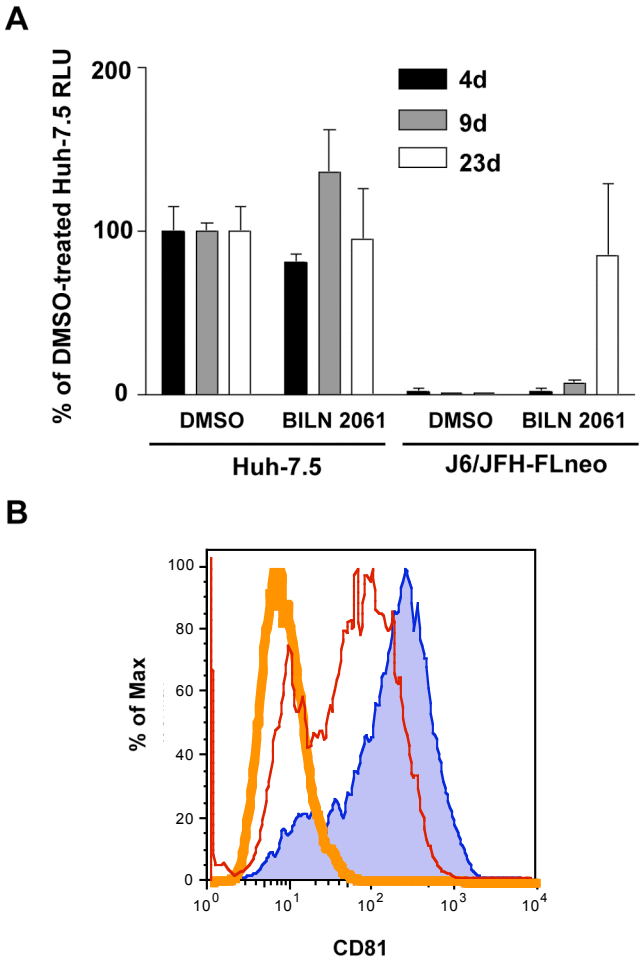

Fig. 4.18 BILN 2061 treated J6/JFH-FLneo replicon cells have increased CD81 surface expression and are permissive for HCVpp infection. (**A**) J6/JFH-FLneo and Huh-7.5 parental cells were treated with BILN 2061 or DMSO for a period of 23d. At 4 (black bars), 9 (gray bars), and 23 d (white bars) post treatment, DMSO and BILN 2061-treated cells were challenged with HCVpp-Luc or VSVGpp-Luc. Luciferase activity was measured at 72 h.p.i. and HCVpp-Luc RLU were normalized to VSVGpp-Luc RLU. Each bar, expressed as the percentage of DMSO-treated Huh-7.5 RLU, is the average value of triplicate wells; error bars show the standard deviations. (**B**) At 23 d post treatment BILN 2061 (red line) and DMSO (orange line)-treated J6/JFH-FLneo and Huh-7.5 (tinted, blue curve) cells were immunostained for CD81 surface expression and analyzed by flow cytometry.

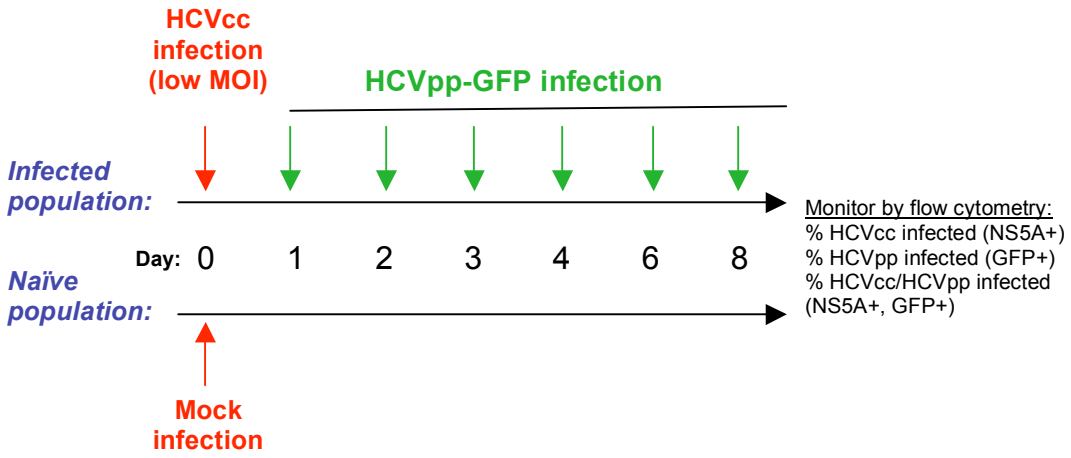

Fig. 4.19 Time course of superinfection with HCVpp. Huh-7.5 cells were infected (infected population) or mock-infected (naïve population) with HCVcc on day 0 and the populations were maintained in parallel. At 1, 2, 3, 4, 6, and 8 d.p.i. the infected and naïve populations were superinfected with HCVpp expressing GFP (HCVpp-GFP). The percent of cells that had become HCVcc infected, HCVpp infected, or HCVcc-HCVpp coinfected was monitored by flow cytometry over the time course.

NS5A negative, was normalized to the percentage of GFP positive cells from the VSVGpp-GFP infection.

After 1 d or 2 d, the infected population was fully permissive for HCVpp (Fig. 4.20A). Beginning at 3 d and continuing through 8 d, there was a decrease in the percentage of GFP positive cells compared to the naïve population, which correlated with increasing numbers of NS5A positive cells in the J6/JFH-infected population (Fig. 4.20A). However, the vast majority of the cells that were HCVpp-susceptible (greater than 80%), were also NS5A positive (Fig. 4.20B). This demonstrated that cells productively infected with J6/JFH were fully permissive for HCV entry. Regarding surface CD81 expression, NS5A positive and negative cells had CD81 expression comparable to naïve cells early in infection (3 d and 4 d; Fig. 4.20C). After 6 d, surface CD81 on NS5A positive cells remained comparable (70%) to naïve cells. However, CD81 expression on NS5A negative cells was greatly reduced (10% of the naïve cell intensity; Fig. 4.20C). Interestingly, the appearance of this distinct $CD81^{low}$ NS5A negative population was coincident with an observed cytopathic effect in the infected population (data not shown) and a 65% reduction in HCVpp-GFP permissiveness in the infected population (Fig. 4.20A). At 6 d and 8 d, NS5A negative cells made up only a small proportion (approximately 10%)

Fig. 4.20 J6/JFH-infection of Huh-7.5 cells promotes the emergence of a CD81^{low} cell population. Huh-7.5 cells were infected with HCVcc (J6/JFH) at an MOI of 0.3 and maintained in parallel with naïve cells (as described in Fig. 4.19). (**A**) At 1, 2, 3, 4, 6, and 8 d.p.i. with J6/JFH, the infected and naïve populations were infected with HCVpp-GFP or VSVGpp-GFP. Cells were harvested at 48 h.p.i. Cells were stained for NS5A and analyzed by flow cytometry for GFP and NS5A expression. The total number of GFP positive cells resulting from HCVpp-GFP infection was normalized to the total number of GFP positive cells in the VSVGpp-GFP infected samples. Values are expressed as the percentage of naïve GFP positive cells. (**B**) The J6/JFH-infected population, which was infected with HCVpp-GFP and stained for NS5A in (A), was grouped into NS5A positive and NS5A negative cells. GFP expression in NS5A positive (black bars) and NS5A negative (white bars) cells was determined and plotted as the percentage of the total GFP positive cells. (**C**) The J6/JFH-infected and naïve populations were analyzed for CD81 surface expression and NS5A expression using immunostaining and flow cytometry at 3, 4, 6, 8, and 17 d.p.i. with J6/JFH. Cells were gated on NS5A positive (green line) or NS5A negative (blue line) cells and CD81 expression was compared to the naïve population (red line). The d.p.i. and percentage of NS5A positive cells at each time point are indicated above the plots.

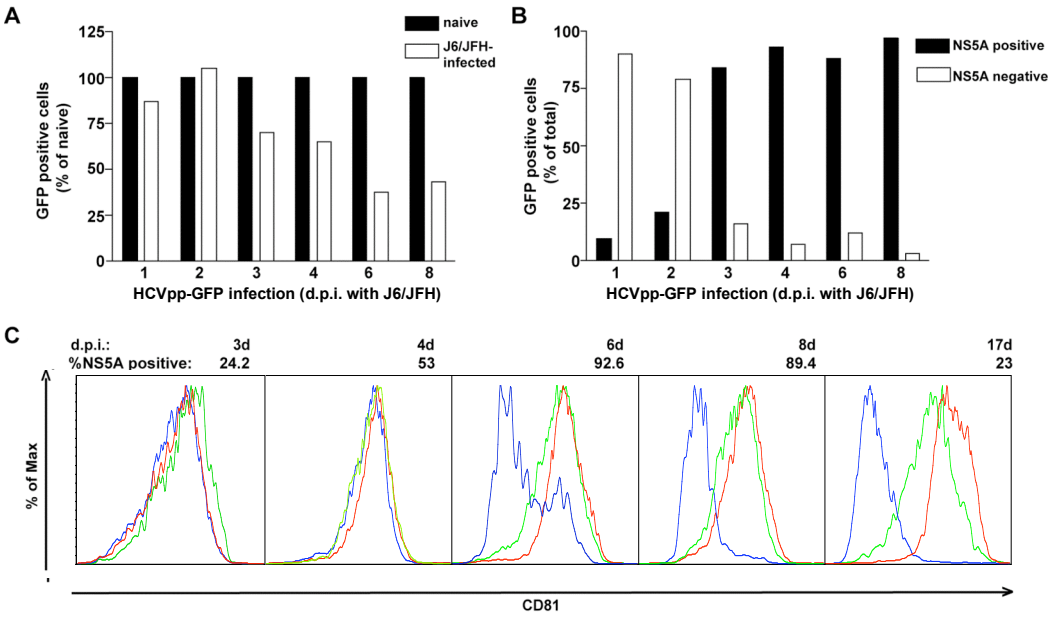
A
naive
J6/JFH-infected
GFP positive cells (% of naive)
125
100
75
50
25
0
1
2
3
4
6
8
HCVpp-GFP infection (d.p.i. with J6/JFH)
B
NS5A positive
NS5A negative
GFP positive cells (% of total)
100
75
50
25
0
1
2
3
4
6
8
HCVpp-GFP infection (d.p.i. with J6/JFH)
C
d.p.i.: 3d 4d 6d 8d 17d
%NS5A positive: 24.2 53 92.6 89.4 23
% of Max
CD81

Fig. 4.20

of the J6/JFH-infected cell population. However, this NS5A negative fraction persisted and increased in frequency to >70% by the final time point, day 17. Notably, the modest decrease in CD81 expression in NS5A positive cells at 6 d and 8 d was more apparent by 17 d (Fig. 4.20C). Unlike the J6/JFH-FLneo population, which had been selected with G418 and undergone multiple passages, I saw no decrease in CD81 RNA levels during the 17 d J6/JFH infection (data not shown). These data suggest that J6/JFH infection selects against cells expressing high levels of CD81, possibly due to a cytopathic effect or retarded growth kinetics, leaving $CD81^{low}$, uninfected cells to emerge. This scenario may also explain the low levels of CD81 and HCVpp resistance that I observed in G418 selected cell populations harboring the J6/JFH-FLneo replicon.

4.5 Discussion

In this chapter, the mechanisms of BVDV and HCV superinfection exclusion were examined. The data presented demonstrate that cells acutely infected with BVDV are protected against superinfection with homologous BVDV. These cells, however, remain susceptible to a heterologous virus, VSV, suggesting a BVDV-specific exclusion. The ability to exclude superinfecting BVDV is established quickly, within 30-60 minutes after

primary infection, but is transient, as persistently infected, passaged cells are not efficiently protected from cp BVDV. The results of this study show that BVDV superinfection exclusion is mediated by dual mechanisms – one at the level of viral entry and a second at the level of viral RNA replication.

I have also described and investigated the mechanisms of superinfection exclusion in human hepatoma cells infected with HCV [(197) and above]. Superinfection exclusion of HCVcc was observed in J6/JFH acutely infected cells and in cells containing full-length and subgenomic replicons derived from HCV genotypes 1a, 1b, or 2a genomes. Treatment with an HCV-specific antiviral agent restored permissiveness in these cells, indicating that the superinfection exclusion phenotype was fully reversible and that it required the presence of HCV RNA or proteins. I determined that the block to superinfection in cells harboring HCV replication was downstream from virus entry and translation of the incoming genome RNA, possibly at the level of RNA replication. An additional, unexpected defect at virus entry was observed in cells harboring a persistent full-length J6/JFH-FLneo replicon. Further analyses revealed that this block to HCV entry was due to the loss of $CD81^{high}$ cells within selected or infected cell populations rather than to a classical superinfection exclusion mechanism.

The first mechanism of superinfection exclusion in cells acutely infected with BVDV is a block at the level of entry. This block was dependent upon expression of the BVDV structural proteins. The importance of the BVDV structural proteins in superinfection exclusion is supported by recent studies by Reimann *et al.,* in which cells constitutively expressing the BVDV structural proteins C-E2 cannot be efficiently infected with BVDV (170). Our study indicates that expression of BVDV glycoprotein E2 appears to play an essential role in the entry block. The importance of E2 in superinfection exclusion is also consistent with the description of an MDBK cell line expressing E2, called MDBK-E2IRESp7, which was shown to be nonpermissive for BVDV infection (76). Moreover, I have demonstrated that expression of the E2 ectodomain alone is sufficient to prevent entry of superinfecting BVDV (Chapter 3).

Exclusion at an early stage of viral infection has been shown for a variety of viruses. One well-characterized mechanism is down regulation of the cell surface receptor after primary viral infection (described above in Section 3.3). Exclusion of a homologous virus can also be due to interference with receptor-mediated surface binding as shown for respiratory syncytial virus (RSV) by using pseudotyped antigenically-related RSV (184, 185). Furthermore, steps post-binding may be blocked. Multiple

mechanisms of VSV superinfection exclusion exist at the level of entry, including a reduced rate of endocytic vesicle formation, decreased internalization of bound ligands, and competition between virions for coated pits (180, 209). Based on our findings, it is possible that the block at BVDV entry might be due to a defect in receptor-mediated interactions on the plasma membrane, virion internalization, fusion or nucleocapsid uncoating. It seems likely, however, considering the data presented in Chapter 3, that the block to BVDV entry is downstream from CD46.

We also demonstrate a second mechanism of BVDV superinfection exclusion at the level of viral RNA replication. Transfected viral RNAs, although fully competent for translation, were not able to replicate in the ncp NADLJiv90^{-}-infected MDBK cells. Exclusion of BVDV at the level of viral RNA replication did not require expression of the viral structural proteins. Instead, the degree of exclusion correlated with the level of primary viral RNA replication. For HCV, a block downstream from entry, uncoating, and translation of the incoming genome RNA, mediated by the viral nonstructural proteins, also exists, but in contrast to BVDV, our data indicate that this is the principle mechanism of superinfection exclusion in HCV-infected cells. Although it remains possible that a transient block at the level of primary translation may exist during acute HCV infection, our data

suggest that in JFH-SGneo replicon cells the superinfection block is due to a direct effect on a downstream event, most likely at one or more steps in RNA replication.

Interference at the level of RNA replication has been previously examined in the HCV replicon system. HCV replication efficiency was inversely correlated with the amount of replicon RNA transfected into Huh-7 cells (130). This effect was dependent on the presence of the HCV NS3-NS5B replicase proteins. In another study, replication capacity of a transfected replicon was reduced in cells that harbored an existing, replicating HCV genome (52). Similarly, in cells acutely infected with BVDV, the block to superinfecting virus at the level of replication was directly correlated to the level of the primary virus replication [(119) and above]. A superinfection block at replication is also consistent with previous observations in other viral systems. For example, Sindbis virus *ts* mutants in two different RNA-negative complementation groups failed to exclude superinfecting viruses at the nonpermissive temperature although complementation could be observed (1, 93), demonstrating that replication of the superinfecting virus was blocked after attachment, penetration, and translation of the superinfecting viral RNA. These observations suggest that viral replication can sequester host factors that are limiting and saturable in

the host cell, thereby interfering with superinfecting virus replication. There may also be competition for replication sites, which are in specialized membrane compartments similar to those observed during classical flavivirus RNA replication (33, 36, 37, 207, 208).

In the course of the HCV superinfection exclusion study I made the surprising observation that G418 selected cells harboring the J6/JFH-FLneo replicon have an additional defect in virus entry. J6/JFH-FLneo cells were resistant to HCVpp bearing glycoproteins from J6 or H77, whereas cells acutely infected with J6/JFH and cells harboring either genotype 1a or 1b replicons, and genotype 2a subgenomic replicon bearing cells were fully permissive. Given that the defect was specific to selected J6/JFH-FLneo, but not subgenomic replicon-containing cells suggested that the phenotype was dependent on J6 C-NS2 expression (or an RNA element harbored in this region). Further analyses revealed that CD81 down regulation was the mechanism responsible for this phenotype. Total and cell surface CD81 protein and CD81 mRNA levels were dramatically reduced in J6/JFH-FLneo cells compared to parental cells. Furthermore, ectopic expression of CD81 rendered J6/JFH-FLneo cells fully permissive for HCVpp infection.

Two possibilities, among others, might explain the low levels of CD81 mRNA in J6/JFH-FLneo cells: (1) HCV-dependent down regulation

of CD81 expression, (2) a selective advantage for cells with low or absent CD81 during G418 selection. Consistent with the latter possibility, prolonged J6/JFH infection yielded a cell population that was increasingly resistant to HCVpp infection, although NS5A positive cells were readily infected with HCVpp. When CD81 surface expression was examined, it became evident that a population of $CD81^{low}$ NS5A negative cells had emerged within the J6/JFH-infected cell culture, coincident with and subsequent to a virus-induced cytopathic effect. The pathway by which J6/JFH infection leads to cell death is unknown, but our data indicate that expression of CD81 and the HCV J6 C-NS2 region are involved. Although I did find some $CD81^{low}$ NS5A positive cells at later stages of J6/JFH infection, the absence of CD81 down regulation during acute infection suggests that this may be due to inefficient infection of cells with lower levels of CD81. Therefore, the main mechanism of this resistance could not be attributed to a classical superinfection exclusion block at the level of virus entry, where replicating HCV prevents a secondary HCV infection. Rather, selection occurs at the population level and resistance is due to an emerging population of $CD81^{low}$ cells that are less permissive for HCV infection. Recently, similar observations during persistent JFH-1 infection

were reported by Zhong *et al*. (221). Clearly, this phenomenon and its relevance *in vivo* warrant further study.

Chapter 5. Analysis of the BVDV and HCV entry pathways

5.1 Introduction

Infection with an enveloped virus requires a fusion event between the viral and a cellular membrane. This event can occur at the cell surface, as demonstrated by HIV and herpes simplex virus (HSV), where binding to one or more receptors induces conformational changes in the envelope glycoprotein allowing membrane fusion at neutral pH. Alternatively, the fusion event can occur within an endosomal compartment in the presence of low pH (reviewed in 183) as has been previously described for classical flaviviruses and alphaviruses (74, 79, 81, 109).

Previous studies of HCV entry have been based on retroviral pseudotypes bearing HCV E1 and E2 glycoproteins (HCVpp) (15, 85). Such pseudotypes were shown to undergo pH-dependent entry into Huh-7 cells in a CD81-dependent manner and could be neutralized by certain α-E2 monoclonal antibodies (85, 220). Additional receptors, including SR-BI and CLDN1 have also been suggested to have a role in HCV entry (15, 176). As described above, using the JFH genotype 2a strain of HCV, it has recently become possible to propagate infectious HCV particles in cell culture (HCVcc), allowing the study of the complete viral lifecycle, including virus entry and fusion events.

In this section, I demonstrate that the entry pathways of BVDV and HCVcc into their respective target cells, MDBK and Huh-7.5, are pH-dependent, although both BVDV and HCV virions are acid-resistant, suggesting that these two viruses may have a similar mechanism of entry. The trigger(s) by which an acid-resistant virus becomes pH-sensitive during entry, as well as the role of putative cellular receptors/coreceptors were investigated.

5.2 Mechanism of BVDV entry

BVDV entry is pH-dependent

To determine if the BVDV entry pathway requires a pH-dependent step, I inhibited the acidification of endosomal compartments in MDBK cells using bafilomycin A1, an inhibitor of vacuolar type H^+-ATPase. As a negative control for this experiment, I utilized herpes simplex virus-1 (HSV-1), a pH-independent virus, which fuses at the plasma membrane (183).

MDBK cells were pre-treated with a range of concentrations of bafilomycin A1 and subsequently infected with ncp NADLJiv90-*luc* or HSV-1 [KOS*dluxori*L, (188)]. At all concentrations tested, BVDV-expressed luciferase activity was reduced in cells treated with bafilomycin

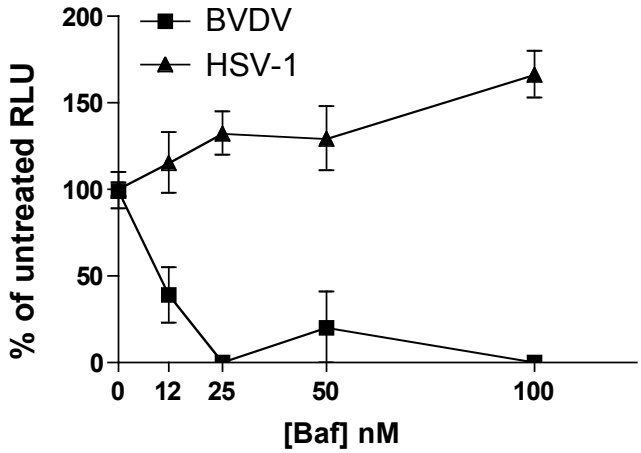

Fig. 5.1 BVDV entry is pH-dependent. MDBK cells were pre-treated with 0, 12, 25, 50 or 100 nM bafilomycin A1 and infected with BVDV NADLJiv90^{-}*luc* or HSV-1 (KOS*dluxoriL*) in the presence of drug. At 24 h.p.i. cells were harvested for luciferase assays. Each point is the mean value of duplicate wells; error bars show the standard errors of the means.

A1 (Fig. 5.1). A 12 nM bafilomycin A1 treatment had an intermediate effect on BVDV infection, while increased concentrations reduced the luciferase activity to background levels. In contrast, HSV-1 luciferase activity was unaffected by the presence of the inhibitor (Fig. 5.1). These data suggest that BVDV entry requires a pH-dependent step.

BVDV infectivity is unaffected by low pH treatment

Enveloped viruses that are internalized by endocytosis are, in general, very sensitive to low pH treatment. Exposure to acidic pH induces a conformational change in the envelope glycoproteins, which prematurely exposes the fusion peptide and thereby diminishes the viral infectivity. Such a scenario occurs in Sindbis (SIN) virions upon treatment with low pH. To determine if BVDV is sensitive to low pH treatment, I treated BVDV virions with a pH 5 or 7 buffer at 37 ºC, neutralized the pH, and infected MDBK cells. Unlike SIN, which was used as a positive control, a pH 5 treatment had no effect on BVDV infectivity (Fig. 5.2). These data suggest that unlike SIN virions, which are primed to undergo fusion upon exposure to low pH, BVDV requires an additional trigger to become acid-sensitive. This hypothesis is supported by the observation that bound BVDV virions could

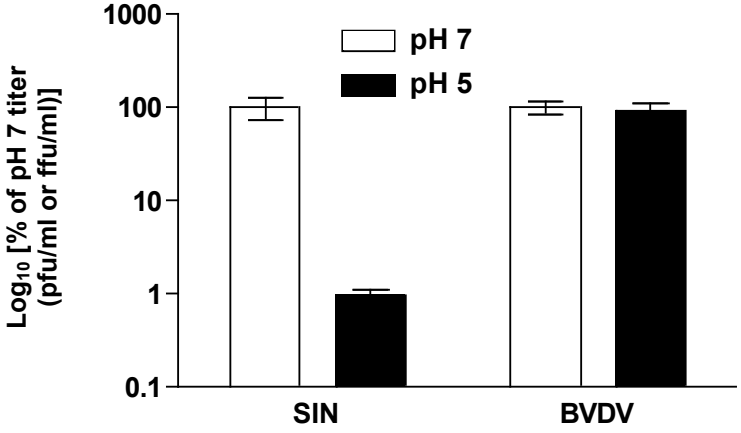

Fig. 5.2 BVDV infectivity is acid-resistant. BVDV or SIN was diluted in citric acid buffer (15 mM citric acid, 150 μM NaCl) at pH 7 (white bars) or pH 5 (black bars) for 10 min at 37 ºC. Samples were then neutralized and titered on either MDBK (BVDV) or BHK-J (SIN) cells. Values, expressed at the percent of pH 7 RLU, are mean titers of duplicate samples titered in duplicate; error bars represent the standard errors of the means.

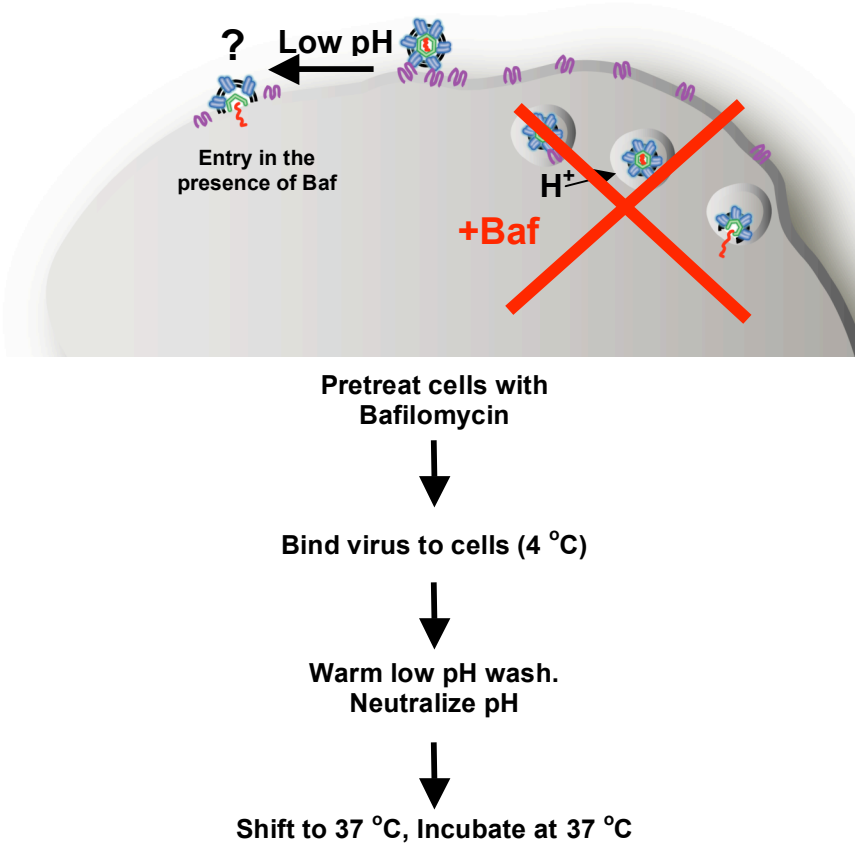

Fig. 5.3 Schematic illustration of entry in the presence of bafilomycin A1. Target cells are pretreated with bafilomycin A1 (+Baf) to block the normal route of virus entry. Virus is added to the cells at 4 ºC to allow binding, but prevent virus internalization. After washing to remove unbound virus, cells are washed with low pH buffer, mimicking the environment of the endosome, to determine if the virus can enter the cell in presence of bafilomycin A1. After the pH of the media is neutralized, the infection is shifted to 37 ºC and incubated in media containing bafilomycin A1.

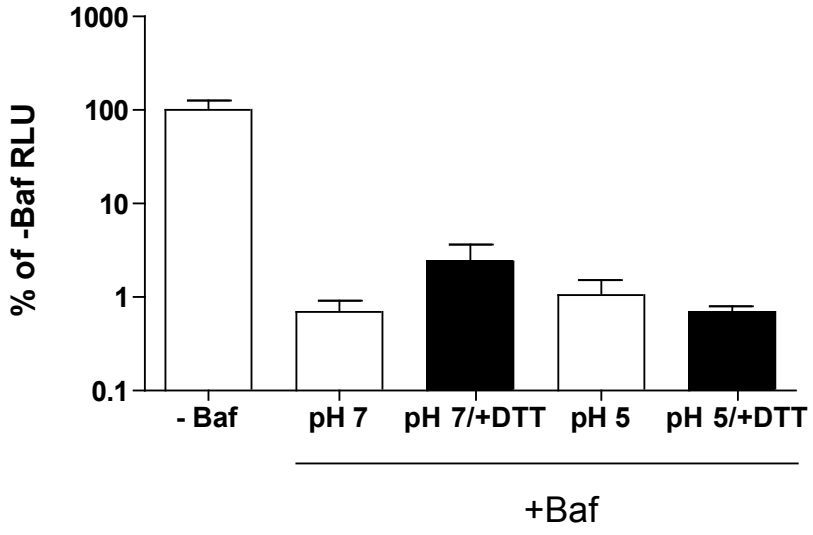

Fig. 5.4 Bound BVDV virions cannot enter a bafilomycin A1 treated cell upon exposure to low pH. MDBK cells were treated with bafilomycin A1 (25 nM), then were infected with BVDV at 4 ºC for 1 h. Cells were washed to remove unbound virus, then washed with citric acid buffer at pH 7 or 5. Cells were incubated in the presence of bafilomycin A1 for 24 h when they were harvested for luciferase assays. Luciferase activity from untreated cells (-Baf) was expressed as 100 percent. Values are the mean value of duplicate wells; error bars show the standard errors of the means.

not enter a bafilomycin A1-treated cell upon exposure to low pH (Figs. 5.3 and 5.4). A recent report proposed a role for disulfide bond reshuffling in the activation of BVDV virions (109). Although, in our hands, the presence of reducing agent in the low pH wash did not enhance BVDV entry into cells treated with bafilomycin A1 (Fig. 5.4).

5.3 Mechanism of HCV entry

HCV entry is pH-dependent

To examine the HCV entry pathway into Huh-7.5 cells, I utilized the HCV reporter virus HCVcc-Rluc (Fig. 5.5A). The expression of Rluc from HCVcc-Rluc serves as a highly sensitive assay for viral RNA replication after infection of permissive cells. To examine the replication kinetics of HCVcc-Rluc in Huh-7.5 cells, virus was bound to cells at 4 ºC. The cells were then shifted to 37 ºC for a 48 h period of infection. After a low MOI infection (~0.01), a small increase in signal was observed after 8-12 h, followed by a logarithmic rise in the luciferase activity between 12 and 24 h.p.i. (Fig. 5.5B).

To determine if HCV entry is dependent on a low pH step, I utilized bafilomycin A1, concanamycin A, and NH_4Cl, agents that prevent acidification of endosomal compartments. As controls for these experiments,

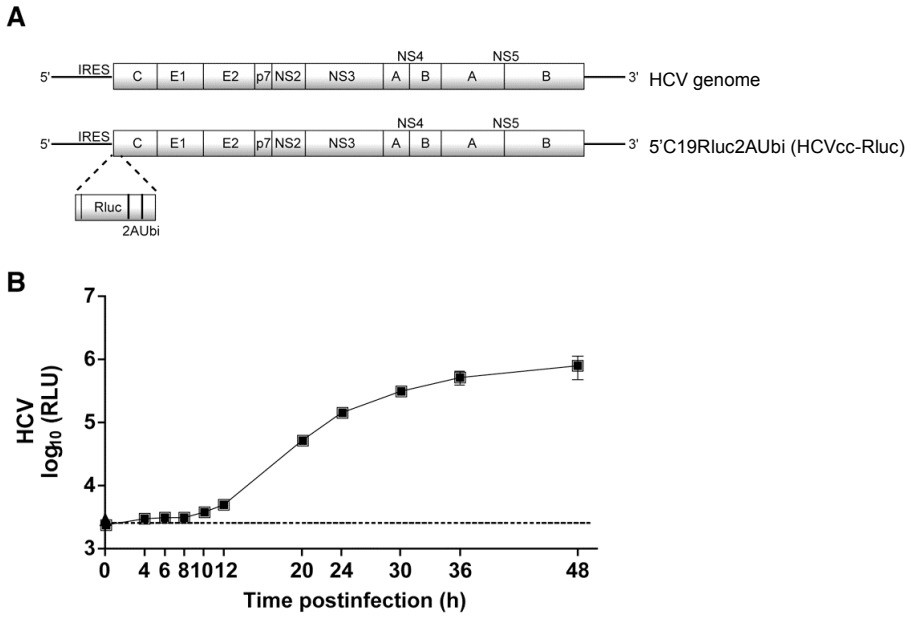

Fig. 5.5 Characterization of HCVcc-Rluc. (A) Schematic of HCV and FL-J6/JFH-5'C19Rluc2AUbi (HCVcc-Rluc) genomes (described fully in Fig. 4.10A). **(B)** Huh-7.5 cells were infected with HCVcc-Rluc for 0, 4, 6, 8, 10, 12, 20, 24, 30, 36, or 48 h. At each time point, cells were harvested and luciferase activity determined. Each point is the average value of triplicate wells; error bars show the standard deviations. The dashed line indicates the background level of the assay from naïve Huh-7.5 cells.

I infected Huh-7.5 cells in parallel with SIN or HSV-1, which are well-characterized, pH-dependent and independent viruses, respectively. SIN undergoes receptor-mediated endocytosis followed by fusion in the acidic environment of the endosome, while HSV-1 fuses at the plasma membrane at neutral pH.

Huh-7.5 cells were pretreated with various concentrations of bafilomycin A1, and then infected with HCV, SIN, or HSV-1. At all concentrations tested, a 3 h pretreatment with bafilomycin A1 reduced HCV expressed luciferase activity to nearly background levels (Fig. 5.6A, -3 h), while having no effect on HSV-1 infection (Fig. 5.6B, -3 h). SIN infection was inhibited in a similar manner to HCV by pretreatment of cells with bafilomycin A1 (data not shown). To confirm that the drug was acting at viral entry and not at subsequent replication steps, bafilomycin A1 was added at 3 h.p.i. with HCV, SIN, or HSV-1, with minimal effects on HCV or SIN luciferase activity (Fig. 5.6A, +3 h, and data not shown). As expected, HSV-1 was unaffected by the presence of bafilomycin A1 at the 3 h.p.i. time point (Fig. 5.6B, +3 h).

To determine the time point p.i. when HCV loses sensitivity to bafilomycin A1 treatment, I performed a time course of bafilomycin A1 addition during HCV infection. Cells were treated with bafilomycin A1 prior

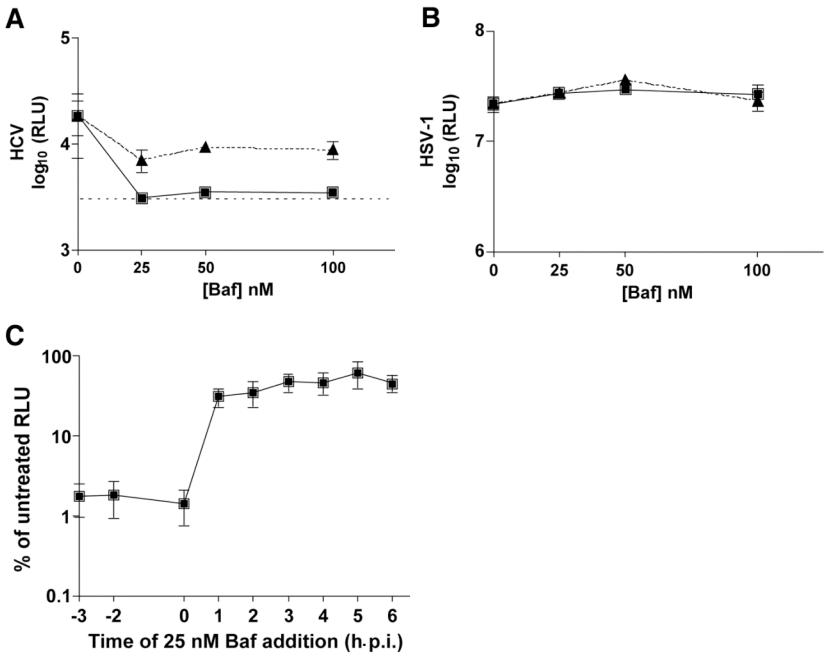

Fig. 5.6 HCV entry is sensitive to bafilomycin A1. (A) Huh-7.5 cells were incubated with bafilomycin A1 (0, 25, 50 or 100 nM) either prior to (squares) or at 3 h.p.i. (triangles) with HCVcc-Rluc. Samples were harvested for luciferase assays at 24 h.p.i. Each point is the average value of triplicate wells; error bars show the standard deviations. The dashed line indicates the background level of the assay from naïve Huh-7.5 cells. **(B)** Huh-7.5 cells were incubated with bafilomycin A1 (0, 25, 50 or 100 nM) either prior to (squares) or at 3 h.p.i. (triangles) with HSV-1. Samples were harvested for luciferase assays at 12 h.p.i. Each point is the average value of triplicate wells; error bars show the standard deviations. **(C)** Huh-7.5 cells were untreated or incubated with bafilomycin A1 prior to (-3 h), at the time of infection (-2 h), or at 0, 1, 2, 3, 4, 5, 6 h.p.i. with HCVcc-Rluc. Samples were harvested for luciferase assays at 24 h.p.i. Values are expressed as the percent of untreated RLU and are the combined data from 2 independent experiments done in triplicate; error bars represent the standard errors of the means.

to HCV infection (-3 h), at the time of infection at 4 ºC (-2 h), after inoculum was removed and cells were shifted to 37 ºC (0 h), or 1, 2, 3, 4, 5, or 6 h.p.i. (Fig. 5.6C). Drug addition at 1 h p.i. or after had little effect on HCV luciferase activity, while if bafilomycin A1 was present at time point -3, -2, or 0 h, the luciferase signal was nearly eliminated (Fig. 5.6C). These data suggest that soon after the temperature shift to 37 ºC, bound HCV virions are able to enter Huh-7.5 cells, thereby becoming insensitive to bafilomycin A1 treatment.

To further confirm that HCV requires a pH-dependent entry step, I tested another inhibitor of vacuolar type H^+-ATPase, concanamycin A. Concanamycin A inhibited HCV and SIN entry into Huh-7.5 cells, but had minimal effect on downstream replication events (Fig. 5.7A and data not shown). Pre- or post- infection treatment with concanamycin A had no effect on HSV-1 infection (Fig. 5.7B). Infection in the presence of NH_4Cl, a lysosomotropic agent, was also tested for its ability to inhibit HCV entry. Pretreatment with 25 mM NH_4Cl inhibited HCV (Fig. 5.7C), but similar inhibition was also observed when the drug was added at 3 h.p.i. (data not shown). This observation was unlike that for SIN, which was inhibited in a dose-dependent manner by pretreatment with NH_4Cl, but the inhibition was much decreased when the drug was present from only 3 h.p.i. (data not

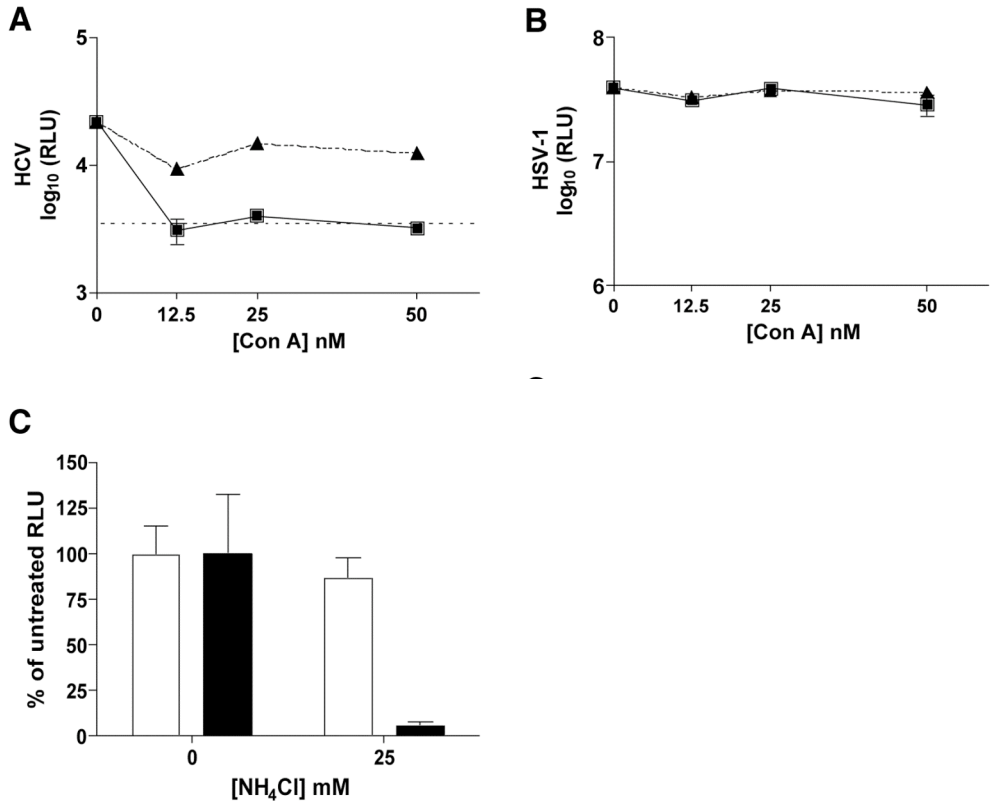

Fig. 5.7 HCV entry is sensitive to concanamycin A and NH_4Cl. (A) Huh-7.5 cells were incubated with concanamycin A (0, 12.5, 25 or 50 nM) prior to (squares) or at 3 h.p.i. (triangles) with HCVcc-Rluc. Samples were harvested for luciferase assays at 24 h.p.i. The dashed line indicates the background level of the assay from naïve Huh-7.5 cells. **(B)** Huh-7.5 cells were incubated with concanamycin A (0, 12.5, 25, or 50 nM) prior to (squares) or at 3 h.p.i. (triangles) with HSV-1. Samples were harvested for luciferase assays at 12 h.p.i. **(C)** Huh-7.5 cells were untreated (0 nM) or incubated with 25 mM NH_4Cl prior to infection with HCVcc-Rluc (black bars) or HSV-1 (white bars). Samples were harvested for luciferase assays at 24 h.p.i. In A, B, and C, each point or bar is the average value of triplicate wells; error bars show the standard deviations.

shown). HSV-1 infection was unaffected by the presence of 25 mM NH_4Cl, indicating that the decrease in HCV luciferase activity for the 3 h.p.i. treatment was not likely due to nonspecific or cytotoxic effects of NH_4Cl on the Huh-7.5 cells (Fig. 5.7C). These data suggest that HCV may require an additional low pH step for downstream replication events that is inhibited by NH_4Cl. Taken together, HCV sensitivity to bafilomycin A1, concanamycin A, and NH_4Cl demonstrates that HCV entry requires a low pH step.

HCV infectivity is unaffected by low pH treatment

As stated above for BVDV, a common feature of viruses that enter cells by endocytosis is their sensitivity to low pH treatment. To determine if HCV infectivity is sensitive to acidic pH, I treated virions with pH 5 or 7 buffers. After neutralization, the virus was used to infect Huh-7.5 cells. SIN virus was again used as a control, being a well-characterized acid-sensitive virus that is readily inactivated by low pH treatment. Treatment at pH 5 for 10 min at 37 ºC had minimal effect on HCV infectivity, but reduced SIN luciferase activity to less than 1% of the pH 7-value (Fig. 5.8A). The observed insensitivity of HCV to low pH treatment is reminiscent of the related pestivirus BVDV [(109) and above] and suggests that HCV, as well, requires an additional trigger to become acid-sensitive.

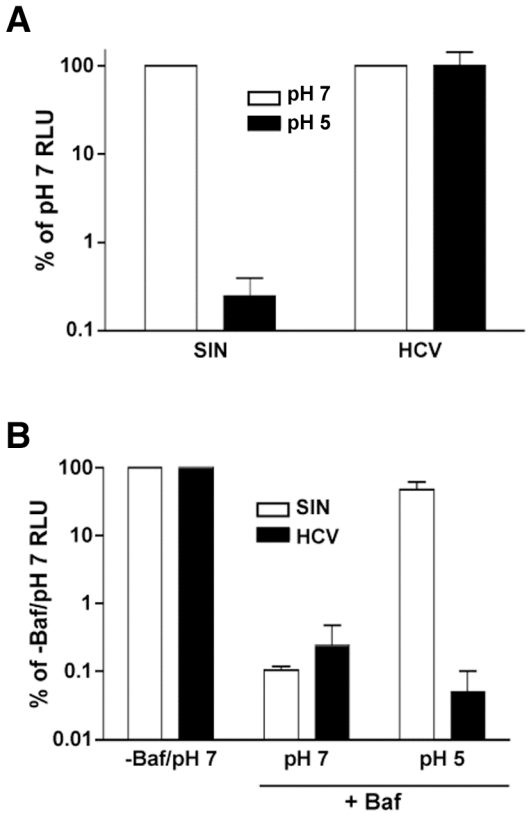

Fig. 5.8 HCV infectivity is resistant to acidic pH. (A) HCV or SIN was diluted in citric acid buffer (15 mM citric acid, 150 mM NaCl) at pH 7 (white bars) or pH 5 (black bars) for 10 min at 37 ºC. Samples were then neutralized and used to infect Huh-7.5 cells. Samples were harvested at 24 h (SIN) or 48 h (HCV) for luciferase assays. Values, expressed as the percent of pH 7 RLU, are the combined data from 2 independent experiments done in triplicate; error bars represent the standard errors of the means. **(B)** Huh-7.5 cells were treated with bafilomycin A1 (25 nM), then were infected with HCV (black bars) or SIN (white bars) at 4 ºC for 2 h. Cells were washed to remove unbound virus, then washed with citric acid buffer at pH 7 or 5. Cells were incubated in the presence of bafilomycin A1 for 24 h when they were harvested for luciferase assays. Luciferase activity from untreated cells washed with pH 7-buffer (-Baf/pH 7) was expressed as 100 percent. Values are the combined data from 2 independent experiments done in triplicate; error bars represent the standard errors of the means.

HCV fails to enter bafilomycin A1 treated cells when exposed to low pH

Many viruses that utilize the acidic environment of the endosome to trigger glycoprotein-mediated fusion can be induced to fuse at the plasma membrane with a brief low pH treatment (Fig. 5.3). Whereas free virus is inactivated, cell bound virus can enter and initiate infection. Using SIN as a control, I tested whether HCV bound at the plasma membrane could enter when exposed to low pH. Huh-7.5 cells were pretreated with bafilomycin A1 to prevent productive entry via endosomal acidification. Cells were then infected with HCV or SIN at 4 ºC. After washing to remove unbound virus, the cells were washed with pre-warmed buffer at pH 5 or 7, then incubated in the presence of bafilomycin A1 at 37 ºC. While there was no increase in HCV luciferase activity from samples washed with pH 5, SIN luciferase activity increased to nearly 50% of the untreated values in samples that had been washed with pH 5 buffer (Fig. 5.8B). Therefore, cell surface bound HCV is unable to enter at the plasma membrane under the same conditions as SIN. These results suggest that cell bound HCV remains acid-resistant and requires an additional trigger for low pH-induced infection.

In the case of BVDV, the presence of reducing agent in addition to low pH has been reported to allow some, albeit inefficient, entry and replication (109). Therefore, I reproduced this experiment with HCV by

including 10 mM DTT in the pH 5 buffer. No enhancement of the luciferase signal was observed (data not shown). However, this experiment is difficult to interpret since treatment of HCV with DTT, either at pH 5 or pH 7, abrogated detectable HCV infection (data not shown). It is unclear if DTT is mediating this effect by destabilizing the HCV glycoproteins or cell surface receptors like CD81, which contains a disulfide bond in its large extracellular loop that is required for E2 binding (82, 162).

HCV entry is not dependent on cathepsin B or L

As observed above for HCV, Ebola virus (EboV) entry is sensitive to inhibitors of endosomal acidification (189, 212), but acid pH cannot induce glycoprotein (GP)-dependent membrane fusion (91). A recent study demonstrated that infection with VSV virions pseudotyped with EboV GP (VSV-EboV GP) depends on the action of pH-dependent endosomal proteases, cathepsin B (CatB) and cathepsin L (CatL) (35). I therefore tested if endosomal proteolysis by CatB or CatL is required for HCV entry.

Huh-7.5 cells pretreated with CA-074, an inhibitor of CatB, or with FYdmk, an inhibitor of both CatB and CatL, were infected with either HCV, HIV particles bearing the VSV-G protein on their surface (HIV-VSV-G), or VSV-EboV GP (35). Both HCV and HIV-VSV-G infections were

unaffected by CA-074 or FYdmk, although either inhibitor reduced the efficiency of VSV-EboV GP infection by approximately 80% compared to untreated cells (Fig. 5.9). This experiment demonstrates that HCV infection is not sensitive to inhibitors of CatB and CatL, suggesting that, in contrast to EboV, these endosomal proteases do not have a significant role in HCV entry.

Evidence that additional post-binding steps are required to activate HCV for entry

The inability of bound HCV to enter at the plasma membrane after exposure to low pH (Fig. 5.8B) suggested that an additional step(s) was required to activate the virus for pH-dependent entry. For some viruses like avian leukosis virus (151), and Semliki Forest virus and VSV in certain cell types (136), fusion in the presence of inhibited endosomal acidification requires incubation at 37 ºC prior to acid treatment. I examined whether low pH could override the bafilomycin A1 block to HCV infection if the cells were shifted to 37 ºC prior to the pH 5 wash (Fig. 5.10). After 1 h at 37 ºC, the HCV-infected cells were washed with buffer at pH 5 or 7. In contrast to what I observed when the cells were washed immediately with low pH (Fig. 5.11, 0 h.p.i.), luciferase activity from cells that had been incubated at 37 ºC

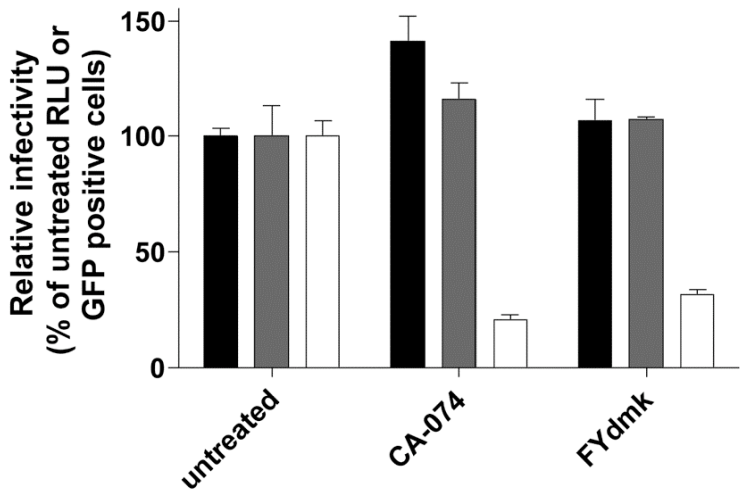

Fig. 5.9 HCV is unaffected by inhibitors of CatB and CatL. Huh-7.5 cells were pretreated with CA-074 (100 mM), a CatB selective inhibitor, or FYdmk (0.1 mM), a CatB/CatL inhibitor, then infected with HCV (black bars), HIV-VSV-G (gray bars), or VSV-EboV GP (white bars) for 2 h at 37 ^{o}C. Cells were incubated in the presence of inhibitor for 24 h. At 24 h.p.i., cells were harvested for luciferase assays (HCV, HIV-VSV-G) or FACS analysis (VSV-EboV GP). The luciferase activity or number of GFP positive cells from untreated cells is expressed as 100 percent. Each bar is the average value of triplicate wells; error bars show the standard deviations.

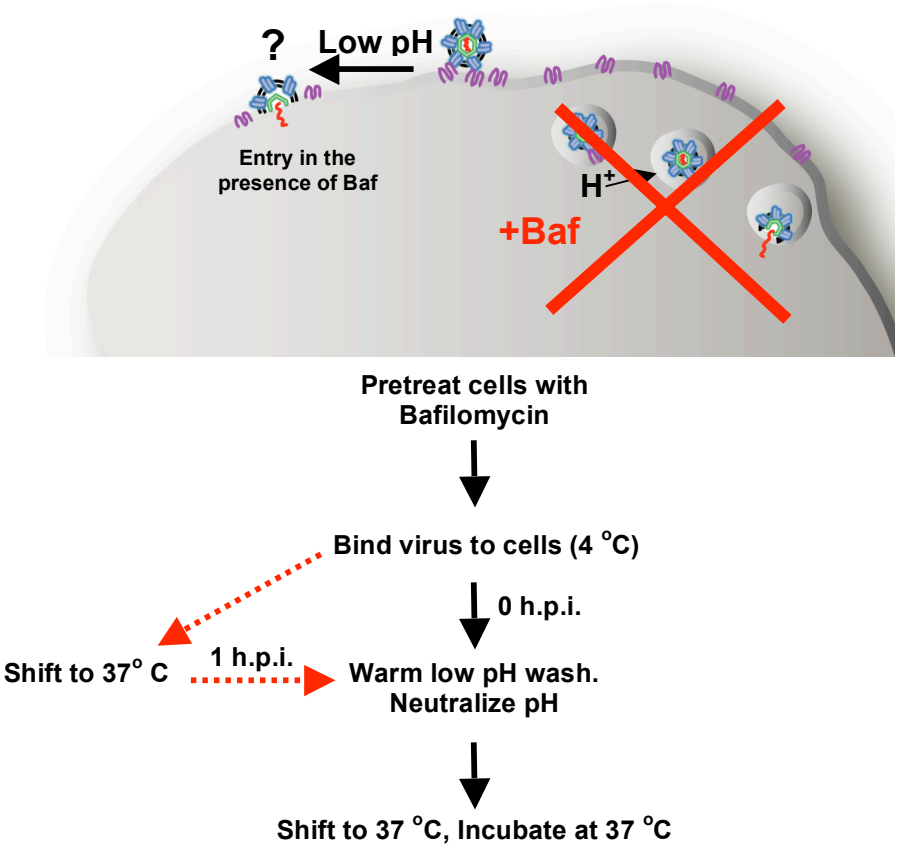

Fig. 5.10 Schematic illustration of entry in the presence of bafilomycin A1 with prior incubation at 37 °C. Same procedure as that described in Fig. 5.3, but instead of washing with low pH immediately after the binding step (0 h.p.i.) the cells were shifted to 37 °C for 1 h. After which, the cells were washed with low pH (1 h.p.i.), neutralized and shifted to 37 °C for incubation.

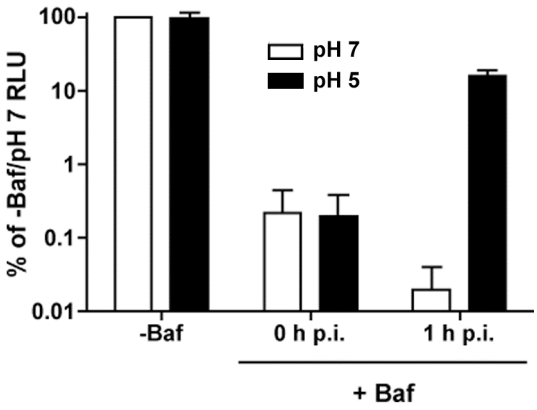

Fig. 5.11 Incubation at 37 ºC allows HCV to enter bafilomycin A1-treated cells. Huh-7.5 cells were treated with bafilomycin A1 (25 nM), then infected with HCV at 4 ºC for 2 h. Cells were washed to remove unbound virus, then washed with citric acid buffer at pH 7 (white bars) or 5 (black bars) immediately (0 h.p.i.) or after 1 h at 37 ºC (1 h.p.i.). Cells were incubated in the presence of bafilomycin A1 for 24 h when they were harvested for luciferase assays. Luciferase activity from untreated cells washed with pH 7-buffer (white bar, -Baf) was expressed as 100 percent. Values are the combined data from 2 independent experiments done in triplicate; error bars represent the standard errors of the means.

prior to the low pH wash increased more than 10-fold, to approximately 15% of the untreated value (Fig. 5.11, 1 h.p.i.). Again, no increase in luciferase activity was observed from cells that had been washed with pH 7 (Fig. 5.11, 1 h.p.i.). These results suggest that HCV requires an event that occurs within 1 h.p.i., possibly at the cell surface or within a forming endosome, for low pH to trigger entry in the presence of bafilomycin A1.

An inhibitor of clathrin-mediated endocytosis reduces the efficiency of HCV entry

To determine if HCV requires clathrin for productive uptake, I utilized a dominant-negative inhibitor of clathrin-mediated endocytosis, AP180c. In addition to its role as an accessory protein in AP-2 mediated uptake, AP180 functions as an alternative endocytic adaptor between clathrin and cargo (152). Because AP180 can bind directly to clathrin via its C-terminal domain (AP180c), this domain can act as a dominant negative of both AP-2 dependent and independent clathrin-mediated endocytosis. AP180c was cloned into a Venezuelan equine encephalitis (VEE) replicon (163), which allowed high levels of expression in Huh-7.5 cells.

Cells were electroporated with VEE-AP180c-GFP or VEE-GFP RNAs and monitored for GFP expression and susceptibility to HCVcc-Rluc

infection. HSV-1, which fuses at the plasma membrane and does not require clathrin, was used as a negative control. At 24 h post electroporation, when VEE-GFP and VEE-AP180c-GFP-transfected cells were 80-100% GFP-positive, cells were infected with HCVcc-Rluc or HSV-1. After 24 h of infection, infected cells were harvested and luciferase activity was determined. In Huh-7.5 cells harboring the VEE-AP180c-GFP replicon, HCV luciferase values were reduced by 44% compared to cells transfected with VEE-GFP (Fig. 5.12). In contrast, HSV-1 infection was supported similarly in both the VEE-AP180c-GFP and VEE-GFP cells; only a modest 16% decrease in HSV-1-driven luciferase activity was observed in the dominant-negative expressing cells. These data suggest a role for clathrin-mediated endocytosis in HCV entry. Further supporting this conclusion, HCV is inhibited by siRNAs which target clathrin heavy chain, as well as chemical inhibitors of clathrin-coated pit formation, such as chlorpromazine (21).

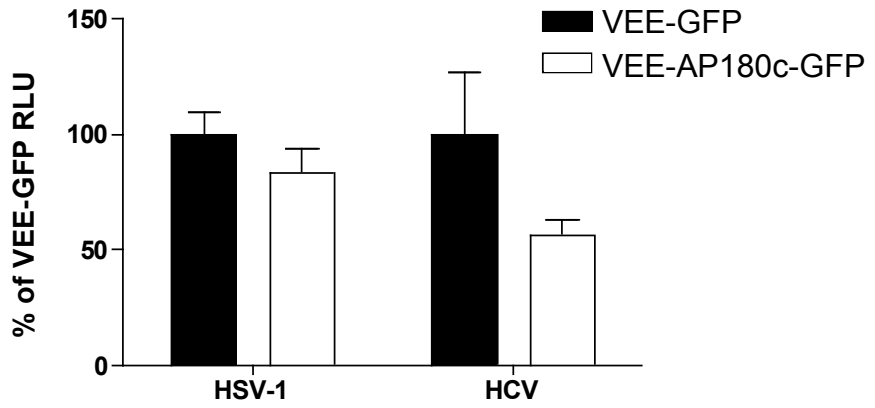

Fig. 5.12 HCV entry is moderately inhibited by a dominant-negative inhibitor of clathrin-mediated endocytosis. Huh-7.5 cells were electroporated with VEE-GFP (black bars) or VEE-AP180c-GFP (white bars) RNA and infected with either HCVcc-Rluc or HSV-1. At 24 h post electroporation, cells were harvested for luciferase assays. Values are the mean value of triplicate wells; error bars show the standard errors of the means. The data shown is representative of at least 2 independent experiments.

5.4 Role of HCV entry factors

SR-BI enhances HCV binding to CHO cells

To examine the role of HCV cellular entry factors in primary binding, CHO cell populations expressing human CD81, human SR-BI, or human CLDN1 were generated. CHO cells are nonpermissive for HCV entry, as demonstrated by their resistance to HCVpp (53), and therefore provide a means to isolate the initial interactions between HCV virions and molecules on the surface of the host cell.

CHO cells, mock-transduced or transduced with CD81, SR-BI or CLDN1, were incubated with HCVcc (J6/JFH) (MOI ~0.5). Cells were washed extensively, and total RNA was harvested for real-time qRT-PCR. While CHO-CD81 and CHO-CLDN1 cells bound similar levels of HCV RNA as mock-transduced cells, HCV RNA bound to CHO-SR-BI cells was increased nearly three-fold over the background level (Fig. 5.13). To confirm that the enhancement of HCV RNA binding to CHO-SR-BI cells was SR-BI dependent, all of the CHO cell populations were incubated with α-SR-BI antibody prior to and during the incubation with HCVcc. The presence of α-SR-BI antibody had no effect on HCV RNA binding to CHO-CD81 and CHO-CLDN1 cells, although it reduced the level of bound HCV RNA on CHO-SR-BI cells to that of mock-transduced cells. These data

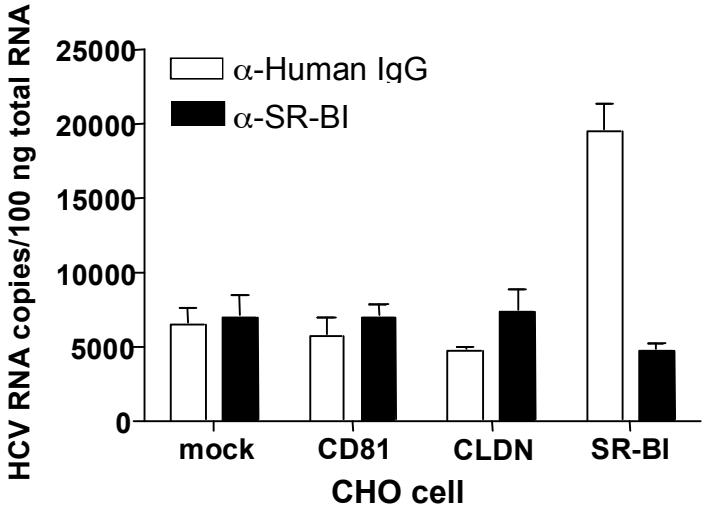

Fig. 5.13 HCVcc binds to CHO cells expressing SR-BI. CHO cells, mock transduced or transduced with CD81, CLDN1, or SR-BI, were preincubated with either anti-SR-BI or anti-human IgG antibodies, then incubated with J6/JFH HCVcc for 2 h at 37 ºC. After washing, total RNA was isolated and HCV RNA was amplified by real-time quantitative RT-PCR. Values are the average of triplicate wells; error bars show the standard deviations.

suggest that the cellular receptor SR-BI may have a role in primary HCV binding to the host cell, whereas CD81 and CLDN1 may act downstream in the entry pathway.

CLDN1 enhances HCV glycoprotein-mediated cell fusion

CLDN1, an integral membrane protein that is a component of tight junctions, has been recently shown to be a required HCV entry factor (53). 293T cells are rendered permissive for HCV entry by expression of CLDN1 and were therefore used in a cell fusion assay to examine the role of CLDN1 in HCV entry. For the fusion assay, 293T "Acceptor" cells expressing an HIV-1 transactivator of transcription (Tat)-inducible GFP reporter were co-cultured with 293T "Donor" cells expressing Tat (Fig. 5.14). A fusion event between donor and acceptor cells will thereby result in GFP expression.

When Donor cells expressing HCV E1/E2 were co-seeded with Acceptor cells harboring CLDN1, the number of GFP-positive foci increased by 7-fold compared to control cultures where Acceptor cells lacked CLDN1 (Fig. 5.15A). Although a pH 5 wash did not amplify the number of GFP foci compared to a pH 7 wash, it did enhance the size and extent of GFP-positive syncytia formation (Fig. 5.15B). A similar

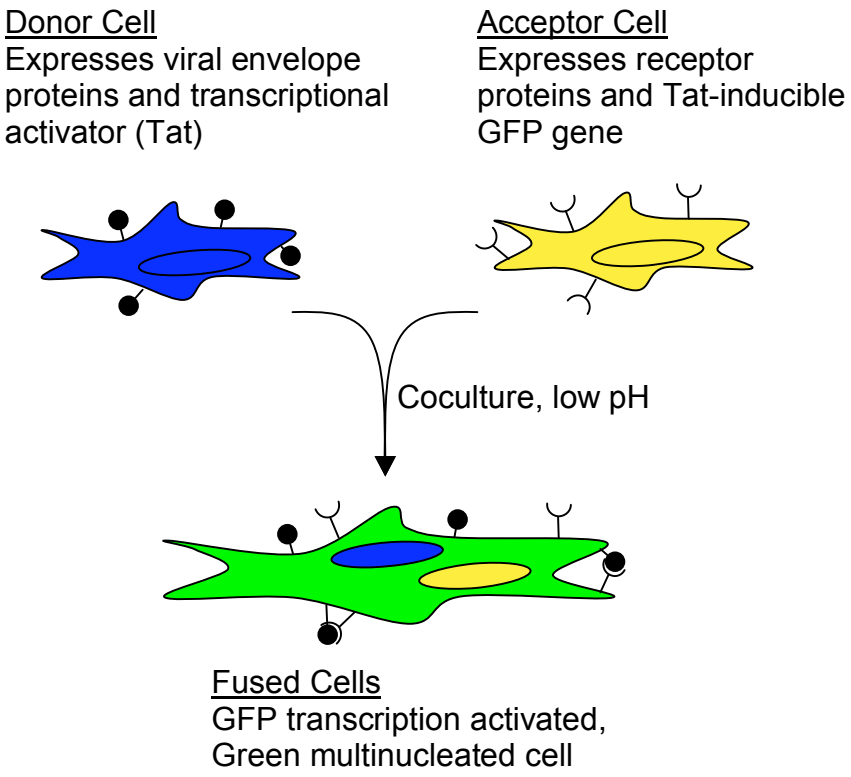

Fig. 5.14 Schematic illustration of cell fusion assay. Donor and Acceptor 293T cells are co-cultured to determine if HCV glycoprotein-mediated cell fusion can occur.

Fig. 5.15 CLDN-1 enhances HCV glycoprotein-mediated fusion in 293T cells. (**A**) 293T Acceptor cells expressing Tat-inducible GFP, as well as mock (-CLDN1, white) or CLDN1 (+CLDN1, black), were co-cultured with 293T Donor cells expressing mock (naïve), HIV-1 Tat, HCV E1E2, or both. Co-cultures were briefly treated with either pH 7 or 5, as indicated below each set of bars, at 24 h post seeding. The number of GFP foci per slide is the mean value from 3 experiments; error bars show the standard deviations. (**B**) Representative examples of typical GFP positive loci observed 48 h post pH treatment. For both VSV G and HCV E1/E2-mediated fusion, pH 5 treatment enhanced syncytia formation, but did not increase the number of GFP foci per well compared to a pH 7 wash.

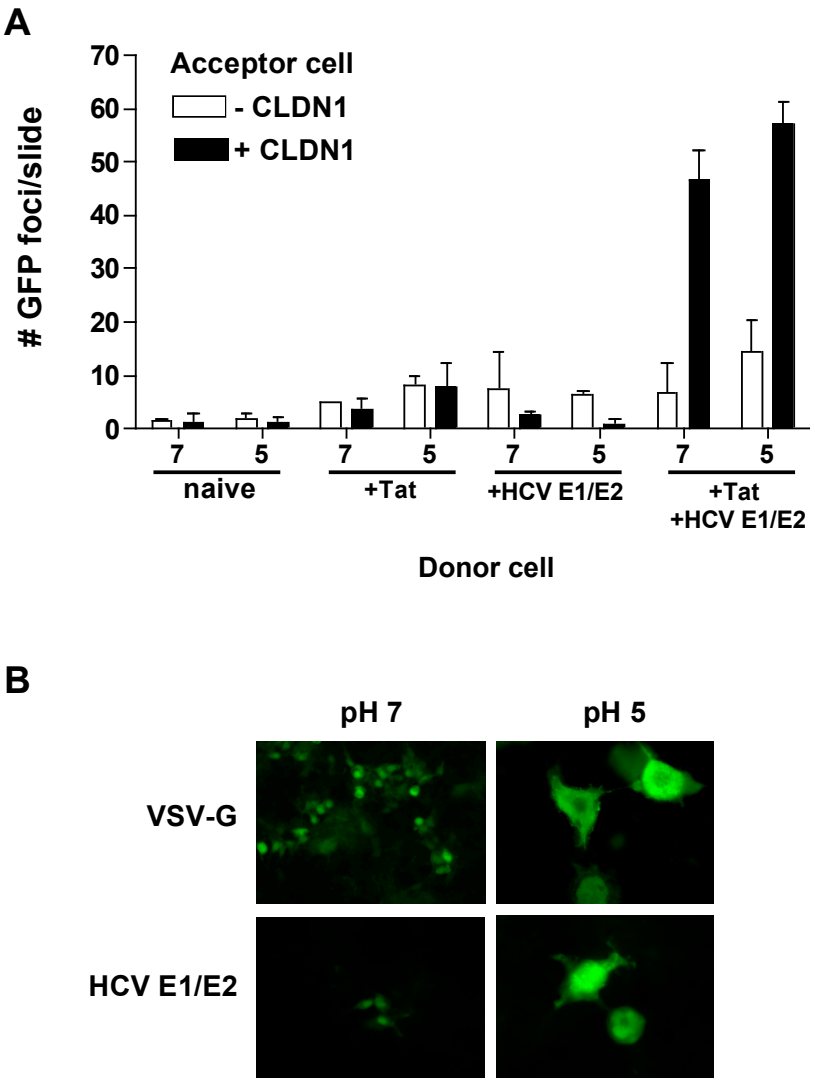
A
GFP foci/slide
70
60
50
40
30
20
10
0
Acceptor cell
- CLDN1
+ CLDN1
7
5
naive
+Tat
+HCV E1/E2
+Tat
+HCV E1/E2
Donor cell
B
pH 7
pH 5
VSV-G
HCV E1/E2

Fig. 5.15

observation was made when Donor cells expressing VSV G on their surface were washed with low pH. These data and the data above suggest that CLDN1 acts downstream from the primary binding step and is required for efficient HCV-glycoprotein-mediated fusion.

5.5 Discussion

The sensitivity of BVDV and HCV to agents that inhibit endosomal acidification strongly suggests that these viruses require a low pH step to enter their respective target cells. Such a pH-dependent route of entry is a common feature among viruses of the *Flaviviridae*. Both BVDV and HCV are also acid-resistant and the inability of these viruses to infect a bafilomycin A1-treated cell after exposure to low pH, under the same conditions that could induce fusion of the alphavirus SIN, suggests that a post-binding maturation step is required to render the virus competent for low pH-triggered entry.

The observation that HCV infectivity is resistant to acidic pH is surprising given its route of transmission through direct blood-to-blood exposure. In contrast, pestiviruses have long been known to be acid resistant, which fits with their need for protection against low pH as they travel through the ruminant digestive system. This shared characteristic of acid

resistance could be the result of a common evolutionary origin and may have been retained by HCV. Alternatively, production of acid-resistant virions may simply reflect a common strategy in the HCV and pestivirus lifecycles.

Low pH induces conformational changes to the envelope glycoproteins of viruses that enter cells by endocytosis, allowing fusion between viral and cellular membranes. Two classes of viral fusion proteins, Class I and Class II, that mediate entry of enveloped viruses have been defined (80). Influenza hemagglutinin (HA) is a prototype class I fusion protein (182). HA is primed for activation during assembly of influenza virions by proteolytic cleavage, which liberates an N-terminal fusion peptide. When exposed to low pH, HA undergoes a dramatic conformational change, which exposes the fusion peptide promoting interaction with membranes for fusion. Class II fusion proteins, found in alphaviruses and classical flaviviruses, are distinct from Class I in their structure, mechanism of action, and apparent evolutionary origin. Alphavirus and flavivirus glycoprotein precursors PE2 and prM, respectively, serve dual roles in virus maturation. As precursors, PE2 and prM act as chaperones to protect the viral fusogens E1 and E from exposure to the low pH environment of the trans-Golgi network, which would otherwise trigger exposure of the fusion peptide and premature fusion. During virion maturation, PE2 and prM are

cleaved by furin, releasing their N terminal fragments, and rendering the viral fusogens competent for pH-triggered fusion during entry (79, 80, 129). These fusion proteins have a well-defined dimer to trimer transition upon exposure to low pH (5, 103, 187). With the exception of the G-proteins of the rhabdoviruses, VSV and rabies virus, the transition of Class I or Class II proteins to the fusogenic state is irreversible (64, 65).

As mentioned above, the prM accessory protein of the classical flaviviruses provides protection during egress from the low pH environment of the cellular secretory pathway upon virion maturation; cleavage of this protein prior to release renders the virus competent for acid catalyzed fusion. For HCV and the pestiviruses, there is no evidence for such a proteolytic maturation event during assembly or release (157, 172, 195), suggesting that activation for subsequent low pH-requiring steps must occur during entry. Activation could theoretically occur at any of the multiple steps involved in the viral entry pathway, for example, binding to a receptor at the cell surface, sequential binding to a receptor and coreceptor, assembly of multiple factors at the cell surface, or within a forming or mature endosome.

In the case of BVDV, evidence exists for activation via disulfide bond reshuffling. The three pestiviral glycoproteins are stabilized by a combination of intra- and inter- molecular disulfide bonds. Treatment with

DTT was reported to decrease BVDV's resistance to acidic pH and to enhance its ability to fuse at the plasma membrane in the presence of low pH (109). Although I was unable to reproduce these results, it has been suggested that DTT might act by mimicking the action of protein disulfide isomerases (PDIs) at the cell surface or within the endocytic pathway that are required to destabilize the BVDV glycoproteins and prime them for fusion upon exposure to low pH. The role of PDIs in the entry of other viruses such as HIV and Moloney murine leukemia virus has been demonstrated (173, 175, 204). In my experiments with HCV, the possible contribution of disulfide bond reshuffling to HCV entry could not be assessed since DTT, at either pH 5 or 7, eliminated detectable HCVcc infection.

Another possibility I explored for HCV is proteolytic activation of the envelope glycoproteins by endosomal proteases. Similar to our observations for HCV, Ebola virus enters via a pH-dependent pathway, but these particles cannot fuse at the plasma membrane upon low pH exposure (91, 189, 212). Infection with VSV particles pseudotyped with EboV GP is inhibited when the activities of the CatB and CatL endosomal proteases are blocked by chemical inhibitors (35). This suggests that EboV entry requires a proteolytic cleavage, which triggers fusion in the endosome. Severe acute

respiratory syndrome coronavirus infection was also shown to be dependent on CatL to cleave its spike glycoprotein within the endosome (179). Additionally, the non-enveloped reoviruses require CatB and CatL for efficient virus disassembly (34, 49). Although inhibitors of CatB/CatL had no effect on HCV infection, it is still possible that different endosomal proteases or other endosomal determinants are required to prime the HCV glycoproteins for fusion.

Alternatively, HCV may be primed for low pH-induced entry by receptor binding or subsequent steps prior to the formation of mature endosomes. Simple binding of HCVcc to cells at 4 °C was not sufficient to activate the virus for low pH-triggered entry at the plasma membrane. One explanation is that HCV entry at the plasma membrane is non-productive for downstream events in the viral life cycle, as previously observed for Semliki Forest virus and VSV in CHO cells (136), and avian leukosis virus (151). However, the fact that low pH could override the bafilomycin A1 block to HCV infection after a shift to incubation at 37 °C, described in Fig. 5.11, suggests that HCV can undergo time- and temperature-dependent activation at the cell surface or in forming endosomes. Further study is necessary to delineate the nature of this event regarding the viral and cellular determinants required, and particular roles of CD81, CLDN1, and SR-BI.

Chapter 6. Unanswered questions and future directions

6.1 Mechanism of E1*E2p7* inhibition of BVDV entry

In this study, I successfully used a functional genomics approach to examine the BVDV life cycle and to identify E2 as a transdominant inhibitor of BVDV entry. Furthermore, the MDBK- E1*E2p7* cells characterized above will provide valuable insights into the molecules required for BVDV to productively enter a cell and the mechanism of BVDV superinfection exclusion at the level of entry.

The observation that CD46 down regulation from the surface of MDBK-E1*E2p7* cells is not the mechanism of BVDV inhibition, suggests that CD46 may not be the only molecule required for BVDV entry. This hypothesis has been proposed previously by Maurer *et al*. (137). In this study, non-permissive cells transduced to express CD46 remained non-permissive for BVDV infection. Moreover, BVDV enters cells by clathrin-mediated endocytosis and CD46 is excluded from endosomes due to a sorting signal (74, 109, 137), suggesting that an additional factor may act downstream from CD46 to mediate subsequent internalization steps. Therefore, although CD46 expression and binding of BVDV to the MDBK-E1*E2p7* cells is unaffected, the possibility of E2-mediated down regulation of an unidentified, essential coreceptor, required for BVDV internalization and fusion, still exists. The requirement for multiple cellular

entry factors is certainly true for HCV and may be likely for BVDV as well, considering that both of these viruses undergo an activation step, which occurs after primary binding (109, 198). MDBK-E1*E2p7* cells may then be resistant to BVDV entry due to the ability of E2 to sequester this additional entry factor away from the cell surface or from other BVDV entry factors.

One may take a variety of approaches to examine BVDV E2-interacting factors in MDBK-E1*E2p7* cells and to define the inhibitory mechanism within them. As a first attempt, E2-associated proteins can be immunoprecipitated from MDBK-E1*E2p7* cell lysates or cells expressing an epitope-tagged E2 protein. This approach will demonstrate if BVDV E2 is associated with a particular cellular molecule and is thereby preventing its function in BVDV entry. Another method to identify the essential factor(s) absent or nonfunctional in these cells is to screen for cDNAs from wild-type MDBK cells that can render MDBK-E1*E2p7* cells permissive for BVDV infection. Moreover, the observed BVDV entry defect in MDBK-E1*E2p7* cells is analogous to that of CRIB cells (cells resistant to infection with BVDV) (60). CRIB cells are also resistant to BVDV entry and harbor functional CD46 on their surfaces. It was originally thought that these cells were deficient in LDL-R (3), a proposed BVDV entry factor, although a

recent study suggests that these cells do in fact express LDL-R and furthermore that this molecule is not required for BVDV infection (108). Even so, CRIB cells can be used in conjunction with MDBK-E1*E2p7* cells to further define a complete set of BVDV entry factors, possibly by cataloging differences in cell surface molecules between these BVDV-resistant cell types and wild type MDBK cells.

6.2 BVDV and HCV superinfection exclusion mechanisms

Superinfection exclusion at the level of RNA replication

Both BVDV and HCV-infected cells establish superinfection blocks at one or more steps in RNA replication. The mechanism by which existing BVDV and HCV RNA replication inhibits superinfecting RNA replication remains to be determined. One hypothesis is that exclusion might be due to insufficient levels of a cellular factor(s) required for virus replication. BVDV and HCV RNA elements or proteins could interact with limiting cellular factors essential for replication and sequester them during the course of infection, thus reducing their availability for an incoming, homologous virus.

To identify these cellular components, we could characterize cellular factors that up regulate BVDV or HCV replication. The observation that levels of replication plateau after infection or transfection of viral RNA, suggests that one or more cellular factors are limiting, controlling the amount of replication that can be supported by the host cell. Therefore, cellular factors, which can increase levels of viral replication, are possible candidates for those that are unavailable for the superinfecting virus and prevent the efficient establishment of its replication. One example of a cellular component required for HCV replication is the liver-specific microRNA, microRNA-122 (miR-122), which facilitates efficient HCV replication (94). Sequestration of miR-122 in HCV replicon-containing cells results in a decrease in HCV RNA replication, which can be restored if miR-122 is ectopically expressed (94). Perhaps levels of miR-122 are reduced over the course of HCV replication or alternatively, miR-122 is inaccessible to the superinfecting virus, preventing the establishment of productive replication.

Another method to identify cellular components that may be limiting for the superinfecting virus is to analyze cellular factors that are closely associated with BVDV and HCV replication complexes. This may be possible by tagging a component of the viral replicase complex, such as

NS5A, with an epitope tag, which can be pulled out from cell lysates with a high affinity antibody. This approach has recently been used to characterize proteins associated with SIN replication complexes (43, 62). Once the required cellular components for HCV or BVDV replication have been identified, cells can be examined for depletion or modulation of this factor during infection and whether its exogenous expression can upregulate replication.

Interference at the level of RNA replication may also be related to the availability of subcellular sites for replication. Positive-strand RNA viruses replicate their RNAs in association with existing or virus-modified subcellular membrane organelles. Bromegrass mosaic virus (BMV), for example, induces spherule-like invaginations into the lumen of the ER that are still connected to the cytosol by a narrow channel. Negative-strand RNA molecules are sequestered in these compartments where they are used as templates for viral genome amplification (178). Likewise, flavivirus RNA replication occurs in a specialized membrane compartment surrounding the nucleus (33, 36, 37, 207, 208). HCV replication complexes are associated with a structure called the "membranous web" and BVDV is also known to extensively reorganize intracellular membranes for sites of replication (50, 69, 194). During primary infection, these specialized areas might become

saturated with replication complexes, blocking access of the superinfecting viral RNA and preventing its entry into functional replication complexes. Alternatively, the availability for building blocks required to create these sites may become limiting. Consistent with this explanation, HCV RNA replication is stimulated by the increased availability of fatty acids (98), which may be important to maintain the integrity of the membranous web as a site of efficient replication. We could therefore further characterize the sites of BVDV and HCV replication in the cell with regard to its location, membrane composition, and associated host factors using a combination of the techniques described above.

An additional question is what criteria regulate the establishment of a particular superinfection defect? Specifically, how is it that BVDV can block superinfecting virus at entry and replication, whereas the block in HCV-infected and replicon cells occurs only at a post-entry step? This may be a consequence of replication style, protein localization, or levels of structural proteins. In addition, assuming that the BVDV entry block is at the coreceptor level, testing whether there is an intracellular interaction between the viral structural proteins and putative receptor/coreceptors could provide a potential explanation. If this is the mechanism of exclusion, it may be that for HCV the conformations of the nascent glycoproteins differ from those on

the mature virion, preventing an intracellular interaction with cellular receptors. Such a scenario would then preclude the establishment of an HCV superinfection block at the level of entry. Given the requirement for specific, host factors and the specialized nature of viral replication sites, it is perhaps not surprising that both BVDV and HCV generate blocks to superinfecting virus at the level of RNA replication. Using the techniques described above, this work will hopefully lead to the identification of the limiting factors for viral RNA replication and how they regulate this intricate process.

Cellular alterations induced by persistent ncp BVDV infection

Our data suggest that cellular changes or alterations within ncp BVDV persistently infected cells contribute to the loss of superinfection exclusion for cp BVDV. Superinfection exclusion was not restored by reinfection of the ncp BVDV persistently infected cells with the original ncp BVDV. In addition, ncp BVDV from persistently infected cells was capable of establishing superinfection exclusion in naïve MDBK cells. Persistent BVDV infection thus appears to induce a cellular alteration that down regulates ncp virus replication and allows cp BVDV superinfection to occur.

Besides the studies discussed in Section 4.2 and 4.3, two other papers have examined pestivirus superinfection exclusion. Baigent *et al*. reported

that calf testis cells could be productively superinfected with cp BVDV 48 h after acute infection with ncp BVDV (7). NS3 and CPE became detectable after an additional 48 h, or 4 days post acute infection (significantly delayed when compared to cp BVDV infection of naïve cells). These data are consistent with the observations reported here. Another earlier study was conducted by Mittelholzer and colleagues for CSFV (147). CSFV is generally noncytopathic and readily establishes persistent infections in cell culture. Persistently infected cultures, serially passaged more than 100 times, yielded cp defective interfering (DI) RNAs that spread through some of the cultures and killed the majority of the cells. The few surviving cells were still infected, but had either lost the cp DI RNA or contained an ncp CSFV variant that was able to "control" replication of remaining DI RNA to a level that was no longer cytopathic. Interestingly, virus production in the persistently infected CSFV cultures prior to the emergence of the cp DI RNAs was about 100-fold lower than after acute infection, analogous to our results for MDBK cells persistently infected with ncp BVDV. Thus, the emergence of a packaged cp DI RNA variant, like superinfection with cp BVDV, was able to spread through culture, replicate to high levels and kill the majority of the cells.

Intriguing questions are raised by all of these studies. First, what are the cellular alterations that down regulate the replication level of the ncp virus after the acute phase of infection? The nature of these cellular changes remains unknown, but it will be interesting to see if this state requires continuing ncp pestivirus replication or if stable epigenetic changes have occurred. This could be determined by curing the persistently infected cells with a BVDV-specific polymerase inhibitor and then determining if these cells can support wild type levels of virus replication.

Another question is how do persistently infected cells remain relatively resistant to superinfection by homologous ncp BVDV, but not to cp BVDV over the time tested? It is interesting that the same mechanism that excludes ncp BVDV does not apply to a superinfecting cp virus (in the case of our BVDV studies) or to the cp CSFV DI characterized by Mittelholzer *et al*. In persistently infected cells as opposed to acute infection, both cp and ncp BVDV may be able to enter the cell more efficiently, encountering lower levels of the E2-mediated block. At the replication level, however, the ncp BVDV remains blocked, whereas the cp BVDV can somehow enter into productive replication possibly due to fundamental differences in its replication mechanism. It is conceivable that due to a greater efficiency of replication initiation or a higher rate of replication, cp

BVDV escapes interaction with a negative cellular factor that is up regulated during persistent infection. Conversely, cp BVDV may not have the same requirement as ncp BVDV for a particular cellular factor that becomes down regulated over the course of infection. One likely candidate is the cellular chaperone protein Jiv. Expression of the 90 amino acid insertion of Jiv (Jiv90) in the cp BVDV NADL genome is sufficient for efficient cleavage at the NS2/3 junction. ncp BVDV, however, remains dependent on the cellular pool of Jiv, which becomes reduced during infection and limits the level of replication (111). To characterize additional cellular factors, which are modulated over the course of infection, one could utilize microarray analysis to examine the gene expression profiles of ncp BVDV acutely and persistently infected cells and compare them to those of cp BVDV-infected cells. It is also possible that the cellular alteration affects the site of ncp BVDV replication and that cp BVDV is more fit to utilize slightly different replication sites. A method to examine this hypothesis would be to compare the replication sites of cp and ncp BVDV, in terms of protein and membrane components, as well as their physical location in the cell, possibly by electron microscopy.

Role of superinfection exclusion in vivo

The notion that cp BVDV arises from ncp BVDV by a rare RNA recombination event leading to fatal MD prompts the question of whether persistently ncp BVDV-infected cells might not exclude superinfecting cp BVDV *in vivo*. If not, how would a cp BVDV variant that arose be propagated? One possibility is that cp BVDV might have a different cell tropism than ncp BVDV. While cp and ncp BVDV may well have different replication efficiencies in a given cell type, it seems unlikely that these variants would infect different target cells since they have identical or nearly identical structural proteins. Alternatively, infection may well be dynamic in persistently infected animals with not all susceptible target cells pre-infected with ncp BVDV. Our study showed a loss of superinfection exclusion in ncp BVDV-infected cells after 1-2 passages. This demonstrates that acutely infected cells that are initially refractory to superinfection may eventually become permissive, thus providing a reservoir of susceptible cells. This would give the founder virus an initial replication advantage over a superinfecting variant but this advantage would diminish over time. Another possibility is that superinfection exclusion may not be efficiently established in all cell types.

The phenomenon of HCV superinfection exclusion has potentially important implications for understanding HCV biology *in vivo*. First, the efficient block for replication of the superinfecting genome would limit the potential for RNA recombination to cells simultaneously infected by two viruses or infected cells that were successfully superinfected before the replication block was established. This may, in part, explain the dearth of natural HCV recombinants that have been identified thus far despite numerous examples of patients harboring more than one HCV genotype (39, 96). Second, even less-fit HCV variants generated during error-prone HCV replication have a chance for at least transient survival assuming that they could productively infect a target cell and efficiently exclude replication of the more fit parental virus. This could provide HCV with a larger pool of variants to deal with immune or other selective pressures that emerge during the course of infection (or treatment). The observation that superinfection exclusion is reversible at the cellular level suggests that interferon (24) or specific antiviral [(153) and this study] treatment may "cure" cells thereby expanding the number of hepatocytes that are permissive for replication of inhibitor-resistant variants. Finally, the phenomenon of superinfection exclusion and the fact that HCV RNA levels are regulated and plateau after

transfection or infection, as discussed above, suggest that there are one or more limiting cellular components required for HCV RNA replication.

HCV JFH-1 induced cytotoxicity in CD81-expressing cells

We observed a J6/JFH-specific cytotoxicity within CD81-expressing cells after prolonged J6/JFH HCVcc infection or selection of G418 resistant populations harboring J6/JFH replicons. This resulted in a population dominated by $CD81^{low}$ cells, rendering them nonpermissive for HCV entry. Notably, this was not the case for subgenomic replicons or for full-length Con1 or H77 replicons. One possibility to explain this genotype-specific difference is that high-level expression of the J6 C-NS2 region driven by the JFH replicase is required for CD81-dependent cytostatic or cytotoxic effects. Similar high levels of expression may not be achieved by the Con1 or H77 adapted replicons. Alternatively, whatever toxic determinants lie within the C-NS2 region may be specific for the genotype 2a isolates tested thus far [J6 and JFH; (221)] and not present in the corresponding genotype 1a (H77) or 1b (Con1) proteins. However, another potentially important difference is the ability of J6/JFH constructs to produce infectious virus in cell culture. In future experiments it will be interesting to explore these possibilities by examining the properties of H77/JFH chimeras that are defective for virus

production versus those harboring adaptations that allow release of infectious virus [(142, 218) and M. Evans *et al.*, in preparation].

Interestingly, the J6/JFH-FLneo population cured with BILN 2061 in the absence of G418 regained CD81 expression and became permissive for HCVpp entry. Several possibilities, either at the population or single cell level could account for restored CD81 expression. At the population level, $CD81^{low}$ cells might lose their growth advantage over surviving $CD81^{high}$ cells in the absence of J6/JFH-FLneo replication or infection. Restoration of CD81 expression was slow and occurred after HCV RNA reached background levels. This might indicate that $CD81^{high}$ cells have only a subtle growth advantage over $CD81^{low}$ cells in the absence of virus. This idea could be explored by sorting cells for $CD81^{high}$ or $CD81^{low}$ expression and comparing their growth rates in the absence or presence of HCV RNA. Alternatively, at the single cell level, slow recovery of CD81 expression could be due to an intrinsically slow rate of CD81 protein accumulation or slowly reversible epigenetic changes that down regulated CD81 expression and occurred due to persistent J6/JFH-FLneo replication and infection. A more complete understanding of the kinetics of CD81 transcription, translation, and protein turnover/stability may provide evidence for this hypothesis.

Another question relates to the mechanism of cytotoxicity and the pathway by which the $CD81^{high}$ cells undergo cell death. Gene expression analysis of an Huh-7.5 population undergoing J6/JFH infection will assist in determining if specific signaling pathways, such as those involved in ER-stress or apoptotic signaling, are activated. In addition, if Huh-7.5 cells are forced to over-express CD81 during J6/JFH infection, the majority of cells die, but some cell clones develop (M. J. Evans, personal communication). Characterization of the survival mechanism in these cells may provide insight into the cause of the cytotoxic effect in susceptible cells.

The *in vivo* relevance of HCV-induced cytotoxicity and the role of the C-NS2 region and CD81 in this process requires further study. One might argue that the genotype specific differences, the high level of replication driven by the thus far unique non-adapted JFH-1 replicase, and the use of Huh-7 or Huh-7.5 hepatoma cells make it unlikely that similar effects will be seen in the HCV-infected liver. Certainly the generally accepted view, that HCV-associated liver damage is immune mediated rather than a direct consequence of hepatocyte infection, is consistent with this view. However, some instances of acute fulminant hepatitis C (54, 68, 101, 219) or rapidly progressive hepatitis in the post-transplant setting (30, 139) could be the result of HCV variants that are cytotoxic, either due to higher replication

levels, the production of toxic viral components, or both. In addition, the level of hepatocyte CD81 expression is clearly one mechanism for controlling HCV infection that may also influence pathogenesis. This could be modulated by the virus, the host-response to virus infection, or therapeutically. In this regard, it will be interesting to examine possible heterogeneity in the level of CD81 expression in HCV-infected and uninfected liver tissue and determine if there is a relationship between CD81 levels, virus infection and cell death.

6.3 Studies of the BVDV and HCV entry pathways

Mechanism of HCV and BVDV activation for pH-triggered entry

The data presented in Chapter 5 demonstrate that both BVDV and HCV are acid-resistant viruses that require activation for pH-triggered entry. Although the mechanism of this activation step remains ambiguous, the pathway, at least for HCV, appears to be both time- and temperature-dependent, given the observation that low pH can allow bound HCV virions to enter a cell in the presence of bafilomycin A1 after prolonged incubation at 37 ºC. Although the effects of the elevated temperature and incubation time warrant further study, several scenarios can be envisioned based on previous work with other enveloped viruses. In the case of avian leukosis

virus and perhaps also for HCV, productive entry could require not only receptor binding but also a forming endosome, encountered only after incubation at 37 °C (151). However, even before receptor mediated endocytosis and formation of mature endosomes, HCV may require interactions that do not occur during binding at 4°C. Given the wealth of factors shown to be required for HCV entry, among them CD81, SR-BI, CLDN1 and GAGs, HCV may require contact with all or at least some of these factors prior to fusion. For example, HCV may be tethered to the cell initially through interactions with GAGs, then attach to the cell surface via a binding determinant, possibly SR-BI, as our data indicates. Productive entry may subsequently necessitate access to CD81 and later to CLDN1, which has been shown to act at a late step in HCV entry and downstream of CD81 (53). These interactions might require lateral diffusion in the plasma membrane or changes at the plasma membrane that occur during endosome formation, either of which could be compromised by low temperature and decreased membrane fluidity.

For BVDV, a time and temperature dependent activation mechanism, similar to HCV, could potentially occur. This event may involve interaction with CD46 and other coreceptors, as well as the rearrangement of disulfide bonds within the envelope glycoproteins. The role for disulfide bond

reshuffling in BVDV entry remains undetermined, at least in the context of my experiments presented above. However, the use of selective inhibitors of protein disulfide isomerases, as opposed to the relatively nonspecific action of DTT, may provide an alternative method to investigate the possible importance of disulfide bond re-organization in activation of BVDV for productive entry. It will also be interesting to determine if HCV undergoes an analogous pathway to acid sensitivity as BVDV or if these two viruses differ in terms of their requirements for protein disulfide isomerases, conformational changes within the envelope glycoproteins, or location of receptor interactions.

Another question is how does an acid-resistant virion differ conformationally from one that is acid-sensitive and therefore, fusion competent? Also, at what stage in the course of their entry pathways do HCV and BVDV become acid-sensitive - at the cell surface, or in the process of internalization by receptor-mediated endocytosis? The detection of specific changes within the virion associated with activation could be used as a marker for particular stages in the virus entry, for example by monitoring changes in epitope exposure over time using a panel of glycoprotein-specific MAbs. Another method would be to bind the virus to bafilomycin A1-treated cells and to perform a time course of low pH pulses

after shifting to 37 ºC in the presence of either a CD81 or CLDN1 antibody. It will be interesting to determine if a low pH wash at a particular time point during entry overcomes the requirement for one or both of these receptors, which have been shown to act downstream of primary binding (41, 53, 106). Alternatively, the blocking antibodies can be added at different time points after the temperature shift prior to washing with low pH. In addition, the virus can be incubated with a soluble form of SR-BI to determine if this treatment renders the virus acid-sensitive and/or increases virus binding to either CD81 or CLDN1. A similar protocol can also be performed with soluble CD81. These experiments will help delineate the kinetics of HCV activation and the role of particular receptors in these changes. In addition, it will be important to determine if the requirements for or timing of HCV activation in Huh-7.5 cells differ from those in polarized cells where CLDN1 resides in the tight junction.

An additional intriguing question relates to the signaling events required for BVDV and HCV productive uptake. For BVDV, the cellular receptor CD46 has 2-3 spliced isoforms of its cytoplasmic tail, which may differ in terms of their signaling to downstream factors. We could first determine if signaling from CD46 is required, and if so, if a particular CD46 isoform is needed during BVDV entry. For HCV, although the cytoplasmic

tail of CD81 is not required (220), SR-BI and its relative, SR-BII, have signaling capability that could coordinate the assembly of other entry factors such as CD81 and CLDN1. Future experiments should be aimed at gaining a better understanding of the steps leading to productive HCV entry, paying particular attention to interaction between the HCV glycoproteins and these cellular entry factors.

Comparing HCVpp and HCVcc entry

The HCVpp system has provided clues to the mechanism of HCV entry into cells, which can now be tested directly using HCVcc. Many of the observations made with HCVpp, such as receptor usage and pH-dependent entry, have now been confirmed in the HCVcc system. For example, the role of CD81 in HCV infection, previously demonstrated using HCVpp (220), is also important for entry of HCVcc (123, 203, 221). As I have found for HCVcc, HCVpp entry is also pH-dependent and sensitive to concanamycin A and NH_4Cl (85). Interestingly, in contrast to the data presented here, Hsu *et al.* reported that HCVpp (genotype 1a, strain H77) were moderately susceptible to inactivation by low pH (85). The basis for this difference is unknown but could reflect differences in the HCV strains used in the two studies or the experimental systems themselves. If incorporation of HCV

E1E2 heterodimers into HCVpp is similar to gp120/gp41 into HIV particles (217), then each HCVpp may harbor less than 10 copies of functional HCV E1E2 heterodimers. In contrast, if HCVcc particles resemble those of the classical flaviviruses, which consist of 90 envelope protein dimers (110), the HCVcc surface may consist of tightly packed glycoprotein oligomers. One could imagine that such a lattice, stabilized by lateral interactions, might be more acid-resistant. Thus, while entry studies using HCVpp and HCVcc have yielded remarkably convergent results, some features may differ. It will also be important to compare HCVcc to HCVcc recovered from infected animals, so-called *ex vivo* HCVcc. *ex vivo* HCVcc retrieved from infected chimpanzees or uPA-SCID mice can be recultured in Huh-7.5 cells (124). This virus can be examined for acid-resistance, receptor usage, and pH-dependence of entry. Entry studies using these different viruses, HCVpp, HCVcc, and *ex vivo* HCVcc, can also be extended to other cell types, including primary hepatocytes.

6.4 Perspectives

These studies have described important features of BVDV and HCV entry and replication, provoked many additional questions, and roused new ideas for future research. It is clear that a better understanding of the virus

host interactions that are required for BVDV and HCV entry, as well as productive replication, may suggest new targets for therapeutic intervention. Future work aims to answer the questions outlined above and will no doubt engender additional projects as well. Moreover, as new technology becomes available, more sophisticated techniques can be applied to the study of BVDV and HCV entry. The ability to tag viral particles using a variety of methods and to track them in real-time using microscopy is an innovative and exciting approach, which provides the potential to follow the virus during the early events of its life cycle. These state of the art techniques can be combined with other approaches suggested above in an attempt to generate a complete picture of the cellular entry pathways of these viruses. With each experiment comes the opportunity to increase our understanding of BVDV and HCV infection and pathogenesis and to help alleviate the personal and economic strain imparted by these viruses on our society.

References

1. **Adams, R. H., and D. T. Brown.** 1985. BHK cells expressing Sindbis virus-induced homologous interference allow the translation of nonstructural genes of superinfecting virus. J Virol **54:**351-7.

2. **Agapov, E. V., C. L. Murray, I. Frolov, L. Qu, T. M. Myers, and C. M. Rice.** 2004. Uncleaved NS2-3 is required for production of infectious bovine viral diarrhea virus. J Virol **78:**2414-25.

3. **Agnello, V., G. Abel, M. Elfahal, G. B. Knight, and Q. X. Zhang.** 1999. Hepatitis C virus and other flaviviridae viruses enter cells via low density lipoprotein receptor. Proc Natl Acad Sci U S A **96:**12766-71.

4. **Air, G. M., and W. G. Laver.** 1989. The neuraminidase of influenza virus. Proteins **6:**341-56.

5. **Allison, S. L., J. Schalich, K. Stiasny, C. W. Mandl, C. Kunz, and F. X. Heinz.** 1995. Oligomeric rearrangement of tick-borne encephalitis virus envelope proteins induced by an acidic pH. J Virol **69:**695-700.

6. **Baginski, S. G., D. C. Pevear, M. Seipel, S. C. Sun, C. A. Benetatos, S. K. Chunduru, C. M. Rice, and M. S. Collett.** 2000. Mechanism of action of a pestivirus antiviral compound. Proc Natl Acad Sci U S A **97:**7981-6.

7. **Baigent, S. J., G. Zhang, M. D. Fray, H. Flick-Smith, S. Goodbourn, and J. W. McCauley.** 2002. Inhibition of beta interferon transcription by noncytopathogenic bovine viral diarrhea virus is through an interferon regulatory factor 3-dependent mechanism. J Virol **76:**8979-88.

8. **Bartenschlager, R.** 2006. Hepatitis C virus molecular clones: from cDNA to infectious virus particles in cell culture. Curr Opin Microbiol **9:**416-22.

9. **Bartenschlager, R., M. Frese, and T. Pietschmann.** 2004. Novel insights into hepatitis C virus replication and persistence. Adv Virus Res **63:**71-180.

10. **Bartenschlager, R., and V. Lohmann.** 2001. Novel cell culture systems for the hepatitis C virus. Antiviral Res **52:**1-17.

11. **Barth, H., C. Schafer, M. I. Adah, F. Zhang, R. J. Linhardt, H. Toyoda, A. Kinoshita-Toyoda, T. Toida, T. H. Van Kuppevelt, E. Depla, F. Von Weizsacker, H. E. Blum, and T. F. Baumert.** 2003. Cellular binding of hepatitis C virus envelope glycoprotein E2 requires cell surface heparan sulfate. J Biol Chem **278:**41003-12.

12. **Bartosch, B., and F. L. Cosset.** 2006. Cell entry of hepatitis C virus. Virology **348:**1-12.

13. **Bartosch, B., J. Dubuisson, and F. L. Cosset.** 2003. Infectious hepatitis C virus pseudo-particles containing functional E1-E2 envelope protein complexes. J Exp Med **197:**633-42.

14. **Bartosch, B., G. Verney, M. Dreux, P. Donot, Y. Morice, F. Penin, J. M. Pawlotsky, D. Lavillette, and F. L. Cosset.** 2005. An interplay between hypervariable region 1 of the hepatitis C virus E2 glycoprotein, the scavenger receptor BI, and high-density lipoprotein promotes both enhancement of infection and protection against neutralizing antibodies. J Virol **79:**8217-29.

15. **Bartosch, B., A. Vitelli, C. Granier, C. Goujon, J. Dubuisson, S. Pascale, E. Scarselli, R. Cortese, A. Nicosia, and F. L. Cosset.** 2003. Cell entry of hepatitis C virus requires a set of co-receptors that include the CD81 tetraspanin and the SR-B1 scavenger receptor. J Biol Chem **278:**41624-30.

16. **Bassin, R. H., S. Ruscetti, I. Ali, D. K. Haapala, and A. Rein.** 1982. Normal DBA/2 mouse cells synthesize a glycoprotein which interferes with MCF virus infection. Virology **123:**139-51.

17. **Bazan, J. F., and R. J. Fletterick.** 1989. Detection of a trypsin-like serine protease domain in flaviviruses and pestiviruses. Virology **171:**637-9.

18. **Behrens, S. E., C. W. Grassmann, H. J. Thiel, G. Meyers, and N. Tautz.** 1998. Characterization of an autonomous subgenomic pestivirus RNA replicon. J Virol **72:**2364-72.

19. **Berg, A., T. Pietschmann, A. Rethwilm, and D. Lindemann.** 2003. Determinants of foamy virus envelope glycoprotein mediated resistance to superinfection. Virology **314:**243-52.

20. **Bick, M. J., J. W. Carroll, G. Gao, S. P. Goff, C. M. Rice, and M. R. MacDonald.** 2003. Expression of the zinc-finger antiviral protein inhibits alphavirus replication. J Virol **77:**11555-62.

21. **Blanchard, E., S. Belouzard, L. Goueslain, T. Wakita, J. Dubuisson, C. Wychowski, and Y. Rouille.** 2006. Hepatitis C virus entry depends on clathrin-mediated endocytosis. J Virol **80:**6964-72.

22. **Blight, K. J., A. A. Kolykhalov, and C. M. Rice.** 2000. Efficient initiation of HCV RNA replication in cell culture. Science **290:**1972-4.

23. **Blight, K. J., J. A. McKeating, J. Marcotrigiano, and C. M. Rice.** 2003. Efficient replication of hepatitis C virus genotype 1a RNAs in cell culture. J Virol **77:**3181-90.

24. **Blight, K. J., J. A. McKeating, and C. M. Rice.** 2002. Highly permissive cell lines for subgenomic and genomic hepatitis C virus RNA replication. J Virol **76:**13001-14.

25. **Bolin, S. R., A. W. McClurkin, R. C. Cutlip, and M. F. Coria.** 1985. Severe clinical disease induced in cattle persistently infected with noncytopathic bovine viral diarrhea virus by superinfection with cytopathic bovine viral diarrhea virus. Am J Vet Res **46:**573-6.

26. **Branch, A. D., D. D. Stump, J. A. Gutierrez, F. Eng, and J. L. Walewski.** 2005. The hepatitis C virus alternate reading frame (ARF) and its family of novel products: the alternate reading frame protein/F-protein, the double-frameshift protein, and others. Semin Liver Dis **25:**105-17.

27. **Bratt, M. A., and H. Rubin.** 1968. Specific interference among strains of Newcastle disease virus. 3. Mechanisms of interference. Virology **35:**395-407.

28. **Bratt, M. A., and H. Rubin.** 1968. Specific interference among strains of Newcastle disease virus. II. Comparison of interference by active and inactive virus. Virology **35:**381-94.

29. **Brown, R. S.** 2005. Hepatitis C and liver transplantation. Nature **436:**973-8.

30. **Cameron, A. M., and R. W. Busuttil.** 2006. The status of liver transplantation for hepatitis C. Expert Opin Biol Ther **6:**993-1002.

31. **Carroll, S. S., J. E. Tomassini, M. Bosserman, K. Getty, M. W. Stahlhut, A. B. Eldrup, B. Bhat, D. Hall, A. L. Simcoe, R. LaFemina, C. A. Rutkowski, B. Wolanski, Z. Yang, G. Migliaccio, R. De Francesco, L. C. Kuo, M. MacCoss, and D. B. Olsen.** 2003. Inhibition of hepatitis C virus RNA replication by 2'-modified nucleoside analogs. J Biol Chem **278:**11979-84.

32. **Cattaneo, R.** 2004. Four viruses, two bacteria, and one receptor: membrane cofactor protein (CD46) as pathogens' magnet. J Virol **78:**4385-8.

33. **Cauchi, M. R., E. A. Henchal, and P. J. Wright.** 1991. The sensitivity of cell-associated dengue virus proteins to trypsin and the detection of trypsin-resistant fragments of the nonstructural glycoprotein NS1. Virology **180:**659-67.

34. **Chandran, K., and M. L. Nibert.** 2003. Animal cell invasion by a large nonenveloped virus: reovirus delivers the goods. Trends Microbiol **11:**374-82.

35. **Chandran, K., N. J. Sullivan, U. Felbor, S. P. Whelan, and J. M. Cunningham.** 2005. Endosomal proteolysis of the Ebola virus glycoprotein is necessary for infection. Science **308:**1643-5.

36. **Chu, P. W., and E. G. Westaway.** 1987. Characterization of Kunjin virus RNA-dependent RNA polymerase: reinitiation of synthesis in vitro. Virology **157:**330-7.

37. **Chu, P. W., and E. G. Westaway.** 1985. Replication strategy of Kunjin virus: evidence for recycling role of replicative form RNA as template in semiconservative and asymmetric replication. Virology **140:**68-79.

38. **Cocquerel, L., C. Voisset, and J. Dubuisson.** 2006. Hepatitis C virus entry: potential receptors and their biological functions. J Gen Virol **87:**1075-84.

39. **Colina, R., D. Casane, S. Vasquez, L. Garcia-Aguirre, A. Chunga, H. Romero, B. Khan, and J. Cristina.** 2004. Evidence of intratypic recombination in natural populations of hepatitis C virus. J Gen Virol **85:**31-7.

40. **Cormier, E. G., R. J. Durso, F. Tsamis, L. Boussemart, C. Manix, W. C. Olson, J. P. Gardner, and T. Dragic.** 2004. L-SIGN (CD209L) and DC-SIGN (CD209) mediate transinfection of liver cells by hepatitis C virus. Proc Natl Acad Sci U S A **101:**14067-72.

41. **Cormier, E. G., F. Tsamis, F. Kajumo, R. J. Durso, J. P. Gardner, and T. Dragic.** 2004. CD81 is an entry coreceptor for hepatitis C virus. Proc Natl Acad Sci U S A **101:**7270-4.

42. **Crise, B., L. Buonocore, and J. K. Rose.** 1990. CD4 is retained in the endoplasmic reticulum by the human immunodeficiency virus type 1 glycoprotein precursor. J Virol **64:**5585-93.

43. **Cristea, I. M., J. W. Carroll, M. P. Rout, C. M. Rice, B. T. Chait, and M. R. MacDonald.** 2006. Tracking and elucidating alphavirus-host protein interactions. J Biol Chem **281:**30269-78.

44. **Demaison, C., K. Parsley, G. Brouns, M. Scherr, K. Battmer, C. Kinnon, M. Grez, and A. J. Thrasher.** 2002. High-level transduction and gene expression in hematopoietic repopulating cells using a human immunodeficiency [correction of imunodeficiency]

virus type 1-based lentiviral vector containing an internal spleen focus forming virus promoter. Hum Gene Ther **13:**803-13.

45. **Deng, R., and K. V. Brock.** 1992. Molecular cloning and nucleotide sequence of a pestivirus genome, noncytopathic bovine viral diarrhea virus strain SD-1. Virology **191:**867-9.

46. **Deregt, D., S. R. Bolin, J. van den Hurk, J. F. Ridpath, and S. A. Gilbert.** 1998. Mapping of a type 1-specific and a type-common epitope on the E2 (gp53) protein of bovine viral diarrhea virus with neutralization escape mutants. Virus Res **53:**81-90.

47. **Drummer, H. E., A. Maerz, and P. Poumbourios.** 2003. Cell surface expression of functional hepatitis C virus E1 and E2 glycoproteins. FEBS Lett **546:**385-90.

48. **Dunn, S. J., S. W. Park, V. Sharma, G. Raghu, J. M. Simone, R. Tavassoli, L. M. Young, M. A. Ortega, C. H. Pan, G. J. Alegre, I. B. Roninson, G. Lipkina, A. Dayn, and T. A. Holzmayer.** 1999. Isolation of efficient antivirals: genetic suppressor elements against HIV-1. Gene Ther **6:**130-7.

49. **Ebert, D. H., J. Deussing, C. Peters, and T. S. Dermody.** 2002. Cathepsin L and cathepsin B mediate reovirus disassembly in murine fibroblast cells. J Biol Chem **277:**24609-17.

50. **Egger, D., B. Wolk, R. Gosert, L. Bianchi, H. E. Blum, D. Moradpour, and K. Bienz.** 2002. Expression of hepatitis C virus proteins induces distinct membrane alterations including a candidate viral replication complex. J Virol **76:**5974-84.

51. **Elbers, K., N. Tautz, P. Becher, D. Stoll, T. Rumenapf, and H. J. Thiel.** 1996. Processing in the pestivirus E2-NS2 region: identification of proteins p7 and E2p7. J Virol **70:**4131-5.

52. **Evans, M. J., C. M. Rice, and S. P. Goff.** 2004. Genetic interactions between hepatitis C virus replicons. J Virol **78:**12085-9.

53. **Evans, M. J., T. von Hahn, D. M. Tscherne, A. J. Syder, M. Panis, B. Wolk, T. Hatziioannou, J. A. McKeating, P. D. Bieniasz, and C.**

M. Rice. 2007. Claudin-1 is a hepatitis C virus co-receptor required for a late step in entry. Nature.

54. **Farci, P., H. J. Alter, A. Shimoda, S. Govindarajan, L. C. Cheung, J. C. Melpolder, R. A. Sacher, J. W. Shih, and R. H. Purcell.** 1996. Hepatitis C virus-associated fulminant hepatic failure. N Engl J Med **335:**631-4.

55. **Fetzer, C., B. A. Tews, and G. Meyers.** 2005. The carboxy-terminal sequence of the pestivirus glycoprotein E(rns) represents an unusual type of membrane anchor. J Virol **79:**11901-13.

56. **Flint, M., C. Logvinoff, C. M. Rice, and J. A. McKeating.** 2004. Characterization of infectious retroviral pseudotype particles bearing hepatitis C virus glycoproteins. J Virol **78:**6875-82.

57. **Flint, M., C. Maidens, L. D. Loomis-Price, C. Shotton, J. Dubuisson, P. Monk, A. Higginbottom, S. Levy, and J. A. McKeating.** 1999. Characterization of hepatitis C virus E2 glycoprotein interaction with a putative cellular receptor, CD81. J Virol **73:**6235-44.

58. **Flint, M., J. M. Thomas, C. M. Maidens, C. Shotton, S. Levy, W. S. Barclay, and J. A. McKeating.** 1999. Functional analysis of cell surface-expressed hepatitis C virus E2 glycoprotein. J Virol **73:**6782-90.

59. **Flint, M., T. von Hahn, J. Zhang, M. Farquhar, C. T. Jones, P. Balfe, C. M. Rice, and J. A. McKeating.** 2006. Diverse CD81 proteins support hepatitis C virus infection. J Virol **80:**11331-42.

60. **Flores, E. F., and R. O. Donis.** 1995. Isolation of a mutant MDBK cell line resistant to bovine viral diarrhea virus infection due to a block in viral entry. Virology **208:**565-75.

61. **Frolov, I., T. A. Hoffman, B. M. Pragai, S. A. Dryga, H. V. Huang, S. Schlesinger, and C. M. Rice.** 1996. Alphavirus-based expression vectors: strategies and applications. Proc Natl Acad Sci U S A **93:**11371-7.

62. **Frolova, E., R. Gorchakov, N. Garmashova, S. Atasheva, L. A. Vergara, and I. Frolov.** 2006. Formation of nsP3-specific protein complexes during Sindbis virus replication. J Virol **80:**4122-34.

63. **Gao, G., X. Guo, and S. P. Goff.** 2002. Inhibition of retroviral RNA production by ZAP, a CCCH-type zinc finger protein. Science **297:**1703-6.

64. **Gaudin, Y.** 2000. Reversibility in fusion protein conformational changes. The intriguing case of rhabdovirus-induced membrane fusion. Subcell Biochem **34:**379-408.

65. **Gaudin, Y., C. Tuffereau, D. Segretain, M. Knossow, and A. Flamand.** 1991. Reversible conformational changes and fusion activity of rabies virus glycoprotein. J Virol **65:**4853-9.

66. **Geib, T., C. Sauder, S. Venturelli, C. Hassler, P. Staeheli, and M. Schwemmle.** 2003. Selective virus resistance conferred by expression of Borna disease virus nucleocapsid components. J Virol **77:**4283-90.

67. **Gorbalenya, A. E., A. P. Donchenko, E. V. Koonin, and V. M. Blinov.** 1989. N-terminal domains of putative helicases of flavi- and pestiviruses may be serine proteases. Nucleic Acids Res **17:**3889-97.

68. **Gordon, F. D., H. Anastopoulos, U. Khettry, M. Loda, R. L. Jenkins, W. D. Lewis, and C. Trey.** 1995. Hepatitis C infection: a rare cause of fulminant hepatic failure. Am J Gastroenterol **90:**117-20.

69. **Gosert, R., D. Egger, V. Lohmann, R. Bartenschlager, H. E. Blum, K. Bienz, and D. Moradpour.** 2003. Identification of the hepatitis C virus RNA replication complex in Huh-7 cells harboring subgenomic replicons. J Virol **77:**5487-92.

70. **Grakoui, A., D. W. McCourt, C. Wychowski, S. M. Feinstone, and C. M. Rice.** 1993. A second hepatitis C virus-encoded proteinase. Proc Natl Acad Sci U S A **90:**10583-7.

71. **Grassmann, C. W., O. Isken, and S. E. Behrens.** 1999. Assignment of the multifunctional NS3 protein of bovine viral diarrhea virus

during RNA replication: an in vivo and in vitro study. J Virol **73:**9196-205.

72. **Grassmann, C. W., O. Isken, N. Tautz, and S. E. Behrens.** 2001. Genetic analysis of the pestivirus nonstructural coding region: defects in the NS5A unit can be complemented in trans. J Virol **75:**7791-802.

73. **Griffin, S. D., L. P. Beales, D. S. Clarke, O. Worsfold, S. D. Evans, J. Jaeger, M. P. Harris, and D. J. Rowlands.** 2003. The p7 protein of hepatitis C virus forms an ion channel that is blocked by the antiviral drug, Amantadine. FEBS Lett **535:**34-8.

74. **Grummer, B., S. Grotha, and I. Greiser-Wilke.** 2004. Bovine viral diarrhoea virus is internalized by clathrin-dependent receptor-mediated endocytosis. J Vet Med B Infect Dis Vet Public Health **51:**427-32.

75. **Gu, B., C. Liu, J. Lin-Goerke, D. R. Maley, L. L. Gutshall, C. A. Feltenberger, and A. M. Del Vecchio.** 2000. The RNA helicase and nucleotide triphosphatase activities of the bovine viral diarrhea virus NS3 protein are essential for viral replication. J Virol **74:**1794-800.

76. **Harada, T., N. Tautz, and H. J. Thiel.** 2000. E2-p7 region of the bovine viral diarrhea virus polyprotein: processing and functional studies. J Virol **74:**9498-506.

77. **Hartley, J. W., R. A. Yetter, and H. C. Morse, 3rd.** 1983. A mouse gene on chromosome 5 that restricts infectivity of mink cell focus-forming recombinant murine leukemia viruses. J Exp Med **158:**16-24.

78. **Hausmann, Y., G. Roman-Sosa, H. J. Thiel, and T. Rumenapf.** 2004. Classical swine fever virus glycoprotein E rns is an endoribonuclease with an unusual base specificity. J Virol **78:**5507-12.

79. **Heinz, F. X., and S. L. Allison.** 2000. Structures and mechanisms in flavivirus fusion. Adv Virus Res **55:**231-69.

80. **Heinz, F. X., and S. L. Allison.** 2001. The machinery for flavivirus fusion with host cell membranes. Curr Opin Microbiol **4:**450-5.

81. **Helenius, A., J. Kartenbeck, K. Simons, and E. Fries.** 1980. On the entry of Semliki forest virus into BHK-21 cells. J Cell Biol **84:**404-20.

82. **Higginbottom, A., E. R. Quinn, C. C. Kuo, M. Flint, L. H. Wilson, E. Bianchi, A. Nicosia, P. N. Monk, J. A. McKeating, and S. Levy.** 2000. Identification of amino acid residues in CD81 critical for interaction with hepatitis C virus envelope glycoprotein E2. J Virol **74:**3642-9.

83. **Hijikata, M., H. Mizushima, T. Akagi, S. Mori, N. Kakiuchi, N. Kato, T. Tanaka, K. Kimura, and K. Shimotohno.** 1993. Two distinct proteinase activities required for the processing of a putative nonstructural precursor protein of hepatitis C virus. J Virol **67:**4665-75.

84. **Holzmayer, T. A., D. G. Pestov, and I. B. Roninson.** 1992. Isolation of dominant negative mutants and inhibitory antisense RNA sequences by expression selection of random DNA fragments. Nucleic Acids Res **20:**711-7.

85. **Hsu, M., J. Zhang, M. Flint, C. Logvinoff, C. Cheng-Mayer, C. M. Rice, and J. A. McKeating.** 2003. Hepatitis C virus glycoproteins mediate pH-dependent cell entry of pseudotyped retroviral particles. Proc Natl Acad Sci U S A **100:**7271-6.

86. **Hulst, M. M., and R. J. Moormann.** 1997. Inhibition of pestivirus infection in cell culture by envelope proteins E(rns) and E2 of classical swine fever virus: E(rns) and E2 interact with different receptors. J Gen Virol **78 (Pt 11):**2779-87.

87. **Ikeda, H., F. Laigret, M. A. Martin, and R. Repaske.** 1985. Characterization of a molecularly cloned retroviral sequence associated with Fv-4 resistance. J Virol **55:**768-77.

88. **Ikeda, M., M. Yi, K. Li, and S. M. Lemon.** 2002. Selectable subgenomic and genome-length dicistronic RNAs derived from an infectious molecular clone of the HCV-N strain of hepatitis C virus replicate efficiently in cultured Huh7 cells. J Virol **76:**2997-3006.

89. **Iqbal, M., H. Flick-Smith, and J. W. McCauley.** 2000. Interactions of bovine viral diarrhoea virus glycoprotein E(rns) with cell surface glycosaminoglycans. J Gen Virol **81:**451-9.

90. **Iqbal, M., and J. W. McCauley.** 2002. Identification of the glycosaminoglycan-binding site on the glycoprotein E(rns) of bovine viral diarrhoea virus by site-directed mutagenesis. J Gen Virol **83:**2153-9.

91. **Ito, H., S. Watanabe, A. Sanchez, M. A. Whitt, and Y. Kawaoka.** 1999. Mutational analysis of the putative fusion domain of Ebola virus glycoprotein. J Virol **73:**8907-12.

92. **Jabbar, M. A., and D. P. Nayak.** 1990. Intracellular interaction of human immunodeficiency virus type 1 (ARV-2) envelope glycoprotein gp160 with CD4 blocks the movement and maturation of CD4 to the plasma membrane. J Virol **64:**6297-304.

93. **Johnston, R. E., K. Wan, and H. R. Bose.** 1974. Homologous interference induced by Sindbis virus. J Virol **14:**1076-82.

94. **Jopling, C. L., M. Yi, A. M. Lancaster, S. M. Lemon, and P. Sarnow.** 2005. Modulation of hepatitis C virus RNA abundance by a liver-specific MicroRNA. Science **309:**1577-81.

95. **Jordan, R., L. Wang, T. M. Graczyk, T. M. Block, and P. R. Romano.** 2002. Replication of a cytopathic strain of bovine viral diarrhea virus activates PERK and induces endoplasmic reticulum stress-mediated apoptosis of MDBK cells. J Virol **76:**9588-99.

96. **Kalinina, O., H. Norder, S. Mukomolov, and L. O. Magnius.** 2002. A natural intergenotypic recombinant of hepatitis C virus identified in St. Petersburg. J Virol **76:**4034-43.

97. **Kapadia, S. B., H. Barth, T. Baumert, J. A. McKeating, and F. V. Chisari.** 2007. Initiation of hepatitis C virus infection is dependent on cholesterol and cooperativity between CD81 and scavenger receptor B type I. J Virol **81:**374-83.

98. **Kapadia, S. B., and F. V. Chisari.** 2005. Hepatitis C virus RNA replication is regulated by host geranylgeranylation and fatty acids. Proc Natl Acad Sci U S A **102:**2561-6.

99. **Karpf, A. R., E. Lenches, E. G. Strauss, J. H. Strauss, and D. T. Brown.** 1997. Superinfection exclusion of alphaviruses in three mosquito cell lines persistently infected with Sindbis virus. J Virol **71:**7119-23.

100. **Kato, T., T. Date, M. Miyamoto, A. Furusaka, K. Tokushige, M. Mizokami, and T. Wakita.** 2003. Efficient replication of the genotype 2a hepatitis C virus subgenomic replicon. Gastroenterology **125:**1808-17.

101. **Kato, T., A. Furusaka, M. Miyamoto, T. Date, K. Yasui, J. Hiramoto, K. Nagayama, T. Tanaka, and T. Wakita.** 2001. Sequence analysis of hepatitis C virus isolated from a fulminant hepatitis patient. J Med Virol **64:**334-9.

102. **Kitadokoro, K., D. Bordo, G. Galli, R. Petracca, F. Falugi, S. Abrignani, G. Grandi, and M. Bolognesi.** 2001. CD81 extracellular domain 3D structure: insight into the tetraspanin superfamily structural motifs. Embo J **20:**12-8.

103. **Klimjack, M. R., S. Jeffrey, and M. Kielian.** 1994. Membrane and protein interactions of a soluble form of the Semliki Forest virus fusion protein. J Virol **68:**6940-6.

104. **Kohl, W., A. Grone, V. Moennig, and G. Herrler.** 2007. Expression of the surface glycoprotein E2 of Bovine viral diarrhea virus by recombinant vesicular stomatitis virus. J Gen Virol **88:**157-65.

105. **Kolykhalov, A. A., E. V. Agapov, K. J. Blight, K. Mihalik, S. M. Feinstone, and C. M. Rice.** 1997. Transmission of hepatitis C by intrahepatic inoculation with transcribed RNA. Science **277:**570-4.

106. **Koutsoudakis, G., A. Kaul, E. Steinmann, S. Kallis, V. Lohmann, T. Pietschmann, and R. Bartenschlager.** 2006. Characterization of the early steps of hepatitis C virus infection by using luciferase reporter viruses. J Virol **80:**5308-20.

107. **Krey, T., A. Himmelreich, M. Heimann, C. Menge, H. J. Thiel, K. Maurer, and T. Rumenapf.** 2006. Function of bovine CD46 as a cellular receptor for bovine viral diarrhea virus is determined by complement control protein 1. J Virol **80:**3912-22.

108. **Krey, T., E. Moussay, H. J. Thiel, and T. Rumenapf.** 2006. Role of the low-density lipoprotein receptor in entry of bovine viral diarrhea virus. J Virol **80:**10862-7.

109. **Krey, T., H. J. Thiel, and T. Rumenapf.** 2005. Acid-resistant bovine pestivirus requires activation for pH-triggered fusion during entry. J Virol **79:**4191-200.

110. **Kuhn, R. J., W. Zhang, M. G. Rossmann, S. V. Pletnev, J. Corver, E. Lenches, C. T. Jones, S. Mukhopadhyay, P. R. Chipman, E. G. Strauss, T. S. Baker, and J. H. Strauss.** 2002. Structure of dengue virus: implications for flavivirus organization, maturation, and fusion. Cell **108:**717-25.

111. **Lackner, T., A. Muller, M. Konig, H. J. Thiel, and N. Tautz.** 2005. Persistence of bovine viral diarrhea virus is determined by a cellular cofactor of a viral autoprotease. J Virol **79:**9746-55.

112. **Lackner, T., A. Muller, A. Pankraz, P. Becher, H. J. Thiel, A. E. Gorbalenya, and N. Tautz.** 2004. Temporal modulation of an autoprotease is crucial for replication and pathogenicity of an RNA virus. J Virol **78:**10765-75.

113. **Lai, V. C., C. C. Kao, E. Ferrari, J. Park, A. S. Uss, J. Wright-Minogue, Z. Hong, and J. Y. Lau.** 1999. Mutational analysis of bovine viral diarrhea virus RNA-dependent RNA polymerase. J Virol **73:**10129-36.

114. **Lamarre, D., P. C. Anderson, M. Bailey, P. Beaulieu, G. Bolger, P. Bonneau, M. Bos, D. R. Cameron, M. Cartier, M. G. Cordingley, A. M. Faucher, N. Goudreau, S. H. Kawai, G. Kukolj, L. Lagace, S. R. LaPlante, H. Narjes, M. A. Poupart, J. Rancourt, R. E. Sentjens, R. St George, B. Simoneau, G. Steinmann, D. Thibeault, Y. S. Tsantrizos, S. M. Weldon, C. L. Yong, and M. Llinas-**

Brunet. 2003. An NS3 protease inhibitor with antiviral effects in humans infected with hepatitis C virus. Nature **426:**186-9.

115. **Lamb, R. A., and P. W. Choppin.** 1983. The gene structure and replication of influenza virus. Annu Rev Biochem **52:**467-506.

116. **Langedijk, J. P., P. A. van Veelen, W. M. Schaaper, A. H. de Ru, R. H. Meloen, and M. M. Hulst.** 2002. A structural model of pestivirus E(rns) based on disulfide bond connectivity and homology modeling reveals an extremely rare vicinal disulfide. J Virol **76:**10383-92.

117. **Lavillette, D., A. W. Tarr, C. Voisset, P. Donot, B. Bartosch, C. Bain, A. H. Patel, J. Dubuisson, J. K. Ball, and F. L. Cosset.** 2005. Characterization of host-range and cell entry properties of the major genotypes and subtypes of hepatitis C virus. Hepatology **41:**265-74.

118. **Lecot, S., S. Belouzard, J. Dubuisson, and Y. Rouille.** 2005. Bovine viral diarrhea virus entry is dependent on clathrin-mediated endocytosis. J Virol **79:**10826-9.

119. **Lee, Y. M., D. M. Tscherne, S. I. Yun, I. Frolov, and C. M. Rice.** 2005. Dual mechanisms of pestiviral superinfection exclusion at entry and RNA replication. J Virol **79:**3231-42.

120. **Levy, S., and T. Shoham.** 2005. The tetraspanin web modulates immune-signalling complexes. Nat Rev Immunol **5:**136-48.

121. **Levy, S., S. C. Todd, and H. T. Maecker.** 1998. CD81 (TAPA-1): a molecule involved in signal transduction and cell adhesion in the immune system. Annu Rev Immunol **16:**89-109.

122. **Liang, D., I. F. Sainz, I. H. Ansari, L. H. Gil, V. Vassilev, and R. O. Donis.** 2003. The envelope glycoprotein E2 is a determinant of cell culture tropism in ruminant pestiviruses. J Gen Virol **84:**1269-74.

123. **Lindenbach, B. D., M. J. Evans, A. J. Syder, B. Wolk, T. L. Tellinghuisen, C. C. Liu, T. Maruyama, R. O. Hynes, D. R. Burton, J. A. McKeating, and C. M. Rice.** 2005. Complete replication of hepatitis C virus in cell culture. Science **309:**623-6.

124. **Lindenbach, B. D., P. Meuleman, A. Ploss, T. Vanwolleghem, A. J. Syder, J. A. McKeating, R. E. Lanford, S. M. Feinstone, M. E. Major, G. Leroux-Roels, and C. M. Rice.** 2006. Cell culture-grown hepatitis C virus is infectious in vivo and can be recultured in vitro. Proc Natl Acad Sci U S A **103:**3805-9.

125. **Lindenbach, B. D., and C. M. Rice.** 1997. trans-Complementation of yellow fever virus NS1 reveals a role in early RNA replication. J Virol **71:**9608-17.

126. **Lindenbach, B. D., H. J. Thiel, and C. M. Rice.** 2007. Flaviviridae: the viruses and their replication, p 1101-1152. In D. M. Knipe and P.M. Howley (ed.), Fields Virology, 5th ed. Lippincott-Raven Publishers, Philadelphia, Pa.

127. **Liszewski, M. K., and J. P. Atkinson.** 1992. Membrane cofactor protein. Curr Top Microbiol Immunol **178:**45-60.

128. **Liszewski, M. K., T. W. Post, and J. P. Atkinson.** 1991. Membrane cofactor protein (MCP or CD46): newest member of the regulators of complement activation gene cluster. Annu Rev Immunol **9:**431-55.

129. **Lobigs, M., and H. Garoff.** 1990. Fusion function of the Semliki Forest virus spike is activated by proteolytic cleavage of the envelope glycoprotein precursor p62. J Virol **64:**1233-40.

130. **Lohmann, V., S. Hoffmann, U. Herian, F. Penin, and R. Bartenschlager.** 2003. Viral and cellular determinants of hepatitis C virus RNA replication in cell culture. J Virol **77:**3007-19.

131. **Lohmann, V., F. Korner, J. Koch, U. Herian, L. Theilmann, and R. Bartenschlager.** 1999. Replication of subgenomic hepatitis C virus RNAs in a hepatoma cell line. Science **285:**110-3.

132. **Lorenz, I. C., J. Marcotrigiano, T. G. Dentzer, and C. M. Rice.** 2006. Structure of the catalytic domain of the hepatitis C virus NS2-3 protease. Nature **442:**831-5.

133. **Lozach, P. Y., A. Amara, B. Bartosch, J. L. Virelizier, F. Arenzana-Seisdedos, F. L. Cosset, and R. Altmeyer.** 2004. C-type

lectins L-SIGN and DC-SIGN capture and transmit infectious hepatitis C virus pseudotype particles. J Biol Chem **279:**32035-45.

134. **Mahon, G. M., and I. P. Whitehead.** 2001. Retrovirus cDNA expression library screening for oncogenes. Methods Enzymol **332:**211-21.

135. **Major, M. E., B. Rehermann, and S. M. Feinstone.** 2001. Hepatitis C viruses. p. 1127-1161. In D. M. Knipe, P.M. Howley, R. M. Chanock, T. P. Monath, B. Roizman, S. E. Straus (ed.), Fields Virology, 4rd ed. Lippincott-Raven Publishers, Philadelphia, PA

136. **Marsh, M., and R. Bron.** 1997. SFV infection in CHO cells: cell-type specific restrictions to productive virus entry at the cell surface. J Cell Sci **110 (Pt 1):**95-103.

137. **Maurer, K., T. Krey, V. Moennig, H. J. Thiel, and T. Rumenapf.** 2004. CD46 is a cellular receptor for bovine viral diarrhea virus. J Virol **78:**1792-9.

138. **Mayo, M. J.** 2003. Extrahepatic manifestations of hepatitis C infection. Am J Med Sci **325:**135-48.

139. **McCaughan, G. W., D. J. Koorey, and S. I. Strasser.** 2005. Liver transplantation for viral hepatitis. Hosp Med **66:**8-12.

140. **McClurkin, A. W., S. R. Bolin, and M. F. Coria.** 1985. Isolation of cytopathic and noncytopathic bovine viral diarrhea virus from the spleen of cattle acutely and chronically affected with bovine viral diarrhea. J Am Vet Med Assoc **186:**568-9.

141. **McKeating, J. A., L. Q. Zhang, C. Logvinoff, M. Flint, J. Zhang, J. Yu, D. Butera, D. D. Ho, L. B. Dustin, C. M. Rice, and P. Balfe.** 2004. Diverse hepatitis C virus glycoproteins mediate viral infection in a CD81-dependent manner. J Virol **78:**8496-505.

142. **McMullan, L. K., A. Grakoui, M. J. Evans, K. Mihalik, M. Puig, A. D. Branch, S. M. Feinstone, and C. M. Rice.** 2007. Evidence for a functional RNA element in the hepatitis C virus core gene. Proc Natl Acad Sci U S A.

143. **Mendez, E., N. Ruggli, M. S. Collett, and C. M. Rice.** 1998. Infectious bovine viral diarrhea virus (strain NADL) RNA from stable cDNA clones: a cellular insert determines NS3 production and viral cytopathogenicity. J Virol **72:**4737-45.

144. **Meunier, J. C., R. E. Engle, K. Faulk, M. Zhao, B. Bartosch, H. Alter, S. U. Emerson, F. L. Cosset, R. H. Purcell, and J. Bukh.** 2005. Evidence for cross-genotype neutralization of hepatitis C virus pseudo-particles and enhancement of infectivity by apolipoprotein C1. Proc Natl Acad Sci U S A **102:**4560-5.

145. **Meyers, G., T. Rumenapf, and H. J. Thiel.** 1989. Ubiquitin in a togavirus. Nature **341:**491.

146. **Meyers, G., N. Tautz, P. Becher, H. J. Thiel, and B. M. Kummerer.** 1996. Recovery of cytopathogenic and noncytopathogenic bovine viral diarrhea viruses from cDNA constructs. J Virol **70:**8606-13.

147. **Mittelholzer, C., C. Moser, J. D. Tratschin, and M. A. Hofmann.** 1998. Porcine cells persistently infected with classical swine fever virus protected from pestivirus-induced cytopathic effect. J Gen Virol **79 (Pt 12):**2981-7.

148. **Moennig, V., H. R. Frey, E. Liebler, J. Pohlenz, and B. Liess.** 1990. Reproduction of mucosal disease with cytopathogenic bovine viral diarrhoea virus selected in vitro. Vet Rec **127:**200-3.

149. **Moennig, V., and P. G. Plagemann.** 1992. The pestiviruses. Adv Virus Res **41:**53-98.

150. **Monazahian, M., I. Bohme, S. Bonk, A. Koch, C. Scholz, S. Grethe, and R. Thomssen.** 1999. Low density lipoprotein receptor as a candidate receptor for hepatitis C virus. J Med Virol **57:**223-9.

151. **Mothes, W., A. L. Boerger, S. Narayan, J. M. Cunningham, and J. A. Young.** 2000. Retroviral entry mediated by receptor priming and low pH triggering of an envelope glycoprotein. Cell **103:**679-89.

152. **Murphy, J. E., I. T. Pleasure, S. Puszkin, K. Prasad, and J. H. Keen.** 1991. Clathrin assembly protein AP-3. The identity of the 155K protein, AP 180, and NP185 and demonstration of a clathrin binding domain. J Biol Chem **266:**4401-8.

153. **Murray, E. M., J. A. Grobler, E. J. Markel, M. F. Pagnoni, G. Paonessa, A. J. Simon, and O. A. Flores.** 2003. Persistent replication of hepatitis C virus replicons expressing the beta-lactamase reporter in subpopulations of highly permissive Huh7 cells. J Virol **77:**2928-35.

154. **Myers, T. M., V. G. Kolupaeva, E. Mendez, S. G. Baginski, I. Frolov, C. U. Hellen, and C. M. Rice.** 2001. Efficient translation initiation is required for replication of bovine viral diarrhea virus subgenomic replicons. J Virol **75:**4226-38.

155. **Nieland, T. J., M. Penman, L. Dori, M. Krieger, and T. Kirchhausen.** 2002. Discovery of chemical inhibitors of the selective transfer of lipids mediated by the HDL receptor SR-BI. Proc Natl Acad Sci U S A **99:**15422-7.

156. **Op De Beeck, A., L. Cocquerel, and J. Dubuisson.** 2001. Biogenesis of hepatitis C virus envelope glycoproteins. J Gen Virol **82:**2589-95.

157. **Op De Beeck, A., C. Voisset, B. Bartosch, Y. Ciczora, L. Cocquerel, Z. Keck, S. Foung, F. L. Cosset, and J. Dubuisson.** 2004. Characterization of functional hepatitis C virus envelope glycoproteins. J Virol **78:**2994-3002.

158. **Palese, P., K. Tobita, M. Ueda, and R. W. Compans.** 1974. Characterization of temperature sensitive influenza virus mutants defective in neuraminidase. Virology **61:**397-410.

159. **Paton, D. J., J. P. Lowings, and A. D. Barrett.** 1992. Epitope mapping of the gp53 envelope protein of bovine viral diarrhea virus. Virology **190:**763-72.

160. **Pavlovic, D., D. C. Neville, O. Argaud, B. Blumberg, R. A. Dwek, W. B. Fischer, and N. Zitzmann.** 2003. The hepatitis C virus p7

protein forms an ion channel that is inhibited by long-alkyl-chain iminosugar derivatives. Proc Natl Acad Sci U S A **100:**6104-8.

161. **Pestov, D. G., and L. F. Lau.** 1994. Genetic selection of growth-inhibitory sequences in mammalian cells. Proc Natl Acad Sci U S A **91:**12549-53.

162. **Petracca, R., F. Falugi, G. Galli, N. Norais, D. Rosa, S. Campagnoli, V. Burgio, E. Di Stasio, B. Giardina, M. Houghton, S. Abrignani, and G. Grandi.** 2000. Structure-function analysis of hepatitis C virus envelope-CD81 binding. J Virol **74:**4824-30.

163. **Petrakova, O., E. Volkova, R. Gorchakov, S. Paessler, R. M. Kinney, and I. Frolov.** 2005. Noncytopathic replication of Venezuelan equine encephalitis virus and eastern equine encephalitis virus replicons in Mammalian cells. J Virol **79:**7597-608.

164. **Pietschmann, T., A. Kaul, G. Koutsoudakis, A. Shavinskaya, S. Kallis, E. Steinmann, K. Abid, F. Negro, M. Dreux, F. L. Cosset, and R. Bartenschlager.** 2006. Construction and characterization of infectious intragenotypic and intergenotypic hepatitis C virus chimeras. Proc Natl Acad Sci U S A **103:**7408-13.

165. **Pietschmann, T., V. Lohmann, A. Kaul, N. Krieger, G. Rinck, G. Rutter, D. Strand, and R. Bartenschlager.** 2002. Persistent and transient replication of full-length hepatitis C virus genomes in cell culture. J Virol **76:**4008-21.

166. **Pileri, P., Y. Uematsu, S. Campagnoli, G. Galli, F. Falugi, R. Petracca, A. J. Weiner, M. Houghton, D. Rosa, G. Grandi, and S. Abrignani.** 1998. Binding of hepatitis C virus to CD81. Science **282:**938-41.

167. **Premkumar, A., L. Wilson, G. D. Ewart, and P. W. Gage.** 2004. Cation-selective ion channels formed by p7 of hepatitis C virus are blocked by hexamethylene amiloride. FEBS Lett **557:**99-103.

168. **Qu, L., L. K. McMullan, and C. M. Rice.** 2001. Isolation and characterization of noncytopathic pestivirus mutants reveals a role for

nonstructural protein NS4B in viral cytopathogenicity. J Virol **75:**10651-62.

169. **Reimann, I., K. Depner, S. Trapp, and M. Beer.** 2004. An avirulent chimeric Pestivirus with altered cell tropism protects pigs against lethal infection with classical swine fever virus. Virology **322:**143-57.

170. **Reimann, I., G. Meyers, and M. Beer.** 2003. Trans-complementation of autonomously replicating Bovine viral diarrhea virus replicons with deletions in the E2 coding region. Virology **307:**213-27.

171. **Rumenapf, T., G. Meyers, R. Stark, and H. J. Thiel.** 1991. Molecular characterization of hog cholera virus. Arch Virol Suppl **3:**7-18.

172. **Rumenapf, T., G. Unger, J. H. Strauss, and H. J. Thiel.** 1993. Processing of the envelope glycoproteins of pestiviruses. J Virol **67:**3288-94.

173. **Ryser, H. J., E. M. Levy, R. Mandel, and G. J. DiSciullo.** 1994. Inhibition of human immunodeficiency virus infection by agents that interfere with thiol-disulfide interchange upon virus-receptor interaction. Proc Natl Acad Sci U S A **91:**4559-63.

174. **Sakai, A., M. S. Claire, K. Faulk, S. Govindarajan, S. U. Emerson, R. H. Purcell, and J. Bukh.** 2003. The p7 polypeptide of hepatitis C virus is critical for infectivity and contains functionally important genotype-specific sequences. Proc Natl Acad Sci U S A **100:**11646-51.

175. **Sanders, D. A.** 2000. Sulfhydryl involvement in fusion mechanisms. Subcell Biochem **34:**483-514.

176. **Scarselli, E., H. Ansuini, R. Cerino, R. M. Roccasecca, S. Acali, G. Filocamo, C. Traboni, A. Nicosia, R. Cortese, and A. Vitelli.** 2002. The human scavenger receptor class B type I is a novel candidate receptor for the hepatitis C virus. Embo J **21:**5017-25.

177. **Schneider, R., G. Unger, R. Stark, E. Schneider-Scherzer, and H. J. Thiel.** 1993. Identification of a structural glycoprotein of an RNA virus as a ribonuclease. Science **261:**1169-71.

178. **Schwartz, M., J. Chen, M. Janda, M. Sullivan, J. den Boon, and P. Ahlquist.** 2002. A positive-strand RNA virus replication complex parallels form and function of retrovirus capsids. Mol Cell **9:**505-14.

179. **Simmons, G., D. N. Gosalia, A. J. Rennekamp, J. D. Reeves, S. L. Diamond, and P. Bates.** 2005. Inhibitors of cathepsin L prevent severe acute respiratory syndrome coronavirus entry. Proc Natl Acad Sci U S A **102:**11876-81.

180. **Simon, K. O., J. J. Cardamone, Jr., P. A. Whitaker-Dowling, J. S. Youngner, and C. C. Widnell.** 1990. Cellular mechanisms in the superinfection exclusion of vesicular stomatitis virus. Virology **177:**375-9.

181. **Singh, I. R., M. Suomalainen, S. Varadarajan, H. Garoff, and A. Helenius.** 1997. Multiple mechanisms for the inhibition of entry and uncoating of superinfecting Semliki Forest virus. Virology **231:**59-71.

182. **Skehel, J. J., and D. C. Wiley.** 2000. Receptor binding and membrane fusion in virus entry: the influenza hemagglutinin. Annu Rev Biochem **69:**531-69.

183. **Smith, A. E., and A. Helenius.** 2004. How viruses enter animal cells. Science **304:**237-42.

184. **Steck, F. T., and H. Rubin.** 1966. The mechanism of interference between an avian leukosis virus and Rous sarcoma virus. I. Establishment of interference. Virology **29:**628-41.

185. **Steck, F. T., and H. Rubin.** 1966. The mechanism of interference between an avian leukosis virus and Rous sarcoma virus. II. Early steps of infection by RSV of cells under conditions of interference. Virology **29:**642-53.

186. **Stevenson, M., C. Meier, A. M. Mann, N. Chapman, and A. Wasiak.** 1988. Envelope glycoprotein of HIV induces interference

and cytolysis resistance in CD4+ cells: mechanism for persistence in AIDS. Cell **53:**483-96.

187. **Stiasny, K., S. L. Allison, J. Schalich, and F. X. Heinz.** 2002. Membrane interactions of the tick-borne encephalitis virus fusion protein E at low pH. J Virol **76:**3784-90.

188. **Summers, B. C., and D. A. Leib.** 2002. Herpes simplex virus type 1 origins of DNA replication play no role in the regulation of flanking promoters. J Virol **76:**7020-9.

189. **Takada, A., C. Robison, H. Goto, A. Sanchez, K. G. Murti, M. A. Whitt, and Y. Kawaoka.** 1997. A system for functional analysis of Ebola virus glycoprotein. Proc Natl Acad Sci U S A **94:**14764-9.

190. **Tamura, J. K., P. Warrener, and M. S. Collett.** 1993. RNA-stimulated NTPase activity associated with the p80 protein of the pestivirus bovine viral diarrhea virus. Virology **193:**1-10.

191. **Tautz, N., K. Elbers, D. Stoll, G. Meyers, and H. J. Thiel.** 1997. Serine protease of pestiviruses: determination of cleavage sites. J Virol **71:**5415-22.

192. **Tautz, N., T. Harada, A. Kaiser, G. Rinck, S. Behrens, and H. J. Thiel.** 1999. Establishment and characterization of cytopathogenic and noncytopathogenic pestivirus replicons. J Virol **73:**9422-32.

193. **Tautz, N., G. Meyers, R. Stark, E. J. Dubovi, and H. J. Thiel.** 1996. Cytopathogenicity of a pestivirus correlates with a 27-nucleotide insertion. J Virol **70:**7851-8.

194. **Thiel, H. J., P. G. W. Plagemann, and V. Moennig.** 1996. Pestiviruses. p. 1059-1073. In B. N. Fields, D. M. Knipe and P.M. Howley (ed.), Fields Virology, 3rd ed., vol 1. Raven Press, New York, NY.

195. **Thiel, H. J., R. Stark, E. Weiland, T. Rumenapf, and G. Meyers.** 1991. Hog cholera virus: molecular composition of virions from a pestivirus. J Virol **65:**4705-12.

196. **Toth, R. L., P. F. Nettleton, and M. A. McCrae.** 1999. Expression of the E2 envelope glycoprotein of bovine viral diarrhoea virus (BVDV) elicits virus-type specific neutralising antibodies. Vet Microbiol **65:**87-101.

197. **Tscherne, D. M., M. J. Evans, T. von Hahn, C. T. Jones, Z. Stamataki, J. A. McKeating, B. D. Lindenbach, and C. M. Rice.** 2007. Superinfection exclusion in cells infected with hepatitis C virus. J Virol **81:**3693-3703.

198. **Tscherne, D. M., C. T. Jones, M. J. Evans, B. D. Lindenbach, J. A. McKeating, and C. M. Rice.** 2006. Time- and temperature-dependent activation of hepatitis C virus for low-pH-triggered entry. J Virol **80:**1734-41.

199. **Van Itallie, C. M., and J. M. Anderson.** 2006. Claudins and epithelial paracellular transport. Annu Rev Physiol **68:**403-29.

200. **Voisset, C., N. Callens, E. Blanchard, A. Op De Beeck, J. Dubuisson, and N. Vu-Dac.** 2005. High density lipoproteins facilitate hepatitis C virus entry through the scavenger receptor class B type I. J Biol Chem **280:**7793-9.

201. **von Hahn, T., B. D. Lindenbach, A. Boullier, O. Quehenberger, M. Paulson, C. M. Rice, and J. A. McKeating.** 2006. Oxidized low-density lipoprotein inhibits hepatitis C virus cell entry in human hepatoma cells. Hepatology **43:**932-42.

202. **Von Hahn, T., J. C. Yoon, H. Alter, C. M. Rice, B. Rehermann, P. Balfe, and J. A. McKeating.** 2007. Hepatitis C Virus Continuously Escapes From Neutralizing Antibody and T-Cell Responses During Chronic Infection In Vivo. Gastroenterology **132:**667-78.

203. **Wakita, T., T. Pietschmann, T. Kato, T. Date, M. Miyamoto, Z. Zhao, K. Murthy, A. Habermann, H. G. Krausslich, M. Mizokami, R. Bartenschlager, and T. J. Liang.** 2005. Production of infectious hepatitis C virus in tissue culture from a cloned viral genome. Nat Med **11:**791-6.

204. **Wallin, M., M. Ekstrom, and H. Garoff.** 2004. Isomerization of the intersubunit disulphide-bond in Env controls retrovirus fusion. Embo J **23:**54-65.

205. **Webb, N. R., P. M. Connell, G. A. Graf, E. J. Smart, W. J. de Villiers, F. C. de Beer, and D. R. van der Westhuyzen.** 1998. SR-BII, an isoform of the scavenger receptor BI containing an alternate cytoplasmic tail, mediates lipid transfer between high density lipoprotein and cells. J Biol Chem **273:**15241-8.

206. **Weiland, E., R. Stark, B. Haas, T. Rumenapf, G. Meyers, and H. J. Thiel.** 1990. Pestivirus glycoprotein which induces neutralizing antibodies forms part of a disulfide-linked heterodimer. J Virol **64:**3563-9.

207. **Wengler, G., G. Wengler, T. Nowak, and E. Castle.** 1990. Description of a procedure which allows isolation of viral nonstructural proteins from BHK vertebrate cells infected with the West Nile flavivirus in a state which allows their direct chemical characterization. Virology **177:**795-801.

208. **Westaway, E. G.** 1987. Flavivirus replication strategy. Adv Virus Res **33:**45-90.

209. **Whitaker-Dowling, P., J. S. Youngner, C. C. Widnell, and D. K. Wilcox.** 1983. Superinfection exclusion by vesicular stomatitis virus. Virology **131:**137-43.

210. **Whitehead, I., H. Kirk, and R. Kay.** 1995. Expression cloning of oncogenes by retroviral transfer of cDNA libraries. Mol Cell Biol **15:**704-10.

211. **Wiskerchen, M., and M. S. Collett.** 1991. Pestivirus gene expression: protein p80 of bovine viral diarrhea virus is a proteinase involved in polyprotein processing. Virology **184:**341-50.

212. **Wool-Lewis, R. J., and P. Bates.** 1999. Endoproteolytic processing of the ebola virus envelope glycoprotein: cleavage is not required for function. J Virol **73:**1419-26.

213. **Wu, T., Y. Yan, and C. A. Kozak.** 2005. Rmcf2, a xenotropic provirus in the Asian mouse species Mus castaneus, blocks infection by polytropic mouse gammaretroviruses. J Virol **79:**9677-84.

214. **Wunschmann, S., J. D. Medh, D. Klinzmann, W. N. Schmidt, and J. T. Stapleton.** 2000. Characterization of hepatitis C virus (HCV) and HCV E2 interactions with CD81 and the low-density lipoprotein receptor. J Virol **74:**10055-62.

215. **Xu, J., E. Mendez, P. R. Caron, C. Lin, M. A. Murcko, M. S. Collett, and C. M. Rice.** 1997. Bovine viral diarrhea virus NS3 serine proteinase: polyprotein cleavage sites, cofactor requirements, and molecular model of an enzyme essential for pestivirus replication. J Virol **71:**5312-22.

216. **Yanagi, M., R. H. Purcell, S. U. Emerson, and J. Bukh.** 1997. Transcripts from a single full-length cDNA clone of hepatitis C virus are infectious when directly transfected into the liver of a chimpanzee. Proc Natl Acad Sci U S A **94:**8738-43.

217. **Yang, X., S. Kurteva, X. Ren, S. Lee, and J. Sodroski.** 2005. Stoichiometry of envelope glycoprotein trimers in the entry of human immunodeficiency virus type 1. J Virol **79:**12132-47.

218. **Yi, M., Y. Ma, J. Yates, and S. M. Lemon.** 2007. Compensatory mutations in E1, p7, NS2, and NS3 enhance yields of cell culture-infectious intergenotypic chimeric hepatitis C virus. J Virol **81:**629-38.

219. **Yoshiba, M., K. Dehara, K. Inoue, H. Okamoto, and M. Mayumi.** 1994. Contribution of hepatitis C virus to non-A, non-B fulminant hepatitis in Japan. Hepatology **19:**829-35.

220. **Zhang, J., G. Randall, A. Higginbottom, P. Monk, C. M. Rice, and J. A. McKeating.** 2004. CD81 is required for hepatitis C virus glycoprotein-mediated viral infection. J Virol **78:**1448-55.

221. **Zhong, J., P. Gastaminza, G. Cheng, S. Kapadia, T. Kato, D. R. Burton, S. F. Wieland, S. L. Uprichard, T. Wakita, and F. V.**

Chisari. 2005. Robust hepatitis C virus infection in vitro. Proc Natl Acad Sci U S A **102:**9294-9.

222. **Zhong, W., L. L. Gutshall, and A. M. Del Vecchio.** 1998. Identification and characterization of an RNA-dependent RNA polymerase activity within the nonstructural protein 5B region of bovine viral diarrhea virus. J Virol **72:**9365-9.